2007

Responses of respiratory system cells in vitro and in vivo to petrochemical combustion-derived ultrafine particles

Gleeson Murphy, Jr.
Louisiana State University and Agricultural and Mechanical College, gmurph1@lsu.edu

RESPONSES OF RESPIRATORY SYSTEM CELLS *IN VITRO* AND *IN VIVO* TO PETROCHEMICAL COMBUSTION-DERIVED ULTRAFINE PARTICLES

A Dissertation

Submitted to the Graduate Faculty of the
Louisiana State University and
Agricultural and Mechanical College
in partial fulfillment of the
requirements for the degree of
Doctor of Philosophy

In

The Interdepartmental Program in
Veterinary Medical Sciences through the
Department of Comparative Biomedical Sciences

by
Gleeson Murphy, Jr.
B.S., Louisiana State University, 2000
D.V.M., Louisiana State University, 2005
August 2007

To Bryan, Melissa, and Tonya

ACKNOWLEDGEMENTS

First and foremost, I would like to express my appreciation of Dr. Arthur Penn, my major professor and mentor for all of the work presented in this dissertation. He accepted the challenge of guiding me, an inexperienced veterinary student, through the rigorous first years of my research career. He provided me with a strong working knowledge of the fundamentals of research, including the importance of a thorough review of available literature without ignoring the significance of historical literature. His belief in the necessity of communicating research findings was exemplified through his constant encouragement of me to present our results to as many people as possible, at both national meetings and in publications.

The significance and success of our projects has relied heavily upon the cooperation and assistance of the other members of my graduate advisory committee. Dr. Steven Barker was always available for cheerful, insightful, and occasionally divine discussions about analytical chemistry assays that still baffle me; however, in working with Dr. Barker, I gained an appreciation for the importance of interdisciplinary research. Dr. William Henk spent many patient hours with me staring at or discussing the tiny colorful points of light in our cell culture experiments; and, through our interaction, I developed a great passion and appreciation for the art and science of microscopy. As a veterinary pathologist, Dr. Daniel Paulsen was able to provide us with meaningful interpretations of the histopathology resulting from butadiene soot exposure *in vivo*. I would also like to thank Dr. Christopher White, the Dean's representative, for his patience and understanding of my unusual schedule.

I also would like to thank the past and present technical staff of the Inhalation Research Facility, including Terry and the late Ken Ahlert, Brandon LaGroue, and Travis Ball; and several research associates who helped me at every step, namely Marc Boudreaux, Erin Boykin, and Daniel Lundquist. I wish to thank Olga Borkhsenious, Greg McCormick, and Josh Welford of

the School of Veterinary Medicine Microscopy Center and Dr. David Burk of the Socolofsky Microscopy Center for their instruction and assistance with the various microscopy techniques that I used in these studies. Michael Kearney was instrumental in many of the statistical analyses performed during these studies. Finally, I want to thank the faculty, administration, and support staff of the Department of Comparative Biomedical Sciences, especially our graduate advisor Dr. George Strain, and the Associate Dean for Student Affairs Dr. Joseph Taboada.

TABLE OF CONTENTS

ABSTRACT

Environmental contamination with airborne particles has been a human health concern for many years. Epidemiologic studies in urban communities have linked ambient particle exposure to various health effects, including chronic obstructive pulmonary disease, lung cancer, and several cardiovascular disease conditions. The pathogenesis of these conditions with respect to ambient particle exposure is complex because ambient particles are complex in composition. The particles vary greatly in origin, size, surface area, and elemental composition; and a given particle type, such as those generated by petrochemical (gasoline, diesel, industrial substrate) combustion, may be coated with many other compounds, including polynuclear aromatic hydrocarbons (PAHs).

Our laboratory group had previously characterized the generation of PAHs from incomplete combustion of the high volume petrochemical 1,3-butadiene (BD) and briefly described the biological effects of BD's incomplete combustion product, butadiene soot (BDS), *in vitro*. The studies presented here represent a continuation of these initial studies, where we first characterize BDS with respect to particle size distribution and assembly, PAH composition, and elemental content of BDS ultrafine particles. We also describe *in vitro* assays demonstrating that BDS ultrafine particles can transport and transfer adsorbed organic constituents directly to target respiratory cells, without uptake of the particles by the cells. Next, we demonstrate that combustion-derived PAHs adsorbed onto BDS particles are concentrated in lipid droplets of respiratory system cells and that, *in vitro*, these PAHs activate xenobiotic metabolism pathways. We also present an *in vivo* analysis of bronchoalveolar lavage fluid (BALF) with inflammatory cell infiltrates, histopathological evidence of inflammation and particle retention, and gene expression analysis revealing upregulation of several cytokines and AhR-responsive biotransformation enzymes. Finally, we present ultrastructural evidence that BDS particles can be internalized by bronchoepithelial cells *in vitro* and phagocytosed by alveolar macrophages *in vivo*. These studies were designed to characterize and promote BDS as both a

model mixture and a real-life example of a petrochemical product of incomplete combustion with the potential both for environmental contamination and for contributing to health problems.

INTRODUCTORY REMARKS

Environmental contamination with airborne particles has been a human health concern for many years (Seaton *et al.* 1995). Epidemiologic studies in urban communities have linked ambient particle exposure to various health effects, including chronic obstructive pulmonary disease, lung cancer, and even heart failure (Dominici *et al.* 2006; Pope, III *et al.* 2002). The pathogenesis of these conditions is complex because ambient particles are complex in composition. For example, the particles vary greatly in origin, size, surface area, and elemental composition; plus a given particle type, such as those generated by petrochemical (gasoline, diesel, industrial substrate) combustion, may be coated with many other compounds, including polynuclear aromatic hydrocarbons [PAHs] (Lighty *et al.* 2000).

Two examples of petrochemical combustion-derived particulate mixtures that have been the subject of many research projects are diesel exhaust particles (DEPs) and residual oil fly ash (ROFA). DEPs contain various oxygen-containing organics, such as quinones, in addition to PAHs and metal ions, all of which have toxic effects in the lung (Kumagai *et al.* 2002; Li *et al.* 2000; Murphy *et al.* 1999). The toxic effects of ROFA, generated from fossil fuel combustion, have been attributed to transition metals associated with the particles (Antonini *et al.* 2002; Dreher *et al.* 1997).

1,3-butadiene (BD) is a high-volume, aliphatic hydrocarbon byproduct of petroleum refining and is used in the manufacture of synthetic rubber and other elastomers. The United States' capacity for BD production has been estimated to be ~6 x 10^9 lbs/year, with many of the producers being located in Texas and Louisiana (The Innovation Group 2002). Even though most industrial processes are very efficient, fugitive volatiles, *i.e.* those which escape the processing stream or remain unused, are combusted, as strict governmental regulations are in

place limiting the amounts of highly reactive volatile organic compounds, such as BD, that can be released to the atmosphere (United States Environmental Protection Agency 1994). The combustion process, known as flaring, is also a highly-efficient process, where > 98% of the original substrate is completely combusted to carbon dioxide and water. The remaining fractions are referred to as products of incomplete combustion (PICs) or 'soots'. Similar to DEPs and ROFA, these PICs often consist of a mixture of carbonaceous particles to which various other organic species, including PAHs, are adsorbed.

In previous work with our collaborators, we began to characterize the generation of PAHs from combustion of BD (Catallo 1998) and to describe the biological effects of butadiene soot (BDS) *in vitro* (Catallo et al. 2001). The work described herein is a continuation of these initial studies. Our hypotheses were:

1) BDS is composed of particles of a respirable size, thus capable of contributing to ambient air pollution and producing health effects via respiratory system exposure;
2) BDS particles are coated with PAHs that have toxic effects in the respiratory system, including effects promoted by aryl hydrocarbon receptor activation;
3) BDS particles and/or their adsorbed PAH constituents induce an inflammatory response, demonstrable by molecular analysis of cytokine expression or inflammatory cell infiltrates *in vivo*;
4) BDS particles directly interact with cells of the respiratory system, including epithelial cells and alveolar macrophages, causing them to alter gene expression *in vitro* and/or *in vivo*, with or without particle uptake.

In Chapter 1, we characterize BDS with respect to particle size distribution and assembly, PAH composition, and elemental content of BDS ultrafine particles. We also describe *in vitro* assays that

demonstrate that BDS ultrafine particles can transport and transfer adsorbed organic constituents directly to target respiratory cells, without uptake of the particles by the cells.

The experiments described in Chapter 2 demonstrate that combustion-derived PAHs adsorbed onto BDS particles are concentrated in lipid droplets of respiratory system cells and that, *in vitro*, these PAHs concomitantly activate xenobiotic metabolism pathways known to potentiate the toxicity of certain PAHs, including several found in BDS.

In Chapter 3, we present an *in vivo* analysis of bronchoalveolar lavage fluid (BALF) with inflammatory cell infiltrates, histopathological evidence of suppurative inflammation and particle retention, and gene expression analysis revealing upregulation of several cytokines and AhR-responsive biotransformation enzymes. The results demonstrate that brief exposure to BDS causes acute airway inflammation and augments expression of AhR-responsive genes *in vivo*.

In Chapter 4, we present ultrastructural evidence that BDS particles can be internalized by bronchoepithelial cells *in vitro* and phagocytosed by alveolar macrophages *in vivo*.

The studies described above were designed to investigate the aforementioned hypotheses and demonstrate that BDS is both a model mixture and a real-life example of a petrochemical PIC with the potential both for environmental contamination and for contributing to health problems.

REFERENCES

Antonini, J. M., Roberts, J. R., Jernigan, M. R., Yang, H. M., Ma, J. Y., and Clarke, R. W. (2002). Residual oil fly ash increases the susceptibility to infection and severely damages the lungs after pulmonary challenge with a bacterial pathogen. *Toxicol. Sci.* **70**(1), 110-119.

Catallo, W. J. (1998). Polycyclic aromatic hydrocarbons in combustion residues from 1,3-butadiene. *Chemosphere* **37**(1), 143-157.

Catallo, W. J., Kennedy, C. H., Henk, W., Barker, S. A., Grace, S. C., and Penn, A. (2001). Combustion products of 1,3-butadiene are cytotoxic and genotoxic to human bronchial epithelial cells. *Environ. Health Perspect.* **109**(9), 965-971.

Dominici, F., Peng, R. D., Bell, M. L., Pham, L., McDermott, A., Zeger, S. L., and Samet, J. M. (2006). Fine particulate air pollution and hospital admission for cardiovascular and respiratory diseases. *JAMA* **295**(10), 1127-1134.

Dreher, K. L., Jaskot, R. H., Lehmann, J. R., Richards, J. H., McGee, J. K., Ghio, A. J., and Costa, D. L. (1997). Soluble transition metals mediate residual oil fly ash induced acute lung injury. *J. Toxicol. Environ. Health* **50**(3), 285-305.

Kumagai, Y., Koide, S., Taguchi, K., Endo, A., Nakai, Y., Yoshikawa, T., and Shimojo, N. (2002). Oxidation of proximal protein sulfhydryls by phenanthraquinone, a component of diesel exhaust particles. *Chem. Res. Toxicol.* **15**(4), 483-489.

Li, N., Venkatesan, M. I., Miguel, A., Kaplan, R., Gujuluva, C., Alam, J., and Nel, A. (2000). Induction of heme oxygenase-1 expression in macrophages by diesel exhaust particle chemicals and quinones via the antioxidant-responsive element. *J. Immunol.* **165**(6), 3393-3401.

Lighty, J. S., Veranth, J. M., and Sarofim, A. F. (2000). Combustion aerosols: factors governing their size and composition and implications to human health. *J. Air Waste Manag. Assoc.* **50**(9), 1565-1618.

Murphy, S. A., Berube, K. A., and Richards, R. J. (1999). Bioreactivity of carbon black and diesel exhaust particles to primary Clara and type II epithelial cell cultures. *Occup. Environ. Med.* **56**(12), 813-819.

Pope, C. A., III, Burnett, R. T., Thun, M. J., Calle, E. E., Krewski, D., Ito, K., and Thurston, G. D. (2002). Lung cancer, cardiopulmonary mortality, and long-term exposure to fine particulate air pollution. *JAMA* **287**(9), 1132-1141.

Seaton, A., MacNee, W., Donaldson, K., and Godden, D. (1995). Particulate air pollution and acute health effects. *Lancet* **345**(8943), 176-178.

The Innovation Group. Butadiene. Chemical Market Reporter . 3-25-2002. Schnell Publishing Company.
Ref Type: Magazine Article

United States Environmental Protection Agency. Regulatory Impact Analysis for the National Emissions Standards for Hazardous Air Pollutants for Source Categories: Organic Hazardous Air Pollutants from the Synthetic Organic Chemical Manufacturing Industry and Other Processes Subject to the Negotiated Regulation for Equipment Leaks. EPA-453/R-94-019. 1994.
Ref Type: Report

CHAPTER 1

COMBUSTION-DERIVED ULTRAFINE PARTICLES TRANSPORT ORGANIC TOXICANTS TO TARGET RESPIRATORY CELLS*

INTRODUCTION

Increased morbidity and mortality have been associated with exposure to inhaled airborne particulate matter [PM] (Dockery *et al.* 1993; Samet *et al.* 2000; Schwartz *et al.* 1996). In 1997, the U. S. Environmental Protection Agency (EPA) issued revised National Ambient Air Quality Standards (United States Environmental Protection Agency 1997) for airborne PM, which supplemented the 1991 standards by focusing on PM with aerodynamic diameters ≤ 2.5 μm ($PM_{2.5}$). Small increases in levels of ambient $PM_{2.5}$ result in increases (> 1%) in cardiovascular and respiratory mortality (Pope, III *et al.* 2002). Recently, the focus has begun to shift to health effects arising from inhalation of ultrafine particles (diameter < 0.1 μm) that comprise a small fraction of the total mass, but most of the total number, of airborne PM (Peters *et al.* 1997). For equivalent masses of inhaled particles, ultrafine particles provide a greater surface area for adsorption of potentially toxic agents than do the larger sized particles.

Inhaled ultrafine particles can be deposited in the lung and can migrate from there into the systemic circulation and thus to the heart, as well as to more distal organs. Within 5 min of intratracheal instillation, 25-30% of ^{99m}technetium-labeled albumin ultrafine particles (nominal diameter ≤ 80 nm) were detected in the blood (Nemmar *et al.* 2001).

Ambient fine and ultrafine particles arise from multiple sources, both combustion-related (e.g., diesel, petrochemical), and non-combustion-related (e.g., crustal, agricultural). The fine soot particles arising from incomplete combustion of coal and petroleum have been associated

* This chapter was printed in the August issue of *Environmental Health Perspectives* (Penn *et al.* 2005).

with increased mortality (Laden *et al.* 2000). In urban settings, diesel exhaust is a prominent source of fine particles. Organic solvent extracts of diesel exhaust particles (DEPs) induce oxidative stress in respiratory epithelial cells and macrophages (Li *et al.* 2002). Particle-rich diesel exhaust contains relatively high levels of polynuclear aromatic hydrocarbons (PAHs), including the well-characterized carcinogen, benzo(*a*)pyrene (BaP). Other contributors to the burden of airborne particulates include PM arising from flaring of volatile hydrocarbons at refineries and/or incomplete combustion of unused or fugitive hydrocarbons at petrochemical plants. These additional sources of inhalable, PAH-rich particles are of special concern where refineries and/or petrochemical processing plants are concentrated.

1,3-butadiene (BD) is a volatile, "top 40" U.S. production chemical [> 3 x 10^9 lbs produced annually; Occupational Safety and Health Administration (OSHA) 2004]. Industrial petrochemicals, including BD, that escape the production stream or that remain unreacted are burned. The butadiene soot (BDS) produced during incomplete combustion of BD is a complex, PAH-rich mixture of particulates**.** A broad size range of PAHs [up to ~1000 atomic mass units (amu)], including BaP and other carcinogens, is present in BDS. After incubation with BDS extracts in dimethylsulfoxide (DMSO), normal human bronchial epithelial cells, which are putative target cells for inhaled irritants, exhibited plasma membrane blebbing, small but statistically significant increases in the number of binucleate cells, and a diffuse cytoplasmic fluorescence, when viewed under the light microscope (Catallo *et al.* 2001).

There is a growing literature on the pathologic responses of cells of the respiratory and cardiovascular systems after exposure to ultrafine particles (Bermudez *et al.* 2004; Chalupa *et al.* 2004; Dick *et al.* 2003; Nemmar *et al.* 2004). Less attention however, has been paid to how the detailed physical and chemical characteristics of combustion-derived ultrafine particles influence

interactions of these particles and their constituents with target cells. Here, we characterize BDS with respect to particle size distribution and assembly, PAH composition, and elemental content of BDS ultrafine particles. We also describe *in vitro* assays that demonstrate that BDS ultrafine particles can transport and transfer adsorbed organic constituents directly to target respiratory cells, without uptake of the particles by the cells.

METHODS

Generation of BDS. We brought a tank of BD (Aldrich, St. Louis, MO) that had been stored at -20°C to room temperature. The BD (≥ 99% purity) contained approximately 175 ppm *t*-butylcatechol as an inhibitor. The BD gas was passed through a back-flash-protected stainless steel two-stage regulator to a stainless steel Bunsen burner (aperture, 0.85 mm inner diameter; feed pipe, 10 cm). The flame was adjusted until a plume of black smoke rose from the top of the burner. Combustion was carried out in a fume hood with active ventilation. The BD feed rates were 5-7 mL/s under normal atmosphere, with flame heights of approximately 1 cm. We captured the particles passing through the feed pipe on cellulose filters held within a Buchner funnel positioned approximately 15 cm above the pipe outlet and attached to a vacuum pump. The BDS was scraped gently off the filters and stored in aluminum-foil-wrapped glass vials capped with foil-lined lids.

We qualitatively determined the success of each BDS-generating reaction by assessing PAH-associated fluorescence of the product. We extracted 1 mg BDS with 2 mL dichloromethane (DCM; Optima; Fisher, Fairlawn, NJ) for 1 min. Fluorescence of the extract was detected under ultraviolet (UV) light (320 nm excitation).

Particle Size Analysis. The sampling train was set up for size fractionation of BDS particles as follows: burner, RespiCon virtual sampler (TSI; St. Paul, MN), in-line HEPA filter, digital flow

meter, Magnahelic (Dwyer, Michigan City, IN), and house vacuum. Size fractionation was carried out with a RespiCon virtual sampler that was set approximately 15 cm above the top of the burner. The first stage of the RespiCon collected particles < 2.5 μm; the second and third stages collected particles 2.5–10 μm and > 10 μm, respectively. Preweighed filters from each impactor stage were weighed, photographed, and submitted for extraction and gas chromatography/mass spectrometry (GC/MS) analyses for PAHs.

Elemental Analyses. All elemental analyses were carried out by Quantitative Technologies Inc. (Whitehouse, NJ). Carbon, hydrogen, and nitrogen content were determined with a Perkin-Elmer CHN elemental analyzer (model 2400; PerkinElmer, Wellesley, MA). Samples in the analyzer were combusted in a pure oxygen environment. Product gases were separated under steady-state conditions and measured as a function of thermal conductivity. Sulfur was converted to sulfate and then titrated versus standards, with an indicator. Oxygen in BDS was determined with the elemental analyzer fitted with an oxygen accessory kit. The oxygen in the organic starting material was converted by pyrolysis to carbon monoxide, which was separated from other pyrolysates under steady-state conditions and measured as a function of thermal conductivity.

Freshly prepared BDS samples were analyzed by inductively coupled plasma (ICP) spectrometry for the presence of 64 additional elements. Samples were digested with nitric acid in a CEM 2100 microwave oven (CEM, Matthews, NC) and then diluted to volume with 18 Mohm-cm water. Reagent blanks were prepared similarly. Samples were analyzed with a Perkin-Elmer Optima 3000XL ICP spectrometer (PerkinElmer) that had been calibrated with traceable standards from the National Institute of Standards and Technology (NIST) (Gaithersburg, MD). The resulting calibration was confirmed by analysis of an independently prepared calibration check standard. A method blank was analyzed, and its value was subtracted from all sample

analyses. Iron concentrations were determined in pristine reaction vessels in which the level of iron, if any, was below the limit of detection. Of the 64 elements screened, 52, including chromium, nickel, and vanadium, were present at levels < 1 ppm.

Percentage of Adsorbed Organic Components. Three 50-mg samples of BDS, in mini-Buchner funnels fitted with preweighed Whatman #1 filters, were each extracted via vacuum filtration with five successive 10-mL aliquots of DCM. The filters were reweighed after drying in air.

GC/MS Analysis of PAH Components of BDS Particles. The BDS generated by controlled combustion of BD was collected on glass-fiber filters and analyzed for PAHs by GC/MS. An unused filter (negative control) and a solvent-only method blank also were analyzed. The BDS (1 mg) was placed into a 10-mL Pyrex conical tube fitted with a Teflon-lined screw cap. The DCM (2.0 mL, ultra-high-purity grade; Aldrich), was added to each tube after being "spiked" with deuterated NIST reference standards for several PAHs previously identified in BDS (Catallo *et al.* 2001): naphthalene-d_8 (5 μg/mL), anthracene-d_{10} (1 μg/mL), chrysene-d_{12} (1 μg/mL), BaP-d_{12} (5 μg/mL), and perylene-d_{12} (2 μg/mL). The tubes were capped and heated (40°C for 4 hr) in a sand bath. A 200-μL aliquot of each sample extract was filtered through a 0.45-μm nylon filter (Nalgene, Rochester, NY) that had been fitted onto a 1-mL syringe barrel. The filtered samples were placed in conical glass sample vial inserts and submitted for GC/MS analysis. Three sets of BDS $PM_{2.5}$ were analyzed by GC/MS after extraction with DCM. There was insufficient material for analysis in the PM_{10} and larger fractions.

The GC/MS analyses were conducted with an Agilent 5973 mass selective detector/6890 GC/data system (Agilent, Palo Alto, CA) in full scan (40–600 amu), positive ion, electron impact mode. Splitless injections of 1 mL were made onto a 28 m × 0.25 mm, 0.25-μm film thickness,

DB5 fused silica glass capillary column (Agilent), with the purge function initiated at 0.75 min postinjection. The injector temperature was 250°C. The initial column temperature (50°C) was held for 5 min, ramped at 10°C/min to 300°C, and held there for 10 min. The transfer zone of the instrument was held at 320°C, and the source temperature was 200°C. Full-scan spectra were compared with reference library spectra and retention indices (relative to deuterated internal standards) to determine peak identity. The most abundant PAH peak areas were integrated and compared by ratio with the corresponding peak area for the anthracene-d_{10} internal standard. Four compounds (anthracene, chrysene, benzopyrenes, and perylene) were identified directly by comparison with each of their respective deuterated standards.

Scanning Electron Microscopy of Freshly Prepared BDS. The BDS was collected from a plume by passing ethanol-cleaned, 12-mm, circular glass coverslips through the plume. The coverslips were affixed to aluminum stubs with conductive adhesive, sputter-coated with approximately 20 nm gold/palladium and examined by scanning electron microscopy (SEM; FEI Quanta 200 ESEM; FEI, Hillsboro, OR) at 20 kV. Digital images of 1,024 × 884 pixels were recorded.

Transmission Electron Microscopy of Freshly Prepared BDS. Samples of BDS were collected directly from the plume onto 300-mesh, parlodion-coated copper grids that were examined by transmission electron microscopy (TEM; Zeiss EM-10C; Zeiss, Thornwood, NY). To simulate the processing of BEAS-2B cells, freshly prepared BDS was collected on filters, transferred to clean tubes, passed through an ethanol series (50–100%), and infiltrated with epoxy resin. The polymerized resin was sectioned and then examined as described above.

Cell Culture. BEAS-2B cells are a non-tumorigenic line derived from normal human bronchial epithelial cells (Ke *et al.* 1988). BEAS-2B cells (1–1.5 × 10^6) were seeded into T-25 flasks

(Corning, Corning, NY) containing bronchial-epithelial growth medium (BEGM), before expansion in T-150 flasks. BEGM is a basal medium (BioWhittaker, Rockland, ME) supplemented (per 500 mL) with 2 mL of 13 mg/mL bovine pituitary extract and 0.5 mL each 0.5 mg/mL hydrocortisone, 0.5 μg/mL human recombinant epidermal growth factor, 0.5 mg/mL epinephrine, 10 mg/mL transferrin, 5 mg/mL insulin, 0.1 μg/mL retinoic acid, 6.5 μg/mL triiodothyronine, 50 mg/mL gentamicin, and 50 μg/mL amphotericin-B. Cells were grown to 80–90% confluence (37°C, 5% CO_2/95% air), split into 60-mm dishes (~ 2.5×10^5 cells/dish), and expanded until approximately 70% confluent. Medium was changed immediately before BDS addition.

Unextracted Soot Particles. For approximation of routine in vivo exposure conditions to airborne particles, the BDS was not subjected to charge neutralization before addition to cell cultures. The BDS (3 mg) was sprinkled onto the surface of the BEGM overlying the BEAS-2B cells. Cells were incubated from 5 min to 72 hr. Unless otherwise noted, the BDS was not removed nor was the medium changed during the course of the exposures. Unexposed cells served as negative controls. Cells sprinkled with 0.5 mg crystalline BaP served as solid PAH controls. Cells to which 40 μL of a 5-mM BaP solution (in DMSO) was added to 5 mL BEGM, served as fully solubilized PAH controls. Cells with 3 mg graphite (> 98% pure; Sigma, St. Louis, MO) sprinkled directly onto the surface of the BEGM served as controls for cell responses to carbon particles lacking adsorbed organic compounds. In all cases, cell responses were determined with a fluorescence microscope (Zeiss Axiovert 405 M) equipped with a 100 W mercury lamp and a Zeiss 02 filter combination (365/420 nm) for excitation and emission.

Sonicated Soot. For determination of whether disrupting the aggregated BDS ultrafine particles enhanced the responses of BEAS-2B cells, BDS was sonicated (Branson model 450 Sonifier;

Branson Ultrasonics, Danbury, CT) in BEGM (3 mg/5 mL) before application to the cells. The output of the sonifier was at setting 5, with a constant-duty cycle and five consecutive 15-sec pulses, with swirling of the vessel between pulses. Diluted (1:10, 1:20, 1:50, 1:100) particle-BEGM suspensions were added to cells. The time course (15 min to 48 hr) of fluorescent responses of cells to sonicated BDS preparations was compared with that of cells exposed to non-sonicated BDS sprinkled on the surface of the medium.

Post-extraction Soot. For determination of whether organic extraction of soot altered the cell responses, the soot remaining on the Whatman filters (see "Percentage of adsorbed organic components," above) after extraction with DCM was collected and added to BEAS-2B cells (3 mg extracted soot/5 mL BEGM).

Soot Extracts. For determination of whether soot extracts and intact BDS elicit similar cell responses over time, the DCM filtrate was dried under N_2 at room temperature and reconstituted in 1 mL DMSO. Aliquots (60 μL) were mixed with 5 mL BEGM and added to BEAS-2B cells. Cells were examined for fluorescence responses (30 min to 48 hr).

Transwell Incubations. The BEAS-2B cells were plated into wells of a 24-well plate (~ 2×10^5 cells/well). Transwell (Corning) inserts (0.4-μm pores) were placed in each well. Medium (0.5-1.0 mL) and either BDS (0.3-0.6 mg) or soot extracts (50 μL) were added to each Transwell, and cells were viewed under a fluorescence microscope, as described above. Controls included a) wells with medium and cells but no BDS, b) wells with medium only, and c) wells with cells omitted and replaced with Octadecyl silane (ODS)-derivitized polymeric disks. At 48 hr, after aspiration of BEGM and rinsing of the wells with phosphate buffered saline (PBS), the Transwells and media were removed from the 24-well plates. ODS disks were washed with water, filter-extracted with DCM, and analyzed by GC/MS. Cells were rinsed with 0.2% trypsin

in PBS and then removed from the wells by incubation with 0.2% trypsin in PBS at 37°C for 3 min. Cells were washed with PBS, pelleted, and extracted with DCM, as described above.

TEM of BEAS-2B Cells Exposed to BDS. The BEAS-2B cells, grown on Thermanox plastic coverslips (VWR International, West Chester, PA), were exposed for 42 hr to 0.6 mg BDS that had been sprinkled onto 1 mL BEGM in Transwells. Coverslips were washed with PBS and fixed with 1.25% glutaraldehyde/2% formaldehyde in 0.1 M sodium cacodylate. The coverslips were processed and examined as described above.

RESULTS

Generation of BDS. With BD flow rates of 5-7 mL/min, 500-600 mg BDS were collected per 15 min of burn. The DCM extracts of freshly prepared BDS exhibited an intense blue fluorescence under UV light. This is consistent with solubilization by DCM of PAHs formed during the combustion process and adsorbed to the surface of the BDS particles. For undetermined reasons, occasional burns yielded particles that did not fluoresce in DCM, contained no detectable PAHs, and produced no cell fluorescence. These were not used.

Particle Size Distribution. Most particles in freshly generated BDS are of respirable size; > 90% of the collected particles are $PM_{2.5}$ (Table 1.1).

Elemental Analyses. Nearly 94% of BDS by weight is elemental carbon and approximately 2% is hydrogen, consistent with a polyaromatic composition of intact BDS. Together, nitrogen and sulfur account only for approximately 1% of the BDS components. Oxygen represents < 0.1% (Table 1.2). After extraction with DCM, the BDS takes on a more graphitic character compared with the nonextracted BDS, as indicated by the fact that the relative carbon content increases slightly and the relative hydrogen content drops below 1%.

The ICP analysis (Table 1.3) revealed that freshly generated BDS is not enriched in metals. For 52 of 64 elements, the levels were < 1 ppm. Of the remaining 12, calcium and iron,

Table 1.1. Particle size distribution of BDS.

Particle Size Fraction	% in Fraction (mean ± SD)[a]
< 2.5 μm	91.6 (4.1)
2.5-10 μm	5.6 (5.6)
> 10 μm	3.2 (1.9)

More than 90% of freshly generated BDS is of respirable size.
[a]Mean ± SD of percent total mass found in each fraction.
n = 5 replicates.

Table 1.2. Strong polyaromatic character of BDS revealed by elemental analysis.

Substrate	**C**	**H**	**N**	**S**	**O**
BDS	93.88 (0.37)	1.82 (0.07)	0.60 (0.31)	0.39 (0.02)	< 0.10
BDS (washed)	95.95 (0.10)	0.78 (0.11)	0.11 (0.02)	0.35 (0.05)	0.55
Graphite	98.01	< 0.10	< 0.10	0.45	< 0.15

The results represent mean percentages ± SEM for triplicate analyses.

25 and 26 ppm, respectively, were the most prominent. Vanadium, chromium, and nickel, if present, were below the limits of detection with the analytical procedures used.

Percentage of Adsorbed Organic Components. Extraction of BDS with DCM resulted in loss of 16.6 ± 3.3% (mean ± SD; n = 3) of the initial weight of BDS. This loss is consistent with removal of aromatic compounds that had been adsorbed to the surface of the particles before extraction. However, small losses of ultrafine particles during filtration cannot be discounted.

GC/MS Analysis of PAH Components of BDS. Three batches of independently generated BDS $PM_{2.5}$ were analyzed by GC/MS after extraction with DCM. Thirteen of the most abundant PAH components, ranging from acenaphthylene (152 amu) to benzoperylene/indenopyrene (276 amu),

are listed in Table 1.4. Four of these (anthracene, chrysene, benzopyrenes, and perylene; Table 1.4) were identified directly by comparison with results from their respective deuterated analogs.

Table 1.3. ICP spectrometry analysis of elemental composition of BDS.

Element	Concentration (ppm)
Calcium	25
Iron	26
Potassium	4
Sodium	6
Phosphorus	19
Zinc	4

All analyses were in triplicate except for iron (n = 2).

The values presented in Table 1.4 for all 13 PAHs are relative amounts, with each expressed as an intensity relative to anthracene-d_{10}. The PAHs were identified on the basis of their relative retention times (retention index) and by comparison with previously published results (Catallo 1998). The relative abundances of all 13 of these PAHs were consistent between batches. Similarly, there was very little difference in PAH composition between these three batches of BDS and the $PM_{2.5}$ sample from Table 1.1 (data not shown). There was insufficient material for GC/MS analysis in the two other fractions in Table 1.1. Many other PAHs also were detected but at lower levels than those of the 13 major components listed here. These results demonstrate that there is a characteristic chemical composition of BDS, regardless of size, that can be obtained reproducibly if consistent generation and collection schemes for BDS are followed.

Electron Microscopy of BDS and of BDS-treated BEAS-2B Cells. Under SEM, macroscopic BDS is composed of spherical, uniformly sized solid particles approximately 50–70 nm in diameter, which aggregate to form open, lacy clusters (Figure 1.1A). These results were confirmed with TEM analysis of soot collected directly on copper grids (Figure 1.1B), as well as

by analysis of epoxy-embedded BDS samples (data not shown). Under TEM, the diameter of particles was 30–50 nm. The slightly larger apparent diameter of the spherical particle by SEM

Table 1.4. The 13 most prominent PAHs (152–276 amu) present in freshly generated BDS.

PAH	*m/z*	Ratio to IS (Anth-d_{10})			Ratio to specific IS (mg/g soot)		
		#1	#2	#3	#1	#2	#3
Acenapthylene	152	4.6	5.6	1.6			
Fluorene	166	1.4	2.5	0.8			
Anthracene	178	7.2	10.2	6.0	14.4	20.4	12.0
Cyclopentaphenanthrene	190	1.7	2.2	1.7			
Fluoranthene	202	6.2	6.4	6.7			
Acephenanthrylene	202	4.0	4.4	4.3			
Pyrene	202	8.0	9.6	8.7			
Benzofluorenes	216	1.0	2.0	1.0			
Acepyrene	226	7.6	7.2	9.8			
Chrysene	228	1.3	1.4	1.2	1.4	1.5	1.2
Benzopyrenes	252	2.0	2.2	2.5	1.7	2.0	1.7
Perylene	252	1.5	1.7	1.6	0.2	0.5	0.4
Benzoperylene/Indenopyrene	276	1.2	0.4	1.5			

IS, internal standards. The most abundant PAH peak areas were integrated and compared by ratio with the corresponding peak area for the anthracene-d_{10} internal standard. Anthracene, chrysene, benzopyrenes, and perylene were identified directly by comparison with each of their respective deuterated standards.

versus TEM results from the 10–20-nm gold/palladium coating that had been applied to the particles during preparation for SEM. Neither light microscope nor TEM analysis of BDS-treated cells yielded any evidence that the ultrafine particles were taken up by the cells during the same time period in which other cells from the same population displayed punctate fluorescence. There is, however, clear evidence from TEM that BDS ultrafine particles reach the cell surface. In Figure 1.1C, individual BDS particles that settled at the bottom of the culture dish are shown in immediate proximity to a BEAS-2B cell.

***In Vitro* Bioassay of BDS Activity.** Three milligrams of BDS, without carrier or solubilizing agent, sprinkled on the surface of BEGM overlying semiconfluent BEAS-2B cells, elicited a time-dependent set of fluorescence responses. Within 60-120 min, a uniform, diffuse blue fluorescence not localized in any organelles was detected in most cells. By 4 hr, the diffuse fluorescence was replaced by punctate fluorescence, that is, fluorescence localized in discrete, circular (1-2 μm) cytoplasmic vesicles (Figure 1.2). No nuclear fluorescence was detected. Fluorescence intensity in the cytoplasmic vesicles increased during the first 24 hr, then plateaued and remained constant for as long as 72 hr. Cells exposed to graphite did not fluoresce, nor did cells exposed to BDS from which adsorbed PAHs has been extracted with DCM. Extracts (DCM) of BDS -- filtered through 0.45-μm filters, dried, resuspended in DMSO, and diluted in BEGM -- produced rapid fluorescence responses, including the appearance of punctate fluorescent in cytoplasmic vesicles within 30 min (data not shown). The time course of fluorescence responses of the cells combined with the evidence that the BDS particles are not taken up by the cells is consistent with PAHs being transferred to the plasma membrane from the surfaces of the ultrafine particles.

Intact BDS particles cannot be easily suspended in aqueous medium. Sonication was required to disperse the soot floating on the surface of the clear BEGM into the liquid to form an opaque black suspension. Less vigorous dispersion techniques were ineffective. Fluorescent cytoplasmic vesicles appeared more rapidly in cells exposed to sonicated BDS diluted with BEGM than in cells exposed to nonsonicated BDS (Table 1.5). The time required for 50% of the cells to display punctate fluorescence was 60, 90, and 150 minutes, respectively, for the 1:10 and 1:20 dilutions of sonicated samples and for the nonsonicated BDS samples. For the 1:50 and 1:100 dilution samples, the percentage of cells with punctate fluorescence never reached 50%,

even after 24 hr. These results are consistent with increased numbers of ultrafine particles containing adsorbed PAHs being made available to the cells as a result of sonication.

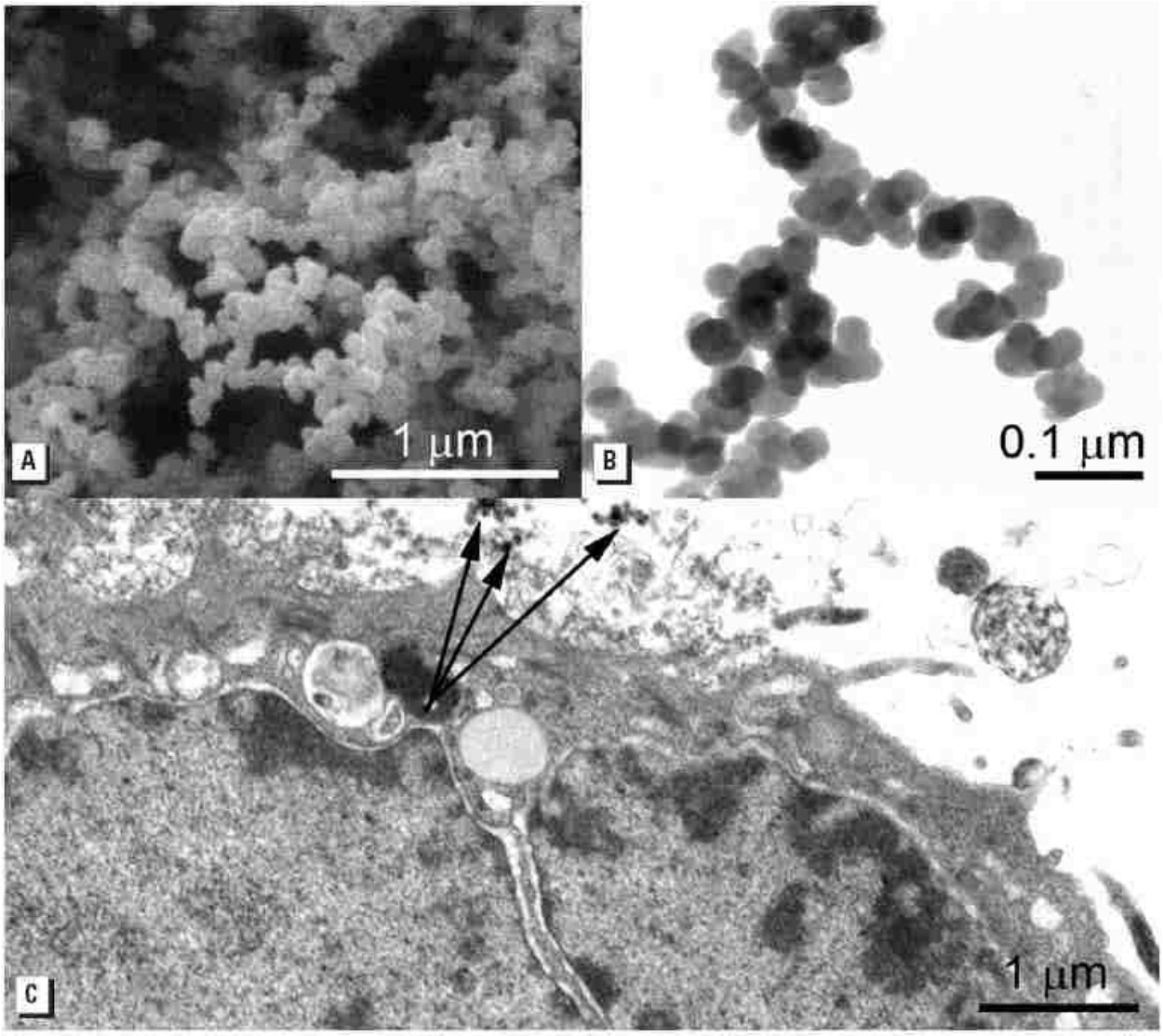

Figure 1.1. (A) An SEM image illustrating the lacy openwork character typical of the BDS aggregates; individual, solid, spherical particles, 50-70 nm in diameter, are the fundamental structural units of the aggregates. (B) A TEM image of BDS showing individual spheres, 30-50 nm in diameter, arranged in branching clusters. The difference in diameter of the spheres in the SEM versus TEM images results from the 10-20 nm gold/palladium conductive coating that was applied to the SEM samples. (C) A TEM image of a portion of the surface of a BEAS-2B cell with individual spherical particles, 30-50 nm in diameter, and small aggregates (arrows) immediately adjacent to the cell membrane. Cells were photographed after 42 hr exposure.

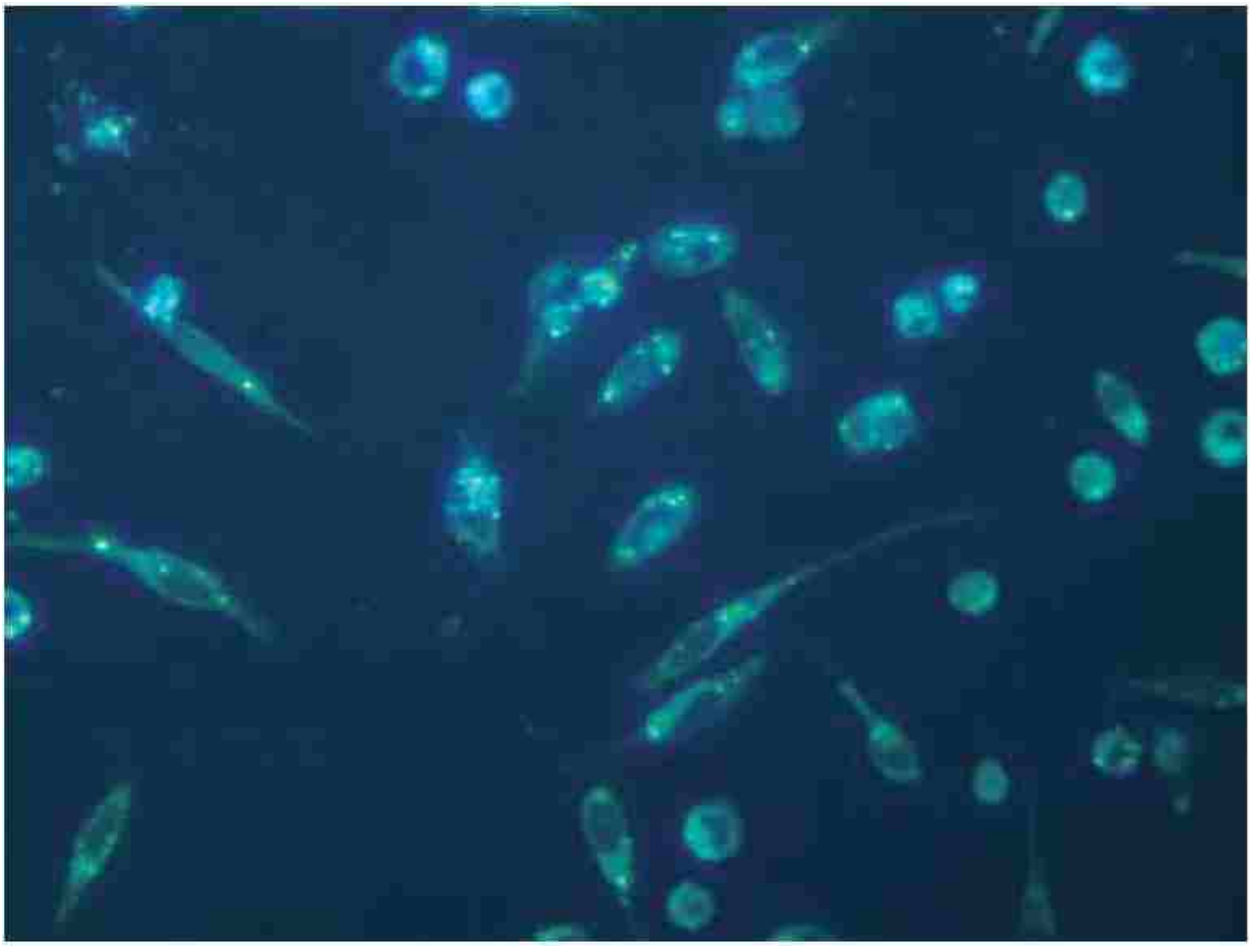

Figure 1.2. Fluorescence localized in punctate cytoplasmic vesicles of BEAS-2B cells. Cells were photographed 4 hr after BDS, without carrier, was sprinkled onto the surface of the BEGM overlying the cells. Excitation/emission wavelengths = 360/420 nm. Magnification, 400X.

Table 1.5. Time lag between the addition of diluted, sonicated BDS suspended in BEGM, and development of punctate fluorescence in BEAS-2B cells.

Dilution of Sonicated BDS	Time to PF_{50}
1:10	60 minutes
1:20	90 minutes
1:50	> 48 hours
1:100	> 48 hours

PF_{50}, punctate fluorescence in 50% of exposed BEAS-2B cells. The corresponding time lag for unsonicated BDS sprinkled onto the surface of BEGM was 150 min.

Additional evidence that the fluorescence responses result from direct interaction of PAH-containing ultrafine particles with cells was obtained by plating BEAS-2B cells in 24-well dishes. Transwell inserts (0.4-μm pore) containing 0.3 mg nonsonicated BDS sprinkled onto 1 mL BEGM were placed in each well. Wells were examined at 4, 8, 24, and 48 hr. Fluorescent vesicles were visible at 4 hr in cells to which BDS had been added directly (no inserts) and at 18-48 hr in cells from the BDS/Transwell group. These results indicate that the fluorescence responses of cells in this case are dependent on accessibility of cells to particles of BDS that are < 0.4 μm in size. Crystals of BaP, which are more dense than the lacy, open aggregates of BDS, elicited punctate blue-violet fluorescence from cells within 4 hr, but only in cells immediately adjacent to BaP crystals that had dropped to the bottom of the dish. When the nonspherical BaP crystals, all larger than 0.4 μm, were floated on BEGM in Transwells, the cells did not fluoresce even after 48 hr (data not shown). In contrast, when crystalline BaP was dissolved first in DMSO and then mixed with BEGM (final BaP concentration = 40 μM) before addition to cells, all cells displayed punctate blue fluorescence within 2 hr.

Confirmation that the material adsorbed to the surface of the BDS ultrafine particles is inherently responsible for the cell fluorescence was obtained by solubilizing dried DCM extracts of BDS in DMSO, diluting them with BEGM, and adding them to Transwells. These extracts elicited diffuse fluorescence within 30–45 min and punctate fluorescence within 2 hr. When the same extracts were mixed with BEGM and added directly to wells lacking Transwells, punctate fluorescence was visible in cells by 30 min and in most cells by 3 hr. These results confirm that the fluorescence is due to uptake by the cells of PAHs desorbed from the surfaces of the ultrafine particles.

At 48 hr, the ODS disks and the cells from both the BDS/Transwell exposure and BDS/no Transwell exposure wells were rinsed, extracted with DCM, and analyzed with GC/MS. The major PAH peaks at 202 *m/z*, previously identified in extracts of BDS (Table 1.4), also are present in the extracts from the wells with BEAS-2B cells and the wells with the ODS disks (Figure 1.3). These peaks, however, are absent from wells to which BDS alone (without cells or the ODS disks) was added. These results, combined with *a*) the absence of evidence for direct uptake of BDS ultrafine particles by the cells, *b*) the time lines for the development of fluorescence, and *c*) the very low levels of metals or other polar constituents in BDS, strongly suggest that nonpolar organic constituents adsorbed to the surface of combustion-derived ultrafine particles are transferred to the plasma membrane and subsequently to the cell interior.

DISCUSSION

An extensive literature details a range of toxic responses, both *in vivo* and *in vitro*, after exposures to PAHs. In this article, we characterize physical and chemical properties of BDS, a complex airborne mixture of particles featuring adsorbed PAHs, produced as a result of incomplete combustion of BD, a major industrial petrochemical. Consideration of these properties is vital to understanding the processes whereby BDS and other ultrafine particulate combustion mixtures deliver and transfer potentially toxic components to target cells. We also describe a simple bioassay to test the effects of BDS and other combustion-derived, PAH-rich particle mixtures on putative target cells. Our results demonstrate that the overwhelming majority of freshly generated BDS particles are of respirable size, have a predictable chemical composition, and act to transport adsorbed, bioactive chemicals (primarily PAHs) to target cells. These results indicate that uptake of airborne ultrafine particles by target cells is not necessary

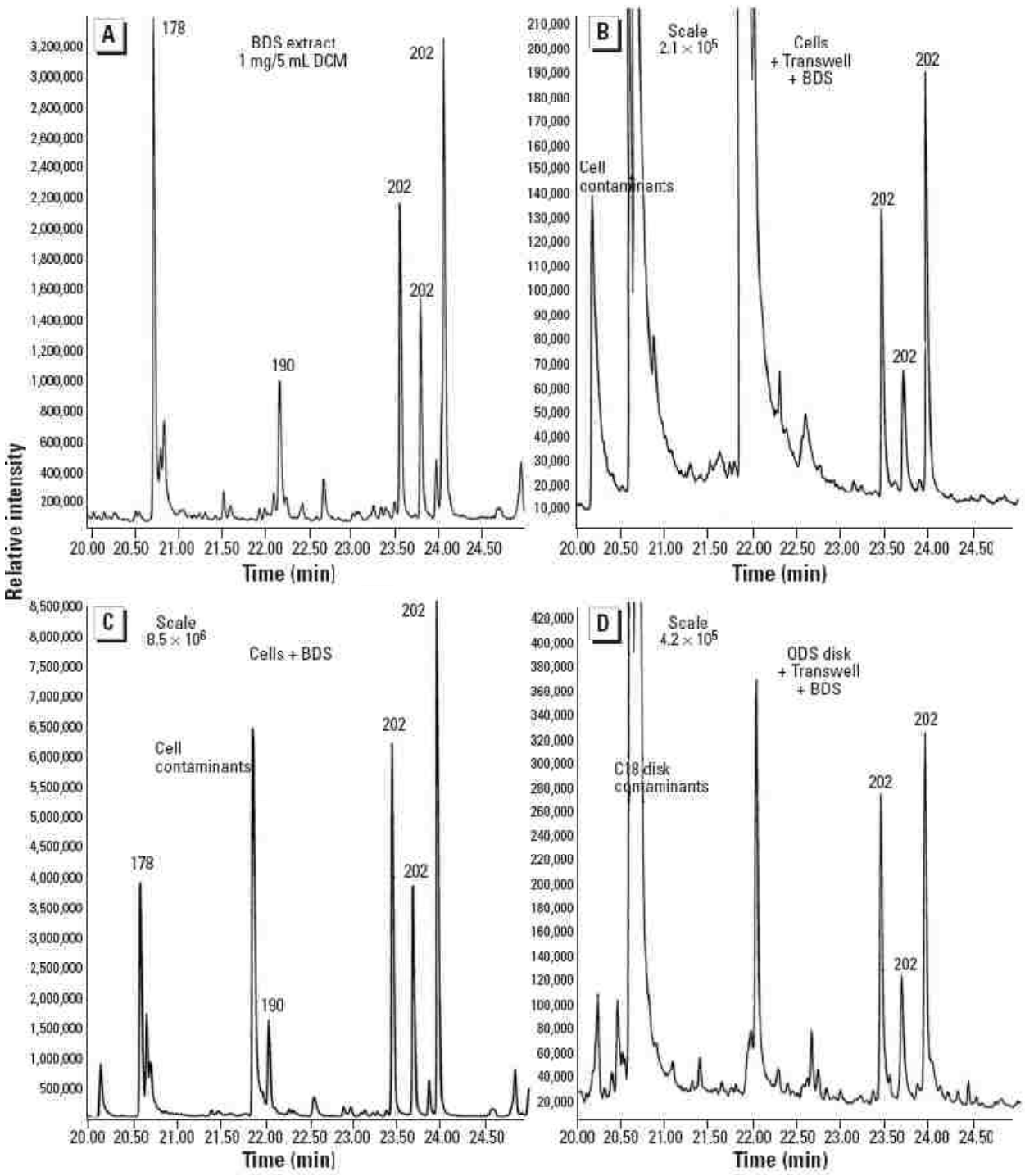

Figure 1.3. GC/MS ion chromatograms of (A) BDS extract (total ion), (B) cells exposed to BDS sprinkled on medium surface [selected ion monitoring (SIM)], (C) BDS added to a Transwell placed over cells (SIM), and (D) BDS added to a Transwell placed over an ODS disk (SIM). The same 202 m/z cluster was observed in all cases. Interference with monitoring of other PAH masses was due to cell or method contaminants, as noted. The GC/MS analyses were conducted as described in "Materials and Methods," except that monitoring was in the selective ion mode.

for the particles to exert their toxic effects on the cells. These findings are especially timely in light of the current focus on toxicologic responses to inhaled airborne particulates.

The approach we used to generate BDS is similar to that described previously for soot generation during combustion of various hydrocarbons, including BD (Cole *et al.* 1984a; 1984b). Those authors focused on some of the less complex hydrocarbon combustion products (benzene, phenylacetylene) and also demonstrated that the key step in the process was most likely a free radical addition reaction of 1,3-butadienyl radical and acetylene. This type of reaction, which occurs in the high-temperature environment of a flame, is favored over a Diels-Alder reaction, which predominates at much lower temperatures. Our results and those of Catallo (1998) provide a more detailed and extensive description of the wide range of unsubstituted PAHs (Table 1.4) that are generated during combustion of C_4 hydrocarbons than was previously presented.

The elemental analyses emphasize the strong polyaromatic nature of BDS and the relative absence of ring substitution (Table 1.2). The very low levels of nitrogen, sulfur, and oxygen (Table 1.2) indicate that amines, nitro compounds, oxides of sulfur, quinones, hydroquinones, or semiquinones are not likely to be the BDS constituents that are primarily responsible for its biologic activity. None of these constituents was noted in multiple GC/MS analyses of BDS (data not shown). We have not yet investigated metabolism of BDS components by respiratory epithelial cells and so cannot address the question of whether oxidative products of that metabolism are involved in the cells' responses to BDS exposure.

Figure 1.1A and 1.1B show that the dimensions of the solid spheres comprising the BDS particles are 30–50 nm in diameter. These dimensions agree with those for elementary soot particles from a variety of sources, including DEPs (Berube *et al.* 1999; Ishiguro *et al.* 1997; Murphy *et al.* 1999); aircraft fuel (Popovitcheva *et al.* 2000), cigarette smoke (Kendall *et al.*

2002), and carbon black (Lahaye and Ehrburgerdolle 1994). The small size of the solid spheres corresponds to very high surface area per gram, maximizing the amount of PAH adsorbed per gram of soot. The small size also means that these particles have greater potential bioavailability.

As a source of potentially toxic particles of respirable size, BDS (and likely other petrochemical soots, as well) rivals or exceeds a number of well-characterized mixtures of airborne particles, including tobacco smoke, diesel exhaust, urban reference dusts, and residual oil fly ash (ROFA). The comparisons to DEPs and ROFA are particularly informative in light of reported toxicologic responses to those particle mixtures. In some urban areas, DEPs, widely regarded as major agents of oxidative damage to cells of the respiratory system (Boland *et al.* 1999; Bonvallot *et al.* 2001; Kawasaki *et al.* 2001; Li *et al.* 2002), comprise 10–30% of the $PM_{2.5}$ and up to 50% of total ambient PM (United States Environmental Protection Agency 2002). In a recent report that focused on mitochondrial dysfunction elicited by DEPs and ultrafine particles, Xia *et al.* (2004) concluded that the effects were "mediated by adsorbed chemicals" including polar (quinones) and (aromatic hydrocarbon) constituents, "rather than by the particles themselves." For the PAHs that we have quantified in BDS (Table 1.4), the concentrations (milligrams per gram of BDS) are greater than or equal to values reported for the same components in DEP extracts (Tong *et al.* 1984). The respirable toxic particles in ROFA, a fuel oil combustion by-product from nonmobile sources, are relatively poor in organic components but rich in metals (Costa and Dreher 1997). Injury to airway cells and alterations in cytokine gene expression in response to ROFA exposure have been reported (Dreher *et al.* 1997; Dye *et al.* 1999; Samet *et al.* 2002). The elemental composition of BDS contrasts strikingly with that of ROFA. The iron level in BDS (Table 1.3) is three orders of magnitude lower than for ROFA (Costa and Dreher 1997). Further, vanadium and nickel levels in BDS are below the

limits of detection (Table 1.3), whereas many of the effects of ROFA on respiratory cells have been attributed to its high vanadium content (Dye *et al.* 1999).

Appearance of fluorescent intracytoplasmic bodies (Figure 1.2) is a well-known response of cells and tissues to exposure to individual PAHs. Tissue fluorescence after injection of colloidal suspensions of BaP and intracellular fluorescence localization of hydrocarbons, including BaP (Richter and Saini 1960), have long been recognized. In a later study, BaP solubilized in serum was taken up by HeLa and monkey kidney cells in culture (Allison and Mallucci 1964). At 24 hr, the cells exhibited a cytoplasmic granule fluorescence that the authors attributed to sequestration of BaP in lysosomes. Subsequently, internalization of high concentrations of BaP and its appearance as crystals in lysosomes of human foreskin fibroblasts 6-18 hr postexposure was described (Kocan *et al.* 1983). Other investigators, although confirming BaP uptake by cells, concluded that low to moderate levels of BaP were localized within lipid vesicles, not lysosomes (Plant *et al.* 1985). Intracellular lipid vesicles are likely repositories for hydrophobic PAHs. Preliminary results from our laboratory indicate that the punctate blue fluorescence is localized within vesicles that are stained with lipid dyes (Murphy G, Henk W, Barker S, Penn A, unpublished data).

The temporal development of the cells' fluorescence responses to ultrafine BDS particles and to crystalline BaP that has sunk to the bottom of the culture dish is consistent with direct transfer of adsorbed PAHs from the particle surface to the cells rather than by diffusion of dissolved PAHs to the cells. The solubility limit of PAHs in aqueous media is exceedingly small; a representative value is 2.3-3.0 ng/mL for BaP (Lakowicz *et al.* 1980). This solubility limit is met in all of our preparations. The amount of soot used in our study ranged from 0.006 to 0.6 mg/mL BEGM. This corresponds to a range of 1×10^3 to 1×10^5 ng PAH/mL BEGM, an

amount that exceeds the solubility of PAHs by several orders of magnitude. Thus, it can be assumed that the BEGM would be saturated with PAHs in all cases and that the fluorescence responses would not vary with the amount of soot added to the system. However, in our studies, the observed responses clearly correlate with the amount of soot added; the time required for punctate fluorescence to develop in the cells was shortened as the amount of soot particles per milliliter of suspension was increased (Table 1.5). Similarly, this time for development of punctate fluorescence was shortened in the case of BaP crystals that had been solubilized in DMSO before being mixed with the BEGM that was applied to the cells.

In the routine situation where BDS was sprinkled onto the surface of the medium, and not sonicated to form a suspension, most of the cells display punctate fluorescence after approximately 4 hr. This is consistent with transport of PAHs by the ultrafine particles directly to the surface of the cells (Figure 1.1C). As noted above, a soot sample collected by impaction is composed of solid, spherical particles (30–50 nm) arranged into lacy, open-work aggregates [Figure 1.1A,B] (Berube *et al.* 1999). Although the density of these individual solid spheres is high, and the entire weight of the aggregates above the liquid line is supported by the spherical particles in direct contact with the liquid surface, the high surface tension of the liquid (and the hydrophobic particle surface) prevents individual spheres from piercing the liquid surface immediately (Cherry 1981). With time, the wettability of the spherical particles directly contacting the liquid surface is increased by the normal adsorption of moisture from the adjacent liquid surface, and the balance is changed so that individual spherical particles on the bottom of the aggregates can pierce the liquid surface, detach, and sink because of their greater density.

The absence of light or electron microscopy evidence for direct cellular uptake of the BDS ultrafine particles or for involvement of endosomes in the process (Murphy G, Henk W,

Barker S, Penn A, unpublished data) raises the question of how the BDS-associated PAHs traverse the plasma membrane and gain entry to the cells (Figure 1.3). Data from lipoprotein studies suggest that the PAH uptake can be accomplished by direct transfer of the PAHs from the BDS ultrafine particles to the plasma membrane, without the ultrafine particles themselves entering the membrane. Uptake of BaP from hydrophobic carriers by human fibroblasts and mouse macrophages occurred in the absence of endocytosis (Plant *et al.* 1985). In all cases, cellular uptake of BaP could be accounted for by a partitioning mechanism. Subsequently, Plant *et al.* (1987) described a three-compartment system to explain rapid membrane uptake of BaP from lipoproteins and phospholipid vesicles and for the much slower release of BaP from the cell membrane to intracellular sites. These proposed events are consistent with our findings of a lag between the appearance of a relatively rapid, diffuse fluorescence of BEAS-2B cells and the appearance of subsequent punctate cytoplasmic fluorescence.

Further support for cellular uptake of hydrophobic molecules but not of their carriers comes from studies on internalization of cholesterol esters by steroid-producing cells. The pathway for this uptake is termed "selective" and is distinct from receptor-mediated endocytosis. In the selective pathway, cholesterol esters, but not the lipoproteins that transport them, are internalized (Glass *et al.* 1983). The cholesterol esters become localized to intracellular perinuclear lipid droplets (Reaven *et al.* 1995). The transfer of cholesterol esters from the lipoproteins to the plasma membrane is temperature independent. The transfer from there to the perinuclear lipid vesicles does not require an intact Golgi apparatus or even an intact cytoskeleton but seems to require at least one sulfhydryl-containing protein at or very near the plasma membrane. Depletion of ATP from the cell seems not to interfere with the process, although depletion of glucose from the medium decreases efficiency of transfer to the cell

interior (Reaven *et al.* 1996). In our experiments, the cells are grown in a serum-free medium lacking lipoproteins. We propose that the BDS ultrafine particles serve as carriers for the PAHs, in a process analogous to that by which the lipoproteins in the "selective" transport process serve as carriers for the cholesterol esters. The energetics of the BDS-associated PAH uptake as well as the intracellular fate and toxicity of these PAHs currently are under investigation in our laboratory.

REFERENCES

Allison, A. C., and Mallucci, L. (1964). Uptake of hydrocarbon carcinogens by lysosomes. *Nature* **203**, 1024-1027.

Bermudez, E., Mangum, J. B., Wong, B. A., Asgharian, B., Hext, P. M., Warheit, D. B., and Everitt, J. I. (2004). Pulmonary responses of mice, rats, and hamsters to subchronic inhalation of ultrafine titanium dioxide particles. *Toxicol. Sci.* **77**(2), 347-357.

Berube, K. A., Jones, T. P., Williamson, B. J., Winters, C., Morgan, A. J., and Richards, R. J. (1999). Physicochemical characterisation of diesel exhaust particles: Factors for assessing biological activity. *Atmospheric Environment* **33**(10), 1599-1614.

Boland, S., Baeza-Squiban, A., Fournier, T., Houcine, O., Gendron, M. C., Chevrier, M., Jouvenot, G., Coste, A., Aubier, M., and Marano, F. (1999). Diesel exhaust particles are taken up by human airway epithelial cells in vitro and alter cytokine production. *Am. J. Physiol* **276**(4 Pt 1), L604-L613.

Bonvallot, V., Baeza-Squiban, A., Baulig, A., Brulant, S., Boland, S., Muzeau, F., Barouki, R., and Marano, F. (2001). Organic compounds from diesel exhaust particles elicit a proinflammatory response in human airway epithelial cells and induce cytochrome p450 1A1 expression. *Am. J. Respir. Cell Mol. Biol.* **25**(4), 515-521.

Catallo, W. J. (1998). Polycyclic aromatic hydrocarbons in combustion residues from 1,3-butadiene. *Chemosphere* **37**(1), 143-157.

Catallo, W. J., Kennedy, C. H., Henk, W., Barker, S. A., Grace, S. C., and Penn, A. (2001). Combustion products of 1,3-butadiene are cytotoxic and genotoxic to human bronchial epithelial cells. *Environ. Health Perspect.* **109**(9), 965-971.

Chalupa, D. C., Morrow, P. E., Oberdorster, G., Utell, M. J., and Frampton, M. W. (2004). Ultrafine particle deposition in subjects with asthma. *Environ. Health Perspect.* **112**(8), 879-882.

Cherry, B. W. (1981). Polymer surfaces, Cambridge University Press, Cambridge Eng.

Cole, J. A., Bittner, J. D., Longwell, J. P., and Howard, J. B. (1984a). Formation Mechanisms of Aromatic-Compounds in Aliphatic Flames. *Combustion and Flame* **56**(1), 51-70.

Cole, J. A., Bittner, J. D., Longwell, J. P., and Howard, J. B. (1984b). Role of C-4 Hydrocarbons in Aromatic Species Formation in Aliphatic Flames. *Acs Symposium Series* **249**, 3-21.

Costa, D. L., and Dreher, K. L. (1997). Bioavailable transition metals in particulate matter mediate cardiopulmonary injury in healthy and compromised animal models. *Environ. Health Perspect.* **105 Suppl 5**, 1053-1060.

Dick, C. A., Singh, P., Daniels, M., Evansky, P., Becker, S., and Gilmour, M. I. (2003). Murine pulmonary inflammatory responses following instillation of size-fractionated ambient particulate matter. *J. Toxicol. Environ. Health A* **66**(23), 2193-2207.

Dockery, D. W., Pope, C. A., III, Xu, X., Spengler, J. D., Ware, J. H., Fay, M. E., Ferris, B. G., Jr., and Speizer, F. E. (1993). An association between air pollution and mortality in six U.S. cities. *N. Engl. J. Med.* **329**(24), 1753-1759.

Dreher, K. L., Jaskot, R. H., Lehmann, J. R., Richards, J. H., McGee, J. K., Ghio, A. J., and Costa, D. L. (1997). Soluble transition metals mediate residual oil fly ash induced acute lung injury. *J. Toxicol. Environ. Health* **50**(3), 285-305.

Dye, J. A., Adler, K. B., Richards, J. H., and Dreher, K. L. (1999). Role of soluble metals in oil fly ash-induced airway epithelial injury and cytokine gene expression. *Am. J. Physiol* **277**(3 Pt 1), L498-L510.

Glass, C., Pittman, R. C., Weinstein, D. B., and Steinberg, D. (1983). Dissociation of tissue uptake of cholesterol ester from that of apoprotein A-I of rat plasma high density lipoprotein: selective delivery of cholesterol ester to liver, adrenal, and gonad. *Proc. Natl. Acad. Sci. U. S. A* **80**(17), 5435-5439.

Ishiguro, T., Takatori, Y., and Akihama, K. (1997). Microstructure of diesel soot particles probed by electron microscopy: First observation of inner core and outer shell. *Combustion and Flame* **108**(1-2), 231-234.

Kawasaki, S., Takizawa, H., Takami, K., Desaki, M., Okazaki, H., Kasama, T., Kobayashi, K., Yamamoto, K., Nakahara, K., Tanaka, M., Sagai, M., and Ohtoshi, T. (2001). Benzene-extracted components are important for the major activity of diesel exhaust particles: effect on interleukin-8 gene expression in human bronchial epithelial cells. *Am. J. Respir. Cell Mol. Biol.* **24**(4), 419-426.

Ke, Y., Reddel, R. R., Gerwin, B. I., Miyashita, M., McMenamin, M., Lechner, J. F., and Harris, C. C. (1988). Human bronchial epithelial cells with integrated SV40 virus T antigen genes retain the ability to undergo squamous differentiation. *Differentiation* **38**(1), 60-66.

Kendall, M., Tetley, T. D., Wigzell, E., Hutton, B., Nieuwenhuijsen, M., and Luckham, P. (2002). Lung lining liquid modifies PM(2.5) in favor of particle aggregation: a protective mechanism. *Am. J. Physiol Lung Cell Mol. Physiol* **282**(1), L109-L114.

Kocan, R. M., Chi, E. Y., Eriksen, N., Benditt, E. P., and Landolt, M. L. (1983). Sequestration and release of polycyclic aromatic hydrocarbons by vertebrate cells in vitro. *Environ. Mutagen.* **5**(5), 643-656.

Laden, F., Neas, L. M., Dockery, D. W., and Schwartz, J. (2000). Association of fine particulate matter from different sources with daily mortality in six U.S. cities. *Environ. Health Perspect.* **108**(10), 941-947.

Lahaye, J., and Ehrburgerdolle, F. (1994). Mechanisms of Carbon-Black Formation - Correlation with the Morphology of Aggregates. *Carbon* **32**(7), 1319-1324.

Lakowicz, J. R., Bevan, D. R., and Riemer, S. C. (1980). Transport of a carcinogen, benzo[a]pyrene, from particulates to lipid bilayers: a model for the fate of particle-adsorbed polynuclear aromatic hydrocarbons which are retained in the lungs. *Biochim. Biophys. Acta* **629**(2), 243-258.

Li, N., Wang, M., Oberley, T. D., Sempf, J. M., and Nel, A. E. (2002). Comparison of the pro-oxidative and proinflammatory effects of organic diesel exhaust particle chemicals in bronchial epithelial cells and macrophages. *J. Immunol.* **169**(8), 4531-4541.

Murphy, S. A., Berube, K. A., and Richards, R. J. (1999). Bioreactivity of carbon black and diesel exhaust particles to primary Clara and type II epithelial cell cultures. *Occup. Environ. Med.* **56**(12), 813-819.

Nemmar, A., Hoylaerts, M. F., Hoet, P. H., and Nemery, B. (2004). Possible mechanisms of the cardiovascular effects of inhaled particles: systemic translocation and prothrombotic effects. *Toxicol. Lett.* **149**(1-3), 243-253.

Nemmar, A., Vanbilloen, H., Hoylaerts, M. F., Hoet, P. H., Verbruggen, A., and Nemery, B. (2001). Passage of intratracheally instilled ultrafine particles from the lung into the systemic circulation in hamster. *Am. J. Respir. Crit Care Med.* **164**(9), 1665-1668.

Penn, A., Murphy, G., Barker, S., Henk, W., and Penn, L. (2005). Combustion-derived ultrafine particles transport organic toxicants to target respiratory cells. *Environ. Health Perspect.* **113**(8), 956-963.

Peters, A., Wichmann, H. E., Tuch, T., Heinrich, J., and Heyder, J. (1997). Respiratory effects are associated with the number of ultrafine particles. *Am. J. Respir. Crit Care Med.* **155**(4), 1376-1383.

Plant, A. L., Benson, D. M., and Smith, L. C. (1985). Cellular uptake and intracellular localization of benzo(a)pyrene by digital fluorescence imaging microscopy. *J. Cell Biol.* **100**(4), 1295-1308.

Plant, A. L., Knapp, R. D., and Smith, L. C. (1987). Mechanism and rate of permeation of cells by polycyclic aromatic hydrocarbons. *J. Biol. Chem.* **262**(6), 2514-2519.

Pope, C. A., III, Burnett, R. T., Thun, M. J., Calle, E. E., Krewski, D., Ito, K., and Thurston, G. D. (2002). Lung cancer, cardiopulmonary mortality, and long-term exposure to fine particulate air pollution. *JAMA* **287**(9), 1132-1141.

Popovitcheva, O. B., Persiantseva, N. M., Trukhin, M. E., Rulev, G. B., Shonija, N. K., Buriko, Y. Y., Starik, A. M., Demirdjian, B., Ferry, D., and Suzanne, J. (2000). Experimental characterization of aircraft combustor soot: Microstructure, surface area, porosity and water adsorption. *Physical Chemistry Chemical Physics* **2**(19), 4421-4426.

Reaven, E., Tsai, L., and Azhar, S. (1995). Cholesterol uptake by the 'selective' pathway of ovarian granulosa cells: early intracellular events. *J. Lipid Res.* **36**(7), 1602-1617.

Reaven, E., Tsai, L., and Azhar, S. (1996). Intracellular events in the "selective" transport of lipoprotein-derived cholesteryl esters. *J. Biol. Chem.* **271**(27), 16208-16217.

Richter, K. M., and Saini, V. K. (1960). UV-fluorescence studies on the in vitro intracellular accumulation of carcinogenic hydrocarbon. *Am. J. Anat.* **107**, 209-235.

Samet, J. M., Dominici, F., Curriero, F. C., Coursac, I., and Zeger, S. L. (2000). Fine particulate air pollution and mortality in 20 U.S. cities, 1987-1994. *N. Engl. J. Med.* **343**(24), 1742-1749.

Samet, J. M., Silbajoris, R., Huang, T., and Jaspers, I. (2002). Transcription factor activation following exposure of an intact lung preparation to metallic particulate matter. *Environ. Health Perspect.* **110**(10), 985-990.

Schwartz, J., Dockery, D. W., and Neas, L. M. (1996). Is daily mortality associated specifically with fine particles? *J. Air Waste Manag. Assoc.* **46**(10), 927-939.

Tong, H. Y., Sweetman, J. A., Karasek, F. W., Jellum, E., and Thorsrud, A. K. (1984). Quantitative-Analysis of Polycyclic Aromatic-Compounds in Diesel Exhaust Particulate Extracts by Combined Chromatographic Techniques. *Journal of Chromatography* **312**(NOV), 183-202.

United States Environmental Protection Agency (1997). National Ambient Air Quality Standards for Particulate Matter. *Federal Registry* **62**(138).

United States Environmental Protection Agency (2002). Health Assessment Document for Diesel Engine Exhaust. *Federal Registry* **67**(170).

Xia, T., Korge, P., Weiss, J. N., Li, N., Venkatesen, M. I., Sioutas, C., and Nel, A. (2004). Quinones and aromatic chemical compounds in particulate matter induce mitochondrial dysfunction: implications for ultrafine particle toxicity. *Environ. Health Perspect.* **112**(14), 1347-1358.

CHAPTER 2

COMBUSTION-DERIVED HYDROCARBONS CONCENTRATE IN CYTOPLASMIC LIPID DROPLETS OF RESPIRATORY CELLS AND STIMULATE ARYL HYDROCARBON RECEPTOR-ASSOCIATED GENE EXPRESSION

INTRODUCTION

Airborne particulates are of increasing concern, not only for their contribution to ambient pollution, but also for the toxic health effects they elicit. The health effects have been attributed both to the particles themselves, especially in the readily inhalable fine (<2.5 μm) and ultrafine (<0.1 μm) size ranges (Oberdorster *et al.* 1994; Li *et al.* 2003), and to inorganic and organic chemicals associated with the particles. Included among the organic chemicals are polynuclear aromatic hydrocarbons (PAHs) that are adsorbed to the surface of the particles (Ma and Ma 2002; Xia *et al.* 2004). Incomplete combustion of organic substrates leads to the generation of complex airborne particulates *e.g.* those found in cigarette smoke, automobile (gasoline or diesel) exhaust, and petrochemical flares.

Diesel exhaust and cigarette smoke are among the most frequently studied 'real-world' examples of complex combustion-derived particulate mixtures. In both cases, there is a growing body of literature that emphasizes the distinction between the toxicity of the particles versus the toxicity of chemicals adsorbed to the particles (Bonvallot *et al.* 2001; Ma and Ma 2002; Li *et al.* 2002; Sayes *et al.* 2007). Another source of complex particulate environmental contamination is flaring of fugitive volatile compounds by industry. In these settings, volatiles that escape the processing stream or that remain unused are combusted, as strict regulations are in place limiting the amounts of highly reactive volatile organic compounds, such as 1,3-butadiene (BD), that can be released to the atmosphere (United States Environmental Protection Agency 1994). BD is a high-volume, aliphatic hydrocarbon byproduct of petroleum refining and is used in the

manufacture of synthetic rubber and other elastomers. The United States' capacity for BD production has been estimated to be ~6 x 10^9 lbs/year, with many of the producers being located in Texas and Louisiana (The Innovation Group 2002). Butadiene soot (BDS), generated from the incomplete combustion of BD, is both a model mixture and a real-life example of a petrochemical product of incomplete combustion with the potential both for environmental contamination and for contributing to health problems (Penn *et al.* 2005). Free BDS particles have been found apposed to the luminal surface of lung epithelium in mice exposed to BDS by inhalation, while alveolar macrophages filled with BDS particles have been identified in the lung parenchyma even four weeks after BDS exposures end (Murphy G, Paulsen DB, Penn A, unpublished observations).

We have previously characterized BDS as a metals-poor, organic-rich mixture of ultrafine (30-50 nm) carbonaceous particles to which hundreds of PAH species are adsorbed (Catallo *et al.* 2001; Penn *et al.* 2005). Sixteen percent of the total weight of fresh BDS is comprised of PAHs, including benzo(a)pyrene [B(a)P] and other carcinogens, many of which display a characteristic blue or blue-green fluorescence in organic solutions. Human bronchoepithelial cells exposed to BDS develop blue fluorescence, which over time becomes localized in discrete cytoplasmic vesicles. Following BDS exposure, these cells display the same profile of extractable PAHs as the parent BDS. The fluorescence does not develop if the cells are exposed to carbon black instead of BDS, or if the BDS is extracted with organic solvents before the soot particles are presented to the cells (Penn *et al.* 2005). The cellular sites of BDS fluorescence localization have not been identified.

Lipid droplets are spherical organelles ranging in diameter from 50 nm at formation up to 200 μm in mature adipocytes, with the majority being ~1 μm in mammalian cells (Murphy

2001). Initially, lipid droplets were regarded as repositories of intracellular lipids used for energy production and membrane maintenance (Dvorak *et al.* 1983). Recent studies on the dynamic behavior of lipid droplets has led to the elucidation of their role in other processes including fatty acid oxidation and inflammatory eicosanoid production in leukocytes, in which lipoxygenases and cyclooxygenases have been found to interact directly with arachidonic acid within lipid droplets (Bozza *et al.* 1996; Weller *et al.* 1999; Pacheco *et al.* 2002; Vieira-de-Abreu *et al.* 2005). During their formation in the membrane of the endoplasmic reticulum (Robenek *et al.* 2004; Andersson *et al.* 2006) and through association with the plasma membrane (Robenek *et al.* 2005a), lipid droplets obtain an array of proteins that are responsible for the organelle's structure, function, and signaling activities (Murphy 2001; Wolins *et al.* 2006). Three of the most extensively characterized of these lipid droplet surface proteins are perilipin, adipose differentiation-related protein (ADFP or adipophilin), and TIP47, collectively referred to as the PAT family of proteins (Brown 2001; Robenek *et al.* 2005b). As the database of the molecular characteristics of lipid droplets has expanded, links to various disease processes have been identified. Skeletal muscle ADFP expression is increased in obese patients during weight loss or during insulin sensitizing protocols for diabetics (Phillips *et al.* 2005). Expression of ADFP is increased significantly in atherosclerotic plaques, and increased ADFP expression in macrophages alters lipid transport by promoting storage of triglycerides and cholesterol while reducing cholesterol efflux (Larigauderie *et al.* 2004).

The compounds that concentrate in lipid droplets are not restricted to lipids. Indeed, a number of proteins including caveolin-1, caveolin-2 (Robenek *et al.* 2004; Fujimoto *et al.* 2001; Ostermeyer *et al.* 2001; Cohen *et al.* 2004) and even the core protein of the hepatitis C virus (Barba *et al.* 1997; Hope *et al.* 2002) have been localized to lipid droplets. Proteomic

characterization has revealed that proteins responsible for lipid transport, lipid metabolism, and droplet structure are physically associated with lipid droplets (Brasaemle *et al.* 2004). Hydrophobic environmental chemicals, including PAHs, are another group of compounds that might concentrate within lipid droplets. Verdin *et al.* (2006a; 2006b) have demonstrated that fluorescent PAHs, including B(a)P, as well as anthracene and fluoranthene, concentrate in the lipid droplets of fungi, which sequester these noxious compounds (pollutant dissipation) and perhaps metabolize them to less toxic derivatives.

The experiments described here demonstrate that combustion-derived PAHs adsorbed onto inhalable ambient particles are concentrated in lipid droplets of respiratory system cells and that these PAHs concomitantly activate xenobiotic metabolism pathways known to potentiate the toxicity of certain PAHs, including several found in BDS.

METHODS

Cell Culture. BEAS-2B cells (1.5×10^6), a human bronchoepithelial cell line (Reddel *et al.* 1988), were seeded into T-25 flasks (Corning, Corning, NY) containing bronchial-epithelial growth medium (BEGM), before expansion in T-150 flasks. BEGM is a basal medium (BEBM; Cambrex, Walkersville, MD) supplemented (per 500 mL) with 2 mL of 13 mg/mL bovine pituitary extract and 0.5 mL each of 0.5 mg/mL hydrocortisone, 0.5 µg/mL human recombinant epidermal growth factor, 0.5 mg/mL epinephrine, 10 mg/mL transferrin, 5 mg/mL insulin, 0.1 µg/mL retinoic acid, 6.5 µg/mL triiodothyronine, and 50 mg/mL gentamicin.

MH-S cells (1×10^6), a murine alveolar macrophage cell line(Mbawuike and Herscowitz 1989), were propagated in T-150 flasks containing RPMI 1640 medium supplemented with 2 mM L-glutamine, 10 mM HEPES, 1 mM sodium pyruvate, 4.5 g/L glucose, 1.5 g/L bicarbonate, 0.05 mM 2-mercaptoethanol, and 10% fetal bovine serum (FBS). BEAS-2B and MH-S cells

were grown to 80–90% confluence (37°C, 5% CO_2/95% air), split into 60-mm dishes (2.5 x 10^5 cells/dish; grown on 25 x 25 mm glass coverslips) or 6-well plates (1 x 10^5 cells/well), and expanded until approximately 90% confluent.

Murine 3T3-L1 preadipocytes (Green and Kehinde 1975; 1976) were plated in 6-well plates and grown to 2 days postconfluence in DMEM containing 4.5 g/L glucose with 10% calf serum, 100 U/mL penicillin, and 100 µg/mL streptomycin. Cells were induced to differentiate by changing the medium to DMEM containing 4.5 g/L glucose, 10% FBS, 100 U/mL penicillin, 100 µg/mL streptomycin, 0.5 mM 3-isobutyl-methylxanthine, 1 µM dexamethasone, and 1.7 µM insulin. After 48 hrs, this medium was replaced with DMEM containing 4.5 g/L glucose supplemented with 10% FBS, 100 U/mL penicillin, and 100 µg/mL streptomycin; and the cells were maintained in this medium until used (Floyd and Stephens 2002; 2003).

BDS Generation and Collection. The process of BDS generation and collection has been described in detail (Penn *et al.* 2005). Briefly, room temperature BD gas (≥ 99% purity; Sigma; St. Louis, MO) was passed through a back-flash-protected stainless steel two-stage regulator to a stainless steel Bunsen burner at flow rates of 5–7 mL/sec under normal atmosphere and ignited. Soot particles passing through the feed pipe were collected on acetone-washed Whatman cellulose filters placed in a porcelain Buchner funnel connected to a vacuum pump. The BDS was scraped gently off the filters and stored in aluminum-foil-wrapped glass vials capped with foil-lined lids.

BDS Exposures. In each exposure, the culture medium was changed immediately before addition of BDS or staining solutions. For the co-localization experiments, 3 mg of BDS were sprinkled onto the surface of the BEGM in each 60 mm dish containing BEAS-2B cells (70% confluent) 24 hours prior to imaging. For sonicated BDS (S-BDS) exposures, a stock solution

was prepared by suspending 10 mg BDS in 50 mL of culture medium and sonicating the suspension with three 15 second pulses of a Branson Sonifier (Model 450, Constant Duty Cycle; Danbury, CT). BEAS-2B cells, MH-S cells, and adipocytes were exposed to 20 μg/mL S-BDS for 24 hours prior to fluorescence imaging. For quantitative RT-PCR experiments, BEAS-2B and MH-S cells were exposed to S-BDS for 0, 1, 12, or 24 hours prior to RNA extraction.

Fluorescent Dye Co-Localization. Organelle-specific fluorescent probes were used to investigate the subcellular localization of BDS-associated fluorescence. The probes were prepared in BEGM, and BEAS-2B cells were exposed as described in Table 2.1. Monodansylcadaverine (MDC; Sigma) was used to label autophagosomes. LysoTracker Red DND-99, to label lysosomes; Dextran-Tetramethylrhodamine (D-TMR), to label endosomes; and Cholesteryl BODIPY 542/563 C_{11}, to label lipid droplets, were obtained from Molecular Probes (Invitrogen; Carlsbad, CA). To investigate peroxisomes as candidate organelles for sequestration of the PAH fluorescence, we transfected BEAS-2B cells with a plasmid whose protein product is a fusion of the red fluorescent protein DsRed2 with the peroxisomal targeting sequence 1 [PTS1] (Gould *et al.* 1989; 1990). Construction of a plasmid, in which the sequence for a DsRed monomeric protein was appended to the lipid droplet localizing sequence for ADFP, is described below. We identified lipid rafts with the Vybrant Lipid Raft Labeling Kit (Invitrogen), which labels the rafts with a fluorescent conjugate of the B subunit of cholera toxin (CT-B). Due to the extremely small size of individual rafts, they are condensed into larger discrete bodies with a CT-B specific antibody for fluorescence observation (Janes *et al.* 1999). The characteristics of the optical filter set for each test agent are listed in Table 2.1.

Fluorescence Microscopy. With a Microfire Megapixel Digital CCD camera, operated by PictureFrame software (Optronics; Goleta, CA), we collected images (Figures 2.1A, 2.1C, 2.2C,

2.3A-C) from a Zeiss Axiovert 405M inverted fluorescence microscope, through a 40X objective (LD Achroplan, 0.60 NA). With a SensiCam QE 12-bit, cooled CCD camera (Cooke; Romulus, MI), operated by SlideBook software (Intelligent Imaging Innovations; Denver, CO), we collected images (Figures 2.1B, 2.2A-B, 2.3D) from a Leica DM RXA2 upright microscope, through 40X (HCX PL APO CS, 1.25 NA), 63X (HCX PL APO CS, 1.32 NA), or 100X (HCX APO U-V-I, 1.30 NA) objectives equipped with differential interference contrast (DIC) optics. Z-plane images captured though the 100X objective were processed by SlideBook, with constrained iterative deconvolution, to confirm co-localization of the BDS-associated fluorescence with pDsRed-Monomer-ADFP. These planes were combined to create a three-dimensional rotating video image of a single BDS-exposed BEAS-2B cell. We used SlideBook to measure lipid droplet dimensions and Adobe Photoshop CS to process all images using only crop, screen, and levels commands.

Table 2.1. Fluorescent probe specifications, exposure parameters, and filter wavelength boundaries for BDS-associated fluorescence co-localization.

Test Agent or Probe	Organelle Labelled	Concentration of Test Agent	Exposure Duration	Ex/Em (nm)
Butadiene Soot (BDS)		20 μg/mL	24 hr	360/470
Monodansylcadaverine	Autophagosomes	0.14 mM	10 min	475/535
Dextran-TMR	Endosomes	2.5 mg/mL	24 hr	560/620
LysoTracker Red	Lysosomes	1.0 μM	10 sec	560/620
pDsRed2-Peroxi	Peroxisomes	N/A	96 hr	560/620
Cholera Toxin Subunit B	Lipid Rafts	1 μg/mL	10 min	475/535
Cholesteryl BODIPY	Lipid Droplets	1.0 μM	10 min	546/600
pDsRed-Mono-C-ADFP	Lipid Droplets	N/A	48 hr	546/600

The concentrations of test agents are the final concentration in BEGM culture medium. For all co-localization experiments, cells were exposed to BDS for 24 hours prior to imaging. In the transfection studies, the exposure duration is the time after transfection that the images were collected. Filters were obtained from Omega® Optical (Brattleboro, VT).

RNA Isolation. BEAS-2B cells and MH-S cells at or near confluence were collected from three wells of a 6-well plate by scraping into 1 mL of Invitrogen TRIzol Reagent and passing them three times through a 23G needle attached to a 1 mL syringe. RNA was purified from this solution with the Qiagen RNeasy Mini Kit. RNA concentrations were measured with a NanoDrop ND-1000 Spectrophotometer (Wilmington, DE). RNA quality and integrity was assessed using the Agilent RNA 6000 Nano Assay Kit and the Agilent 2100 BioAnalyzer (Santa Clara, CA). Total RNA was converted to cDNA using TaqMan Reverse Transcriptase Reagents (Applied Biosystems; Foster City, CA) according to the manufacturer's protocol.

pDsRed-Monomer-C-ADFP Plasmid Preparation and Transformation. Human ADFP PCR primers were as designed by Targett-Adams *et al.* (2003) from the ADFP mRNA sequence in GenBank: a) 5'-GGGGCAGGTTTAATGAGTTTTATG-3'; and b) 5'-CCAGGAAGAAAAAT GGCATCCGTT-3' (Integrated DNA Technologies; Coralville, IA). PCR was performed on 50 ng of BEAS-2B cDNA in Eppendorf MasterMix (Hamburg, Germany) for 30 cycles in an MJ Research (Waltham, MA) PTC-100 thermal cycler. To impart red fluorescence to ADFP expressed within cells, the ADFP PCR product was ligated into the pDsRed-Monomer-C In-Fusion Ready Vector with the In-Fusion Dry-Down PCR Cloning Kit and expanded in Fusion-Blue Competent *E. coli* cells (Clontech; Mountain View, CA) according to the manufacturer's protocols. Plasmid DNA was isolated from the bacteria with the Wizard Plus SV Miniprep system (Promega; Madison, WI). Plasmid insert size was confirmed by double restriction enzyme digestion with *EcoR*I and *Sal*I (New England Biolabs; Beverly, MA); the insert sequence was confirmed by GeneLab (Louisiana State University, School of Veterinary Medicine, Baton Rouge, LA) with the Applied BioSystems BigDye Terminator v3.1 Cycle Sequencing Kit. BEAS-2B cells grown on glass coverslips in 60 mm dishes were transformed with 500 ng of the

plasmid, in the presence of Lipofectamine LTX and PLUS reagents (Invitrogen). After 48 hours, cells were observed for lipid droplet fluorescence, then exposed to S-BDS (20 μg/mL) for 24 hours prior to imaging for co-localization.

Quantitative Real Time RT-PCR. Quantitative RT-PCR (qRT-PCR) was performed on cDNA samples from BEAS-2B and MH-S cells with inventoried TaqMan Gene Expression Assays primer-probe sets (Applied Biosystems) for the genes listed in Table 2.2. Reaction volumes were 25 μL and 40 reaction cycles were performed for each gene in an Applied Biosystems 7300 Real Time PCR System. Relative gene expression was determined by the comparative cycle threshold ($\Delta\Delta C_T$) method, with each gene normalized to β-actin (ACTB) for human cells (Fields *et al.* 2001) or hypoxanthine guanine phosphoribosyl transferase (Hprt1) for mouse cells (Mamo *et al.* 2007), and then compared to the 0 hour control. Results are reported as fold change over control ± standard error of the mean [($2^{-\Delta\Delta C_T}$) ± SEM].

Statistical Analysis. We used the GLM (general linear model) procedure of the SAS statistical package (version 9.1.3; SAS Institute, Inc., Cary, NC) to compare RT-PCR data and used the Dunnett's *t* test to determine statistical differences.

RESULTS

BDS-associated Fluorescence in Bronchial Epithelial Cells is Time-dependent. We followed the time-dependent development of BDS-associated fluorescence in human bronchial epithelial cells by fluorescence microscopy. Figure 2.1 shows the fluorescent responses of BEAS-2B cells exposed to 3 mg of BDS sprinkled on the surface of the medium. The responses progressed from diffuse fluorescence visible at ten minutes post-exposure (Figure 2.1A) to the appearance of bright punctate perinuclear blue-green fluorescence first visible after two hours. During the transition from diffuse to punctate fluorescence, a reticular network was visible throughout the

Table 2.2. Quantitative RT-PCR fold change values in AhR-responsive genes of MH-S and BEAS-2B cells exposed to BDS.

Gene	Applied Biosystems Primer-Probe Set ID Number	1 Hour	12 Hours	24 Hours
MH-S				
Ahr	Mm00478932_m1	1.05 ± 0.17	1.08 ± 0.16	1.15 ± 0.28
Ahrr	Mm00477443_m1	3.56 ± 0.52 *	3.04 ± 0.54 *	3.32 ± 0.62 *
Aldh3a1	Mm00839312_m1	1.42 ± 0.26	1.02 ± 0.50	1.38 ± 0.57
Cyp1a1	Mm00487218_m1	10.45 ± 2.97 *	4.78 ± 0.94 *	6.37 ± 1.94 *
Cyp1b1	Mm00487229_m1	69.21 ± 15.81 *	16.77 ± 3.45 *	17.56 ± 3.49 *
Tiparp	Mm00724822_m1	7.84 ± 1.16 *	2.09 ± 0.33 *	1.97 ± 0.46 *
BEAS-2B				
ALDH3A1	Hs00167469_m1	1.54 ± 0.8	7.27 ± 1.2 *	4.63 ± 2.6 *
CYP1A1	Hs00153120_m1	21.52 ± 15.4	191.01 ± 29.4 *	108.38 ± 44.3 *
CYP1B1	Hs00164383_m1	6.07 ± 2.9 *	4.91 ± 0.7	3.50 ± 1.5
TIPARP	Hs00604497_m1	13.11 ± 6.8 *	4.35 ± 0.6	3.46 ± 1.5

Results are reported as fold change over control ± standard error of the mean [$(2^{-\Delta\Delta C_T})$ ± SEM].
N=4 for each gene analyzed.
*Significant difference (α=0.05) from control sample.

cytoplasm. Ultraviolet excitation wavelengths (~360 nm) typically provided the brightest emission spectra for visualization of the BDS-associated fluorescence as shown in Figures 2.1A and 2.1C; however, the reticular network shown in Figure 2.1B was best demonstrated with a longer excitation wavelength (~480 nm). The intensity of the fluorescence within the punctate bodies increased through 4 hours of exposure (Figure 2.1C) and persisted at least through 72 hours. The differential interference contrast (DIC) image in Figure 2.2A demonstrates that in BEAS-2B cells the fluorescent bodies appear as sub-micron (0.78 ± 0.05 μm) refractile entities, and that some exposed cells develop prominent peripheral membrane blebs.

BDS-associated Fluorescence Localizes to Lipid Droplets in Bronchial Epithelial Cells. Based on the light microscope observations of size, shape and perinuclear distribution of the

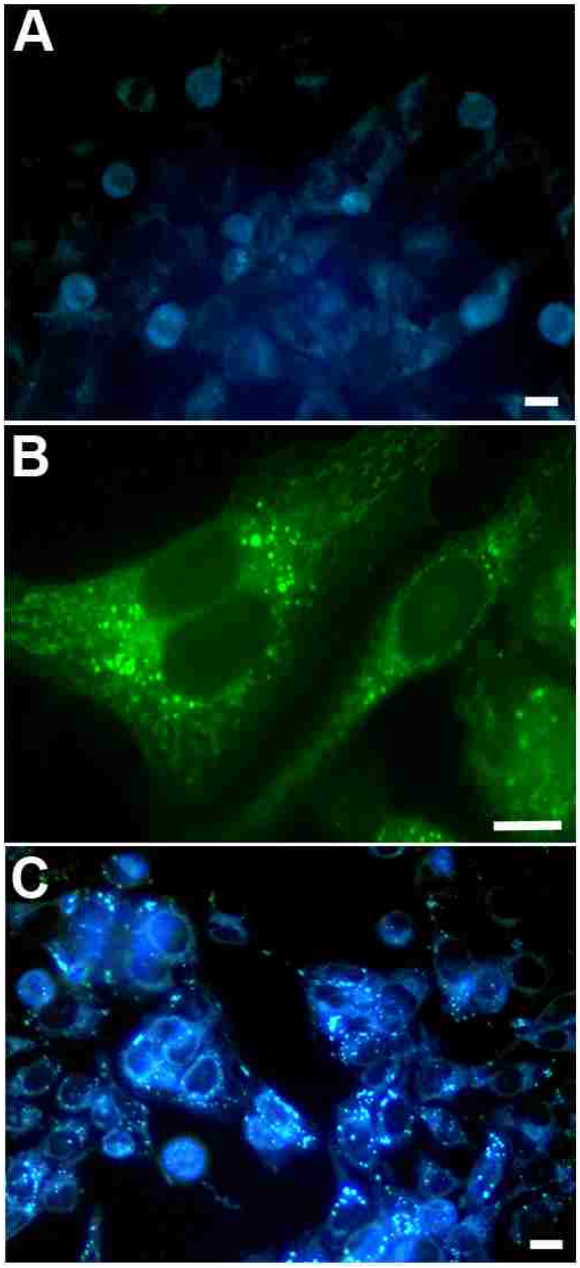

Figure 2.1. Time-dependent fluorescent responses of BEAS-2B cells exposed to petrochemical combustion-derived ultrafine particles (BDS) sprinkled on the surface of the culture medium. Diffuse fluorescence is visible within 10 min (A). A reticular network is visible during the transition from diffuse to punctate fluorescence at 2 hours post-exposure (B). Punctate fluorescence increases through the first 4 hours of exposure to BDS (C). Ultraviolet excitation wavelengths (~360 nm) typically provided the brightest emission spectra for visualization of the BDS-associated fluorescence as shown in A and C; however, the reticular network shown in B was best demonstrated with a longer excitation wavelength (~480 nm). Bars = 10 µm.

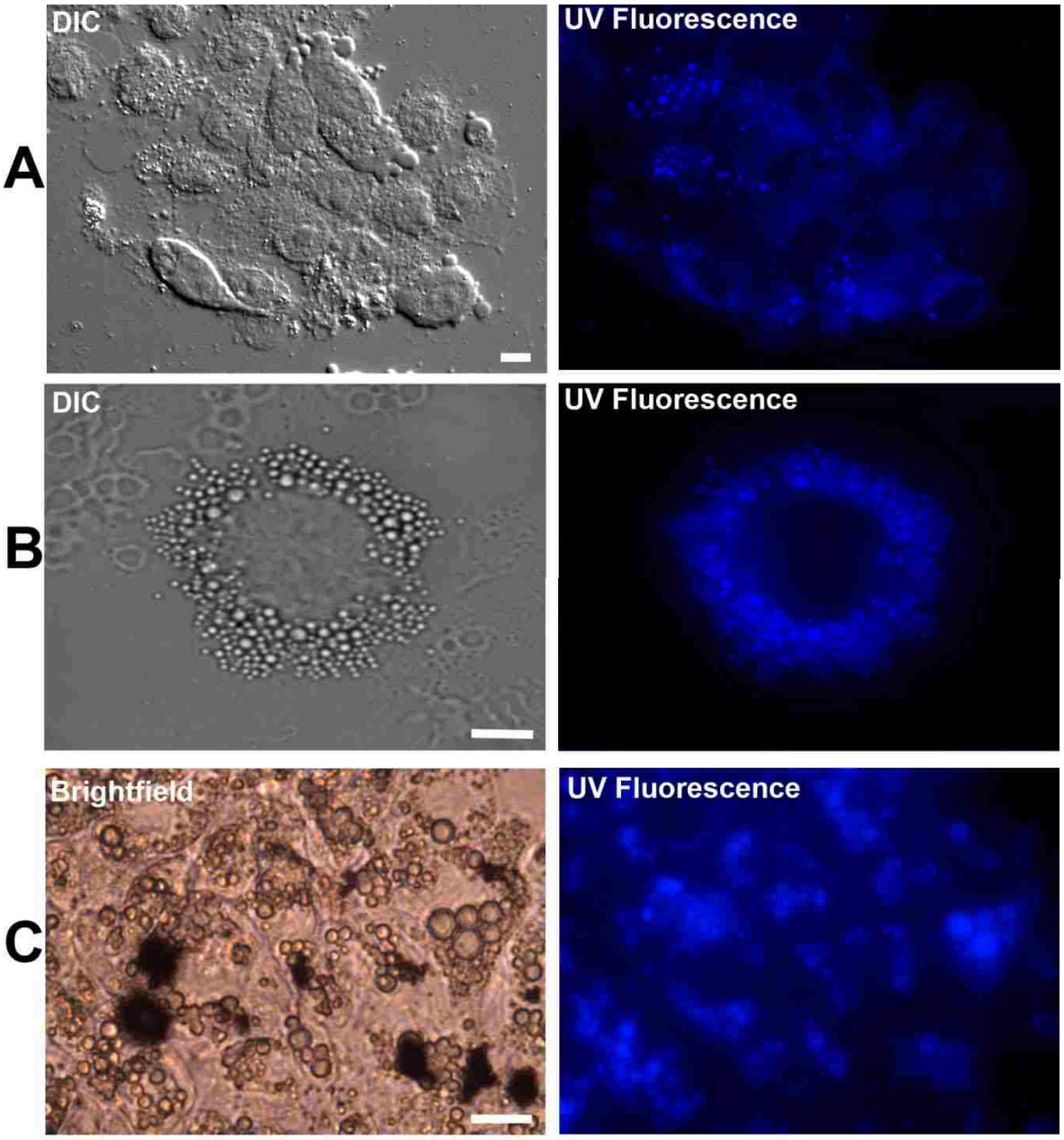

Figure 2.2. Bronchial epithelial cells, alveolar macrophages, and adipocytes display characteristic BDS-associated fluorescence. DIC (A,B) and brightfield photomicrographs (C) paired with UV-fluorescence images of BEAS-2B human bronchoepithelial cells (A), MH-S murine alveolar macrophages (B) and 3T3-L1 murine adipocytes (C) following a 24-hour exposure to sonicated BDS. The fluorescent bodies appear as variably-sized refractile bodies; peripheral membrane blebs are visible on some cells (A). In contrast to BEAS-2B cells, mouse alveolar macrophages displayed larger droplets, all of which were fluorescent (B). Large droplets in mouse adipocytes displayed BDS-associated fluorescence, as well (C). Black BDS particles are visible in the brightfield panel of C, and the fluorescent panel demonstrates the lack of fluorescence associated with the particles. Bars = 10 μm (A), 7.5 μm (B), and 10 μm (C).

fluorescent compartments, candidate organelles were selected and tested by fluorescence co-localization to identify the subcellular compartment(s) in which the BDS-associated blue fluorescence became concentrated. Due to the wide excitation and emission spectra of the BDS-associated fluorescence, special consideration was necessary in the selection of fluorophores to avoid overlaps in excitation or emission. We determined that fluorophore excitation wavelengths >500 nm were required to avoid eliciting fluorescence in cells exposed to BDS alone, and that ultraviolet excitation wavelengths (350-400nm) were ideal for providing maximal and consistent fluorescent blue (~450-500 nm) BDS-associated emissions (data not presented). Thus, we were limited essentially to red fluorophores for co-localization and were not able to take advantage of the older, more common, and often brighter, blue and green fluorophores.

LysoTracker Red is a membrane permeant fluorescent probe that selectively labels intracellular compartments with low pH, *e.g.* lysosomes (Wubbolts *et al.* 1996). Lysosomes also sequester lipid-containing molecules, *e.g.* low density lipoproteins, acquired through endocytic mechanisms (Brown *et al.* 2000; Dhaliwal and Steinbrecher 2000; Moumtzi *et al.* 2007). Rare co-localization of LysoTracker Red and BDS-associated fluorescence is visible in the merge of Figure 2.3A.

Autophagic vacuoles form when cellular organelles, damaged membranes, or large protein structures are packaged for degradation (Reggiori and Klionsky 2002; 2005). MDC was identified originally as a fluorescent probe that selectively labels autophagic vacuoles (Biederbick *et al.* 1995); however, its specificity has been challenged in that it also labels lysosomes and autolysosomes (Bampton *et al.* 2005; Rodriguez-Enriquez *et al.* 2006). Our results confirmed this. MDC and LysoTracker Red fluorescence often co-localized with one another, while each rarely co-localized with BDS-associated fluorescence (images not shown).

D-TMR is a 10 kDa dextran moiety fused to the tetramethylrhodamine fluorophore. D-TMR preferentially enters cells via endocytosis (Ohkuma and Poole 1978), thus serving to label primary endosomes and later, secondary lysosomes. Figure 2.3B shows the images of D-TMR and BDS fluorescence. No co-localization of the fluorophore with BDS-associated fluorescence was detected.

In BEAS-2B cells transfected with the fluorescent peroxisome marker, DsRed expression was visualized as evenly distributed fluorescent red cytoplasmic inclusions ≤0.5 μm in diameter. Peroxisome fluorescence did not co-localize with BDS-associated fluorescence (data not presented).

For BEAS-2B cells with fluorescence-labeled lipid raft aggregates, there was no co-localization of blue BDS-associated fluorescence and green raft fluorescence (data not presented).

Cholesteryl-BODIPY C_{11} concentrates in hydrophobic compartments within cells via the 'selective' transport pathway, in which cholesteryl esters from high density lipoproteins are routed directly to lipid droplets without prior processing in lysosomes or the Golgi apparatus (Sparrow and Pittman 1990; Reaven *et al.* 1995; 1996). Figure 2.3C shows the co-localization of the red cholesteryl-BODIPY C_{11} and the blue BDS fluorescence as evidenced by the predominance of purple vesicles in the merged image.

To confirm the localization of BDS-associated fluorescence specifically to lipid droplets, we transfected BEAS-2B cells with a plasmid whose protein product is a fusion of DsRed-Monomer-C with ADFP. The resultant cells displayed fluorescent red perinuclear inclusions ~1 μm in size. The merged image of Figure 2.3D shows that the blue fluorescence associated with BDS co-localizes completely with the red fluorescence of the lipid droplets in BEAS-2B cells.

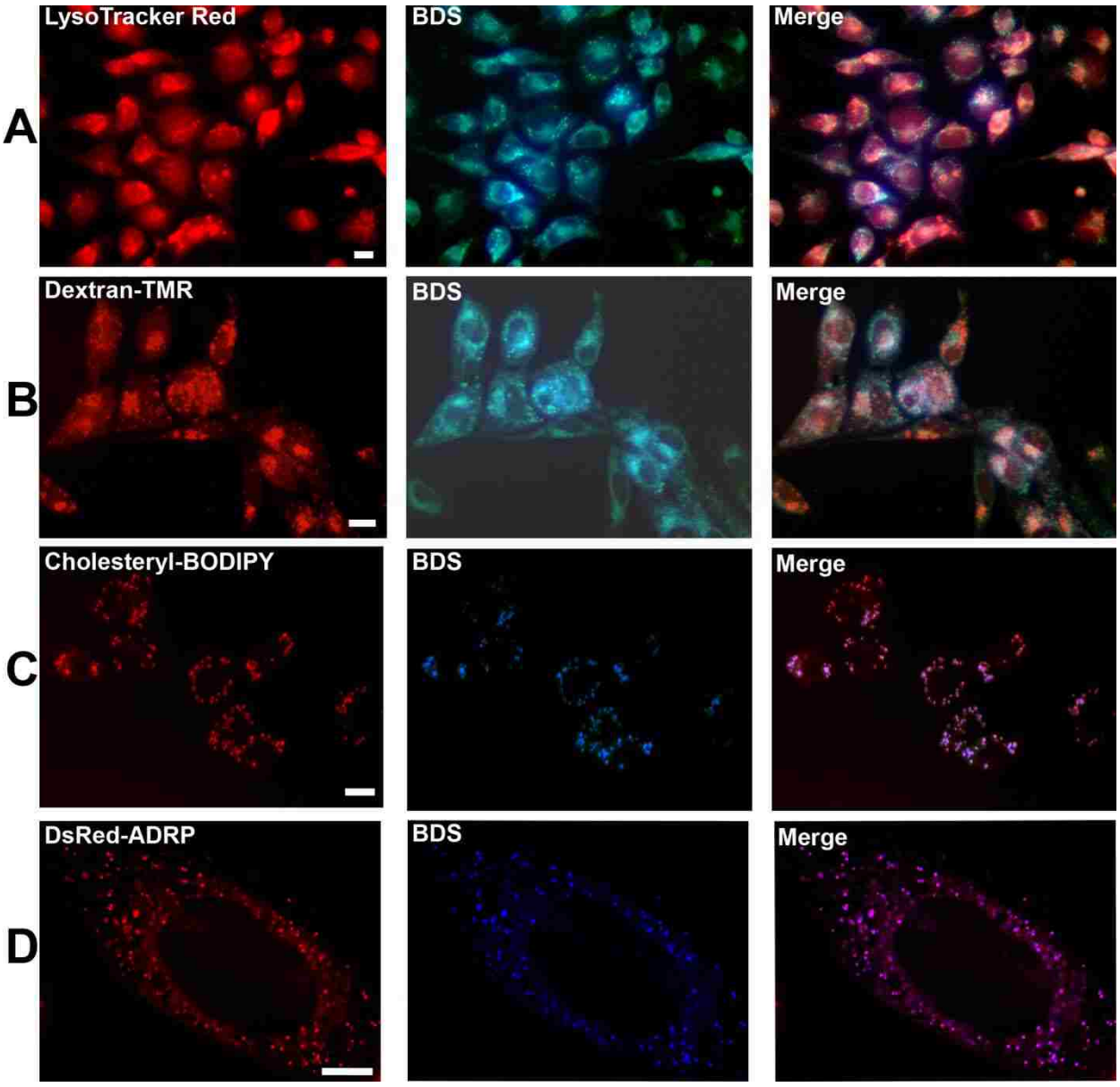

Figure 2.3. Co-localization assays of organelle-specific probes with BDS fluorescence in BEAS-2B cells. The left column shows responses to red fluorescent probes for lysosomes (LysoTracker Red, A), endosomes (Dextran-TMR, B), and lipid droplets (cholesterol-BODIPY, C; DsRed-ADFP, D). The central column shows the concurrent BDS-associated fluorescence following UV excitation. The right column shows the merged images. Complete co-localization is evident for lipid droplets. Video 2.1 is a deconvolved, three-dimensional representation of the cell shown in the merge of D. Bars = 10 μm (A-C) and 5 μm (D).

The video is a three-dimensional rotating representation of the same cell shown in the Figure 2.3D merge (Video 2.1). This video demonstrates the heterogeneity in size of the fluorescent lipid droplets (0.3-1.4 μm), their perinuclear distribution, and their uniform dispersion throughout the cytoplasm of a BEAS-2B cell.

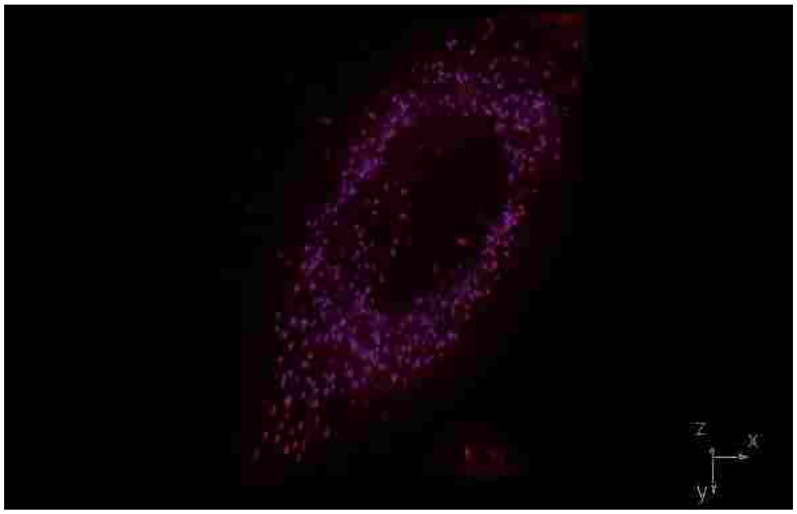

Video 2.1. This video demonstrates the heterogeneity in size of the fluorescent lipid droplets (0.3-1.4 μm), their perinuclear distribution, and their uniform dispersion throughout the cytoplasm of a BEAS-2B cell.

Alveolar Macrophages and Adipocytes Display BDS-associated Fluorescence. Murine alveolar macrophages exposed to BDS generally displayed the same overall characteristic distribution of punctate blue fluorescence as did the BEAS-2B cells. However, as shown in Figure 2.2B, there were cytoplasmic differences between macrophages and BEAS-2B cells, with the former displaying large (1.8 ± 0.2 μm) fluorescent lipid droplets concentrated in the perinuclear region.

Cultured adipocytes exposed to BDS are shown in Figure 2.2C. The large (2.6 ± 0.3 μm) fat droplets of these cells display the same BDS-associated fluorescence seen in BEAS-2B cells, corroborating the observations above that the fluorescent vesicles are consistent with lipid droplets. Furthermore, the development of fluorescence in these cells also was time-dependent

with the fluorescence intensity increasing proportionally with time of exposure to BDS. Adipocytes also were chosen in this context to represent another pulmonary cell type, the lipofibroblast or lipid-laden pulmonary interstitial fibroblast. This cell type is found most commonly in lungs of neonatal mammals where it functions in supplementary surfactant production and retinoid storage (McGowan and Torday 1997; Chen *et al.* 1998).

BDS Induces Aryl-Hydrocarbon Receptor (AhR) Responsive Gene Transcription in MH-S and BEAS-2B cells. We used RT-PCR to measure the expression of the AhR and selected AhR-responsive genes, including the aryl hydrocarbon receptor repressor (Ahrr), aldehyde dehydrogenase 3A1 (Aldh3a1), cytochrome P450 IA1 (Cyp1a1) and IB1 (Cyp1b1), and TCDD-inducible poly(ADP-ribose) polymerase (Tiparp), in MH-S cells exposed to S-BDS for 1, 12, and 24 hours (Table 2.2). Although there was no change in Ahr expression in the macrophages (MH-S), there was greater than a three-fold increase in Ahrr expression across all time points examined. This is consistent with a recent report that expression of Ahrr and the AhR nuclear transporter increases following exposure of cells to the PAH carcinogen 3-methylcholanthrene, even though there is no increase in AhR transcript expression (Yamamoto *et al.* 2004). We also measured significant increases for Cyp1a1, Cyp1b1, and Tiparp, with the highest expression of each gene being recorded one hour post-exposure. Expression of Aldh3a1 was increased, but it was not significantly different from expression in the control cells. A similar trend was noted for selected genes in bronchoepithelial (BEAS-2B) cells, except that ALDH3A1 expression was significantly increased, and the highest values for each gene were at one hour for CYP1B1 and TIPARP, and at 12 hours for ALDH3A1 and CYP1A1 (Table 2.2).

Macrophage inflammatory protein-2 (MIP-2; human interleukin-8 analogue) expression was significantly elevated at 1 and 12 hours post exposure (1.50 ± 0.24 and 1.25 ± 0.16,

respectively) in MH-S cells. In contrast, there were either no significant changes in expression or the expression level was below the level of detection for the following cytokines in MH-S cells: interferon-γ (Ifng), interleukin-1β (Il-1b), interleukin-4 (Il-4), interleukin-6 (Il-6), transforming growth factor β1 (Tgfb1), and tumor necrosis factor (Tnf). Expression of IL-1α and IL-1β was elevated in BEAS-2B cells at each time point, but the increases were not significantly different from control cells (data not presented).

DISCUSSION

The objectives of this study were a) to identify the cytoplasmic compartment where PAHs reside following delivery by inhalable combustion-derived ultrafine particles and b) to determine whether this compartmentalization is associated with altered expression of Phase I biotransformation enzyme and/or cytokine genes. We used organelle-specific probes and fluorescence imaging techniques to identify lipid droplets as the subcellular sites of localization of PAH-associated fluorescence in respiratory epithelial cells. This investigation represents the first time that this organelle has been identified as a site of accumulation and potential repository for organic toxicants associated with combustion-derived ultrafine particles. We also used qRT-PCR to determine that Phase I biotransformation genes were upregulated in a time-dependent manner, while expression of cytokine genes was slight or unchanged.

A role for carbonaceous particles as a PAH delivery system to cells has been previously considered. Bevan *et al.* (1981) and Lakowicz *et al.* (1980) demonstrated that cellular uptake of PAHs is enhanced when the PAHs are adsorbed to high surface area solids such as carbon black particles or asbestos fibers. In an earlier study, we reported that aggregates of non-sonicated BDS particles occasionally were found apposed to cells, but that endocytosis of the particles was not detected. We also demonstrated that organic solvent-extracted BDS particles did not produce

the characteristic fluorescent responses and that the soot-derived PAHs, which produce those responses, can be extracted from the cells (Penn *et al.* 2005). Based on these observations, we propose that BDS particles physically deliver the hydrophobic PAHs to the cells, and that the PAHs are distributed diffusely to lipid bilayers in the plasma membrane and endoplasmic reticulum. A 'reticular' distribution of fluorescence is visible in cells when maximal punctate fluorescence has not yet developed (Figure 2.2B). Partitioning forces then trap the PAHs in the lipophilic environment of lipid droplets once they reach this compartment.

Investigators have used B(a)P-associated fluorescence as a marker for intracellular PAH accumulation, and have described the uptake and partitioning kinetics of B(a)P delivered to cells. Lakowicz *et al.* (1980) showed that the rate-limiting step of PAH transfer from a particulate is desorption of the PAH from the particle into the aqueous environment and that its subsequent incorporation into a lipid phase is very rapid. Subsequently, Plant *et al.* (1987) reported that the rate-limiting step in PAH movement intracellularly is desorption from the inner leaflet of the plasma membrane into the aqueous cytosol. B(a)P would then partition to lipophilic compartments including the membranes of the Golgi apparatus and endoplasmic reticulum, and ultimately lipid droplets. B(a)P was used in these earlier descriptions of PAH movement within cells because of its inherent fluorescence and well-known carcinogenicity. Our results suggest that consideration of hydrophobic compound movement and compartmentalization within cells should be applied to a broader range of compounds, including lipophilic toxins, other xenobiotics and pharmacologic agents. Lipid droplets might act as repositories for such compounds preventing them from exerting their toxic or therapeutic effects, in effect 'protecting' the cell. Alternatively, the sequestration of compounds in lipid droplets may perpetuate their availability

to the cell. The degree of availability may depend upon the characteristics of the lipid droplet surface and its associated proteins charged with regulation of access to the droplets' cargo.

The results presented here and from our unpublished *in vivo* studies indicate that inhaled combustion-derived ultrafine particles can traffic to target organs and deliver the PAHs adsorbed to their surface to intracellular depots, *i.e.* lipid droplets, which then serve as reservoirs for accumulation and possible delayed release of these compounds. By gas chromatography/mass spectrometry (GC/MS) and liquid chromatography/tandem mass spectrometry (LC/MS/MS), we have identified BDS-associated PAHs spanning the size range from 100 amu to more than 400 amu. Among those identified specifically were anthracene, chrysene, benzopyrenes [including B(a)P], and perylene (Catallo *et al.* 2001; Penn *et al.* 2005). The sequestered PAHs, as well as PAHs en route to lipid droplets, likely are available to biotransformation enzymes, especially those enzymes induced by PAH interaction with the AhR. In support of this, we report here that cytochrome P450 IA1 and IB1 transcripts are upregulated in BEAS-2B cells in a time-dependent manner after exposure to BDS. We have observed a similar response in lungs of mice exposed to BDS by inhalation (Murphy G, Paulsen DB, Penn A, unpublished observations). Microsomal cytochrome P450 enzyme activity is responsible for the Phase I metabolism of many PAHs, whereby oxidation of a toxic substrate prepares the substrate for Phase II metabolism and eventual excretion. However, for some compounds, including B(a)P, Phase I metabolism can transform substrates into highly reactive compounds (bioactivation). The most bioactive metabolite of B(a)P is benzo(a)pyrene-7,8-diol-9,10-epoxide (BPDE), which forms guanine adducts in DNA (*e.g.* at specific mutational loci of the p53 gene). These loci often are altered in human lung cancer (Denissenko *et al.* 1996). Buening *et al.* (1978) reported that intraperitoneal injection of BPDE significantly increases pulmonary tumor occurrence in rats. Using normal

mammary epithelial cells exposed to B(a)P *in vitro*, Keshava *et al.* (2005) demonstrated that cytochrome P450 IA1 and IB1 expression is highly variable between individuals, but that expression of these genes is generally induced by exposure to B(a)P, regardless of baseline expression. Although the data seemed to strongly support bioactivation of B(a)P, there was only a weak correlation between CYP1A1 and CYP1B1 induction and B(a)P-DNA adduction. We propose that sequestration of PAHs in lipid droplets may perpetuate their interaction with the AhR, and thus prolong activation of the xenobiotic metabolism pathways.

Experiments in dogs have shown that organic solvent-denuded diesel exhaust particles coated with B(a)P are stripped of the majority of their PAH load within 30 minutes of initial exposure. The released PAHs are detected rapidly in the systemic circulation followed by metabolism that likely occurs in the liver. The pulmonary epithelium does not retain the stripped PAHs long enough to metabolize a significant portion. However, about one-third of the original B(a)P load can be recovered as the parent compound and about one-half as lipophilic metabolites from particles that persist in the airways (free or macrophage associated) more than five months post-exposure, at which time about three-fourths of the particles still are retained in the lungs (Gerde *et al.* 2001). Thus, long-term retention of PAH-laden particles in the lung could allow for long-term concentration of PAHs into the lipid droplets of alveolar macrophages and pulmonary epithelial cells. The availability of these PAHs to the AhR once they are sequestered in lipid droplets remains unknown. Persistent irritation from particle retention in the lung interstitium plus long-term activation of the AhR pathway, constant stimulation of xenobiotic metabolism enzymes, and perpetual inflammation could provide a pro-cancerous environment in the lung parenchyma (Wogan *et al.* 2004).

In conclusion, our results demonstrate that fluorescent PAH compounds adsorbed to inhalable combustion-derived ultrafine particles traffic to lipid droplets of respiratory cells, including bronchial epithelial cells, alveolar macrophages, and adipocytes (as a surrogate for pulmonary lipofibroblasts). Furthermore, *in vitro* exposure of epithelial cells and alveolar macrophages to BDS stimulates AhR-responsive xenobiotic metabolism pathways known to potentiate the toxicity of certain PAHs, including several found in BDS.

REFERENCES

Andersson, L., Bostrom, P., Ericson, J., Rutberg, M., Magnusson, B., Marchesan, D., Ruiz, M., Asp, L., Huang, P., Frohman, M. A., Boren, J., and Olofsson, S. O. (2006). PLD1 and ERK2 regulate cytosolic lipid droplet formation. *J. Cell Sci.* **119**(Pt 11), 2246-2257.

Bampton, E. T., Goemans, C. G., Niranjan, D., Mizushima, N., and Tolkovsky, A. M. (2005). The dynamics of autophagy visualized in live cells: from autophagosome formation to fusion with endo/lysosomes. *Autophagy.* **1**(1), 23-36.

Barba, G., Harper, F., Harada, T., Kohara, M., Goulinet, S., Matsuura, Y., Eder, G., Schaff, Z., Chapman, M. J., Miyamura, T., and Brechot, C. (1997). Hepatitis C virus core protein shows a cytoplasmic localization and associates to cellular lipid storage droplets. *Proc. Natl. Acad. Sci. U. S. A* **94**(4), 1200-1205.

Bevan, D. R., Riemer, S. C., and Lakowicz, J. R. (1981). Effects of particulate matter on rates of membrane uptake of polynuclear aromatic hydrocarbons. *J. Toxicol. Environ. Health* **8**(1-2), 241-250.

Biederbick, A., Kern, H. F., and Elsasser, H. P. (1995). Monodansylcadaverine (MDC) is a specific in vivo marker for autophagic vacuoles. *Eur. J. Cell Biol.* **66**(1), 3-14.

Bonvallot, V., Baeza-Squiban, A., Baulig, A., Brulant, S., Boland, S., Muzeau, F., Barouki, R., and Marano, F. (2001). Organic compounds from diesel exhaust particles elicit a proinflammatory response in human airway epithelial cells and induce cytochrome p450 1A1 expression. *Am. J. Respir. Cell Mol. Biol.* **25**(4), 515-521.

Bozza, P. T., Payne, J. L., Goulet, J. L., and Weller, P. F. (1996). Mechanisms of platelet-activating factor-induced lipid body formation: requisite roles for 5-lipoxygenase and de novo protein synthesis in the compartmentalization of neutrophil lipids. *J. Exp. Med.* **183**(4), 1515-1525.

Brasaemle, D. L., Dolios, G., Shapiro, L., and Wang, R. (2004). Proteomic analysis of proteins associated with lipid droplets of basal and lipolytically stimulated 3T3-L1 adipocytes. *J. Biol. Chem.* **279**(45), 46835-46842.

Brown, A. J., Mander, E. L., Gelissen, I. C., Kritharides, L., Dean, R. T., and Jessup, W. (2000). Cholesterol and oxysterol metabolism and subcellular distribution in macrophage foam cells. Accumulation of oxidized esters in lysosomes. *J. Lipid Res.* **41**(2), 226-237.

Brown, D. A. (2001). Lipid droplets: proteins floating on a pool of fat. *Curr. Biol.* **11**(11), R446-R449.

Buening, M. K., Wislocki, P. G., Levin, W., Yagi, H., Thakker, D. R., Akagi, H., Koreeda, M., Jerina, D. M., and Conney, A. H. (1978). Tumorigenicity of the optical enantiomers of the diastereomeric benzo[a]pyrene 7,8-diol-9,10-epoxides in newborn mice: exceptional activity of (+)-7beta,8alpha-dihydroxy-9alpha,10alpha-epoxy-7,8,9,10-tetrahydrobenzo[a]pyrene. *Proc. Natl. Acad. Sci. U. S. A* **75**(11), 5358-5361.

Catallo, W. J., Kennedy, C. H., Henk, W., Barker, S. A., Grace, S. C., and Penn, A. (2001). Combustion products of 1,3-butadiene are cytotoxic and genotoxic to human bronchial epithelial cells. *Environ. Health Perspect.* **109**(9), 965-971.

Chen, H., Jackson, S., Doro, M., and McGowan, S. (1998). Perinatal expression of genes that may participate in lipid metabolism by lipid-laden lung fibroblasts. *J. Lipid Res.* **39**(12), 2483-2492.

Cohen, A. W., Razani, B., Schubert, W., Williams, T. M., Wang, X. B., Iyengar, P., Brasaemle, D. L., Scherer, P. E., and Lisanti, M. P. (2004). Role of caveolin-1 in the modulation of lipolysis and lipid droplet formation. *Diabetes* **53**(5), 1261-1270.

Denissenko, M. F., Pao, A., Tang, M., and Pfeifer, G. P. (1996). Preferential formation of benzo[a]pyrene adducts at lung cancer mutational hotspots in P53. *Science* **274**(5286), 430-432.

Dhaliwal, B. S., and Steinbrecher, U. P. (2000). Cholesterol delivered to macrophages by oxidized low density lipoprotein is sequestered in lysosomes and fails to efflux normally. *J. Lipid Res.* **41**(10), 1658-1665.

Dvorak, A. M., Dvorak, H. F., Peters, S. P., Shulman, E. S., MacGlashan, D. W., Jr., Pyne, K., Harvey, V. S., Galli, S. J., and Lichtenstein, L. M. (1983). Lipid bodies: cytoplasmic organelles important to arachidonate metabolism in macrophages and mast cells. *J. Immunol.* **131**(6), 2965-2976.

Fields, W. R., Desiderio, J. G., Putnam, K. P., Bombick, D. W., and Doolittle, D. J. (2001). Quantification of changes in c-myc mRNA levels in normal human bronchial epithelial (NHBE) and lung adenocarcinoma (A549) cells following chemical treatment. *Toxicol. Sci.* **63**(1), 107-114.

Floyd, Z. E., and Stephens, J. M. (2002). Interferon-gamma-mediated activation and ubiquitin-proteasome-dependent degradation of PPARgamma in adipocytes. *J. Biol. Chem.* **277**(6), 4062-4068.

Floyd, Z. E., and Stephens, J. M. (2003). STAT5A promotes adipogenesis in nonprecursor cells and associates with the glucocorticoid receptor during adipocyte differentiation. *Diabetes* **52**(2), 308-314.

Fujimoto, T., Kogo, H., Ishiguro, K., Tauchi, K., and Nomura, R. (2001). Caveolin-2 is targeted to lipid droplets, a new "membrane domain" in the cell. *J. Cell Biol.* **152**(5), 1079-1085.

Gerde, P., Muggenburg, B. A., Lundborg, M., and Dahl, A. R. (2001). The rapid alveolar absorption of diesel soot-adsorbed benzo[a]pyrene: bioavailability, metabolism and dosimetry of an inhaled particle-borne carcinogen. *Carcinogenesis* **22**(5), 741-749.

Gould, S. J., Keller, G. A., Hosken, N., Wilkinson, J., and Subramani, S. (1989). A conserved tripeptide sorts proteins to peroxisomes. *J. Cell Biol.* **108**(5), 1657-1664.

Gould, S. J., Keller, G. A., Schneider, M., Howell, S. H., Garrard, L. J., Goodman, J. M., Distel, B., Tabak, H., and Subramani, S. (1990). Peroxisomal protein import is conserved between yeast, plants, insects and mammals. *EMBO J.* **9**(1), 85-90.

Green, H., and Kehinde, O. (1975). An established preadipose cell line and its differentiation in culture. II. Factors affecting the adipose conversion. *Cell* **5**(1), 19-27.

Green, H., and Kehinde, O. (1976). Spontaneous heritable changes leading to increased adipose conversion in 3T3 cells. *Cell* **7**(1), 105-113.

Hope, R. G., Murphy, D. J., and McLauchlan, J. (2002). The domains required to direct core proteins of hepatitis C virus and GB virus-B to lipid droplets share common features with plant oleosin proteins. *J. Biol. Chem.* **277**(6), 4261-4270.

Janes, P. W., Ley, S. C., and Magee, A. I. (1999). Aggregation of lipid rafts accompanies signaling via the T cell antigen receptor. *J. Cell Biol.* **147**(2), 447-461.

Keshava, C., Divi, R. L., Whipkey, D. L., Frye, B. L., McCanlies, E., Kuo, M., Poirier, M. C., and Weston, A. (2005). Induction of CYP1A1 and CYP1B1 and formation of carcinogen-DNA adducts in normal human mammary epithelial cells treated with benzo[a]pyrene. *Cancer Lett.* **221**(2), 213-224.

Lakowicz, J. R., Bevan, D. R., and Riemer, S. C. (1980). Transport of a carcinogen, benzo[a]pyrene, from particulates to lipid bilayers: a model for the fate of particle-adsorbed polynuclear aromatic hydrocarbons which are retained in the lungs. *Biochim. Biophys. Acta* **629**(2), 243-258.

Larigauderie, G., Furman, C., Jaye, M., Lasselin, C., Copin, C., Fruchart, J. C., Castro, G., and Rouis, M. (2004). Adipophilin enhances lipid accumulation and prevents lipid efflux from THP-1 macrophages: potential role in atherogenesis. *Arterioscler. Thromb. Vasc. Biol.* **24**(3), 504-510.

Li, N., Sioutas, C., Cho, A., Schmitz, D., Misra, C., Sempf, J., Wang, M., Oberley, T., Froines, J., and Nel, A. (2003). Ultrafine particulate pollutants induce oxidative stress and mitochondrial damage. *Environ. Health Perspect.* **111**(4), 455-460.

Li, N., Wang, M., Oberley, T. D., Sempf, J. M., and Nel, A. E. (2002). Comparison of the pro-oxidative and proinflammatory effects of organic diesel exhaust particle chemicals in bronchial epithelial cells and macrophages. *J. Immunol.* **169**(8), 4531-4541.

Ma, J. Y., and Ma, J. K. (2002). The dual effect of the particulate and organic components of diesel exhaust particles on the alteration of pulmonary immune/inflammatory responses and metabolic enzymes. *J. Environ. Sci. Health C. Environ. Carcinog. Ecotoxicol. Rev.* **20**(2), 117-147.

Mamo, S., Gal, A. B., Bodo, S., and Dinnyes, A. (2007). Quantitative evaluation and selection of reference genes in mouse oocytes and embryos cultured in vivo and in vitro. *BMC. Dev. Biol.* **7**, 14.

Mbawuike, I. N., and Herscowitz, H. B. (1989). MH-S, a murine alveolar macrophage cell line: morphological, cytochemical, and functional characteristics. *J. Leukoc. Biol.* **46**(2), 119-127.

McGowan, S. E., and Torday, J. S. (1997). The pulmonary lipofibroblast (lipid interstitial cell) and its contributions to alveolar development. *Annu. Rev. Physiol* **59**, 43-62.

Moumtzi, A., Trenker, M., Flicker, K., Zenzmaier, E., Saf, R., and Hermetter, A. (2007). Import and fate of fluorescent analogs of oxidized phospholipids in vascular smooth muscle cells. *J. Lipid Res.* **48**(3), 565-582.

Murphy, D. J. (2001). The biogenesis and functions of lipid bodies in animals, plants and microorganisms. *Prog. Lipid Res.* **40**(5), 325-438.

Oberdorster, G., Ferin, J., and Lehnert, B. E. (1994). Correlation between particle size, in vivo particle persistence, and lung injury. *Environ. Health Perspect.* **102 Suppl 5**, 173-179.

Ohkuma, S., and Poole, B. (1978). Fluorescence probe measurement of the intralysosomal pH in living cells and the perturbation of pH by various agents. *Proc. Natl. Acad. Sci. U. S. A* **75**(7), 3327-3331.

Ostermeyer, A. G., Paci, J. M., Zeng, Y., Lublin, D. M., Munro, S., and Brown, D. A. (2001). Accumulation of caveolin in the endoplasmic reticulum redirects the protein to lipid storage droplets. *J. Cell Biol.* **152**(5), 1071-1078.

Pacheco, P., Bozza, F. A., Gomes, R. N., Bozza, M., Weller, P. F., Castro-Faria-Neto, H. C., and Bozza, P. T. (2002). Lipopolysaccharide-induced leukocyte lipid body formation in vivo: innate immunity elicited intracellular Loci involved in eicosanoid metabolism. *J. Immunol.* **169**(11), 6498-6506.

Penn, A., Murphy, G., Barker, S., Henk, W., and Penn, L. (2005). Combustion-derived ultrafine particles transport organic toxicants to target respiratory cells. *Environ. Health Perspect.* **113**(8), 956-963.

Phillips, S. A., Choe, C. C., Ciaraldi, T. P., Greenberg, A. S., Kong, A. P., Baxi, S. C., Christiansen, L., Mudaliar, S. R., and Henry, R. R. (2005). Adipocyte differentiation-related

protein in human skeletal muscle: relationship to insulin sensitivity. *Obes. Res.* **13**(8), 1321-1329.

Plant, A. L., Knapp, R. D., and Smith, L. C. (1987). Mechanism and rate of permeation of cells by polycyclic aromatic hydrocarbons. *J. Biol. Chem.* **262**(6), 2514-2519.

Reaven, E., Tsai, L., and Azhar, S. (1995). Cholesterol uptake by the 'selective' pathway of ovarian granulosa cells: early intracellular events. *J. Lipid Res.* **36**(7), 1602-1617.

Reaven, E., Tsai, L., and Azhar, S. (1996). Intracellular events in the "selective" transport of lipoprotein-derived cholesteryl esters. *J. Biol. Chem.* **271**(27), 16208-16217.

Reddel, R. R., Ke, Y., Gerwin, B. I., McMenamin, M. G., Lechner, J. F., Su, R. T., Brash, D. E., Park, J. B., Rhim, J. S., and Harris, C. C. (1988). Transformation of human bronchial epithelial cells by infection with SV40 or adenovirus-12 SV40 hybrid virus, or transfection via strontium phosphate coprecipitation with a plasmid containing SV40 early region genes. *Cancer Res.* **48**(7), 1904-1909.

Reggiori, F., and Klionsky, D. J. (2002). Autophagy in the eukaryotic cell. *Eukaryot. Cell* **1**(1), 11-21.

Reggiori, F., and Klionsky, D. J. (2005). Autophagosomes: biogenesis from scratch? *Curr. Opin. Cell Biol.* **17**(4), 415-422.

Robenek, H., Robenek, M. J., Buers, I., Lorkowski, S., Hofnagel, O., Troyer, D., and Severs, N. J. (2005a). Lipid droplets gain PAT family proteins by interaction with specialized plasma membrane domains. *J. Biol. Chem.* **280**(28), 26330-26338.

Robenek, H., Robenek, M. J., and Troyer, D. (2005b). PAT family proteins pervade lipid droplet cores. *J. Lipid Res.* **46**(6), 1331-1338.

Robenek, M. J., Severs, N. J., Schlattmann, K., Plenz, G., Zimmer, K. P., Troyer, D., and Robenek, H. (2004). Lipids partition caveolin-1 from ER membranes into lipid droplets: updating the model of lipid droplet biogenesis. *FASEB J.* **18**(7), 866-868.

Rodriguez-Enriquez, S., Kim, I., Currin, R. T., and Lemasters, J. J. (2006). Tracker dyes to probe mitochondrial autophagy (mitophagy) in rat hepatocytes. *Autophagy.* **2**(1), 39-46.

Sayes, C. M., Reed, K. L., and Warheit, D. B. (2007). Assessing toxicity of fine and nanoparticles: Comparing in vitro measurements to in vivo pulmonary toxicity profiles. *Toxicol. Sci.*

Sparrow, C. P., and Pittman, R. C. (1990). Cholesterol esters selectively taken up from high-density lipoproteins are hydrolyzed extralysosomally. *Biochim. Biophys. Acta* **1043**(2), 203-210.

Targett-Adams, P., Chambers, D., Gledhill, S., Hope, R. G., Coy, J. F., Girod, A., and McLauchlan, J. (2003). Live cell analysis and targeting of the lipid droplet-binding adipocyte differentiation-related protein. *J. Biol. Chem.* **278**(18), 15998-16007.

The Innovation Group. Butadiene. Chemical Market Reporter . 3-25-2002. Schnell Publishing Company. Ref Type: Magazine Article

United States Environmental Protection Agency. Regulatory Impact Analysis for the National Emissions Standards for Hazardous Air Pollutants for Source Categories: Organic Hazardous Air Pollutants from the Synthetic Organic Chemical Manufacturing Industry and Other Processes Subject to the Negotiated Regulation for Equipment Leaks. EPA-453/R-94-019. 1994. Ref Type: Report

Verdin, A., Lounes-Hadj, S. A., Fontaine, J., Grandmougin-Ferjani, A., and Durand, R. (2006a). Effects of anthracene on development of an arbuscular mycorrhizal fungus and contribution of the symbiotic association to pollutant dissipation. *Mycorrhiza.* **16**(6), 397-405.

Verdin, A., Lounes-Hadj, S. A., Laruelle, F., Grandmougin-Ferjani, A., and Durand, R. (2006b). Effect of the high polycyclic aromatic hydrocarbon, benzo[a]pyrene, on the lipid content of Fusarium solani. *Mycol. Res.* **110**(Pt 4), 479-484.

Vieira-de-Abreu, A., Assis, E. F., Gomes, G. S., Castro-Faria-Neto, H. C., Weller, P. F., Bandeira-Melo, C., and Bozza, P. T. (2005). Allergic challenge-elicited lipid bodies compartmentalize in vivo leukotriene C4 synthesis within eosinophils. *Am. J. Respir. Cell Mol. Biol.* **33**(3), 254-261.

Weller, P. F., Bozza, P. T., Yu, W., and Dvorak, A. M. (1999). Cytoplasmic lipid bodies in eosinophils: central roles in eicosanoid generation. *Int. Arch. Allergy Immunol.* **118**(2-4), 450-452.

Wogan, G. N., Hecht, S. S., Felton, J. S., Conney, A. H., and Loeb, L. A. (2004). Environmental and chemical carcinogenesis. *Semin. Cancer Biol.* **14**(6), 473-486.

Wolins, N. E., Brasaemle, D. L., and Bickel, P. E. (2006). A proposed model of fat packaging by exchangeable lipid droplet proteins. *FEBS Lett.* **580**(23), 5484-5491.

Wubbolts, R., Fernandez-Borja, M., Oomen, L., Verwoerd, D., Janssen, H., Calafat, J., Tulp, A., Dusseljee, S., and Neefjes, J. (1996). Direct vesicular transport of MHC class II molecules from lysosomal structures to the cell surface. *J. Cell Biol.* **135**(3), 611-622.

Xia, T., Korge, P., Weiss, J. N., Li, N., Venkatesen, M. I., Sioutas, C., and Nel, A. (2004). Quinones and aromatic chemical compounds in particulate matter induce mitochondrial dysfunction: implications for ultrafine particle toxicity. *Environ. Health Perspect.* **112**(14), 1347-1358.

Yamamoto, J., Ihara, K., Nakayama, H., Hikino, S., Satoh, K., Kubo, N., Iida, T., Fujii, Y., and Hara, T. (2004). Characteristic expression of aryl hydrocarbon receptor repressor gene in human tissues: organ-specific distribution and variable induction patterns in mononuclear cells. *Life Sci.* **74**(8), 1039-1049.

CHAPTER 3

COMBUSTION-DERIVED ULTRAFINE PARTICULATES CAUSE INFLAMMATION IN MURINE AIRWAYS AND UPREGULATE BIOTRANSFORMATION ENZYME GENE EXPRESSION

INTRODUCTION

Fine particles ($PM_{2.5}$; aerodynamic diameter <2.5 μm) contribute to ambient pollution and cardiopulmonary morbidity (Schwartz *et al.* 1996). Since the implementation of a revised edition of the National Ambient Air Quality Standards for Particulate Matter (United States Environmental Protection Agency 1997), studies have correlated $PM_{2.5}$ exposure to increased cardiopulmonary and lung cancer mortality (Pope, III *et al.* 2002; 2004), as well as increased risk of respiratory and cardiovascular disease (Dominici *et al.* 2006; Kunzli *et al.* 2000).

Van Eeden *et al*. (2001) demonstrated that coarse particulate air pollutant ($PM_{10;}$ aerodynamic diameter <10 μm) exposure generates a systemic inflammatory response, *i.e.* an increase in circulating inflammatory cytokines (IL-1β, IL-6, IL-8, and GM-CSF). The cytokines found in the circulation were the same as those produced *in vitro* by alveolar macrophages and bronchial epithelial cells exposed to comparable particulate matter (Fujii *et al.* 2001; Van Eeden *et al.* 2001); thus lung cells produce cytokines that not only can act *in situ*, but also enter the systemic circulation and act upon other organ systems.

In urban areas, combustion of gasoline and diesel fuels as well as industrial organics (simple aliphatics and/or fossil fuels) contributes significantly to the ambient $PM_{2.5}$ fraction (Lighty *et al.* 2000), as well as to the ultrafine particulate ($PM_{0.1}$; aerodynamic diameter <0.1 μm) fraction (Oberdorster and Utell 2002). Ultrafine particles have received little attention from regulatory agencies, but in numerous experimental settings have been found to elicit a range of

toxicological effects, often more severe than those found with comparable exposures to fine particles (Bermudez *et al.* 2004; Lundborg *et al.* 2006).

Ambient urban particles are composed of a complex array of organic and inorganic components, often adsorbed to a carbonaceous core, and each member of the complex may play a role in disease promotion. The surface characteristics and crystal structure of particles may be major determinants of pulmonary inflammation and injury (Sayes *et al.* 2007; Warheit *et al.* 2007). The aqueous inorganic fraction of residual oil fly ash (ROFA), containing the soluble transition metals iron, vanadium, and nickel, induced pulmonary edema, hemorrhage, and a profound inflammatory infiltrate (Dreher *et al.* 1997). Diesel exhaust particles (DEPs) contain a variety of oxygen radical-generating quinones in addition to polyaromatic hydrocarbons (PAHs) and several metal species (Kumagai *et al.* 2002; Li *et al.* 2000; Murphy *et al.* 1999). An extensive body of literature exists characterizing the effects of the parent particles and their isolated constituents *in vitro* and *in vivo*, including studies in humans (Diaz-Sanchez *et al.* 1997; Salvi *et al.* 1999) The endpoints of many of these studies describe inflammatory cell infiltration as well as inflammatory cytokine production by bronchial epithelial cells and alveolar macrophages, with most of the effects attributed to the PAH and quinone fractions (Campen *et al.* 2005; Ma and Ma 2002; Rao *et al.* 2005).

Combustion of low molecular weight hydrocarbons, as in the case of industrial flaring of fugitive volatiles, is another source of complex particulate environmental contamination. 1,3-butadiene (BD) is a high-volume, aliphatic hydrocarbon byproduct of petroleum refining and is used in the manufacture of synthetic rubber and other elastomers. Butadiene soot (BDS), generated from the incomplete combustion of BD, is both a model mixture and a real-life example of a petrochemical product of incomplete combustion with the potential both for

environmental contamination and for contributing to health problems (Penn *et al.* 2005). BDS is an organic-rich mixture of ultrafine (30-50 nm) carbonaceous particles to which hundreds of PAH species, including benzo(a)pyrene [B(a)P] and other carcinogens, are adsorbed. In contrast to ROFA and DEPs, BDS is oxygen- and metals-*poor* (Catallo *et al.* 2001; Penn *et al.* 2005). Both human bronchoepithelial cells and mouse alveolar macrophages display a distinct punctate blue, PAH-associated cytoplasmic fluorescence following exposure to BDS *in vitro*. The fluorescence is localized to cytoplasmic lipid droplets (Murphy et al, manuscript submitted). The fluorescence does not develop if the PAHs have been extracted from the particles and the same spectrum of PAHs present in the parent BDS can be extracted from the fluorescent cells (Penn *et al.* 2005). *In vivo* responses to BDS exposure have not been reported. We hypothesized that inhalation of the PAH-rich BDS should result in a) activation of aryl hydrocarbon receptor (AhR)-associated genes, as is the case with other PAH-rich mixtures, *e.g*. cigarette smoke, and b) up-regulation of inflammatory cytokines, as is the case with DEP.

The questions addressed in this study were:

- Can freshly-generated BDS, known to consist of particles in the ultrafine size range, inhaled by mice reach the alveoli of their lungs?
- Do inhaled BDS particles induce a pulmonary inflammatory response *in vivo*?
- Does exposure to BDS alter gene expression in the lungs? For example, do PAHs associated with BDS particles upregulate expression of xenobiotic biotransformation enzyme genes in lung tissue? Is cytokine gene expression altered?

Here, we present an analysis of bronchoalveolar lavage fluid (BALF) with inflammatory cell infiltrates, histopathological evidence of suppurative inflammation and particle retention, and gene expression analysis which reveals upregulation of several cytokines and AhR

responsive biotransformation enzymes. These results demonstrate that brief exposure to BDS causes acute airway inflammation and augments expression of AhR-responsive genes.

METHODS

Animals. Eighteen 6 week old female Balb/cJ mice were obtained from Jackson Laboratories (Stock 000651, Bar Harbor, ME). After a one week acclimation period, animals were housed individually in suspended steel wire cages at the AAALAC-accredited Inhalation Research Facility at Louisiana State University. The mice were handled in accordance with the NIH *Guide for the Care and Use of Laboratory Animals* (Institute of Laboratory Animal Resources 1996); and all procedures were approved by the Louisiana State University Institutional Animal Care and Use Committee. Food and water were provided *ad libitum* between exposures, but food and water were removed during the exposures to prevent their contamination with particles and/or chemical residues.

BDS Exposures. Room temperature BD gas (Aldrich, St. Louis, MO) was passed through a two-stage regulator (Model LB 150 C; Aldrich), then through a rotameter (Model FM-1050; Matheson, Montgomeryville, PA) to regulate BD flow at 300 mL/min. After passing through a flash arrester, the BD was delivered to a stainless steel Bunsen burner housed in a 0.25 m^3 generation chamber constructed of stainless steel and plexiglass. The burner was lit remotely by a piezoelectric igniter. Each BD flare was allowed to burn for 35-45 sec to maintain an average BDS particle concentration of 6.5 mg/m^3 in the connected adjacent stainless steel and glass 1.0 m^3 inhalation chamber in which the animals were exposed. BDS was drawn from the generation chamber to the exposure chamber by a static pressure differential. Particle concentration in the exposure chamber was monitored in real-time with a DustTrak (Model 8520; TSI Inc., St. Paul, MN); and this concentration was calibrated daily by gravimetric filter comparison. BD gas

concentrations in the exposure chamber were measured by a MIRAN sapphIRe infrared spectrometer (The Foxboro Co., Foxboro, MA) and maintained at an average of 21 ppm throughout the exposures. HEPA-filtered air flow rates in control and exposure chambers were maintained at approximately 140 L/min. Ten animals were exposed to BDS four hours per day for four days, and eight were exposed only to HEPA-filtered air for the same time. Six BDS-exposed mice and four control mice were euthanized [intraperitoneal injection of 0.2 ml Beuthanasia-D Special (Schering-Plough, Union, NJ)] immediately following exposure on the fourth day. We assessed airway hyperreactivity in the remaining four animals from each group by whole body unrestrained plethysmography (Buxco, Troy, NY) beginning one hour post-exposure (Hamelmann *et al.* 1997). These animals were euthanized the following day for sample collection. In another study, four mice were exposed to 50 mg/m^3 BDS for two days, and they were allowed to rest for seven days prior to sample collection. Four mice exposed to HEPA-filtered air were used as controls.

Sample Collection. Following euthanasia, we lavaged the lungs twice with 0.5 mL phosphate-buffered saline passed through a 19 gauge cannula anchored in the trachea. We immediately placed the pooled bronchoalveolar lavage fluid (BALF) on ice. We isolated and excised the left lung for storage in RNAlater (Applied Biosystems, Foster City, CA). We perfused the right lung with 0.4 mL of freshly prepared 0.02 M periodate-0.1 M lysine-0.25% paraformaldehyde (PLP) fixative in phosphate buffer (pH 7.4), then excised and stored the lungs in PLP for 24–48 hr before standard histological sectioning and processing for hematoxylin and eosin staining and histopathological evaluation by a board-certified veterinary pathologist. Characteristics of the macrophages and neutrophilic infiltration on the histological sections were scored as described in Table 3.1.

BALF Analysis. We performed three hundred cell leukocyte differential counts on modified Wright's-stained cytocentrifuge slide preparations of 400 µL aliquots of raw BALF. The leukocytes were categorized by type (macrophage, neutrophil, eosinophil) and particle burden (Figure 3.1). Particle burden was based upon the amount of cytoplasm occupied by gold or black particles. Macrophages in category 1 (MΦ1) had minimal or undetectable particulate burden. Macrophages were categorized as 2 (MΦ2) if greater than five obvious particles were present but < 50% of the cytoplasm was occupied by them. Macrophages with > 50% of their cytoplasm occupied by particles and/or with particles obscuring > 25% of the nucleus were categorized in group 3 (MΦ3). Of the other leukocytes considered (neutrophils, eosinophils, lymphocytes), only neutrophils were found.

RNA Isolation. Each lung stored in RNAlater was removed from the solution within 24-48 hours of sample collection, gently blotted of excess solution, and placed into a clean 2 mL microcentrifuge tube with 1 mL TRIzol Reagent (Invitrogen, Carlsbad, CA) and a 4.5 mm copper-coated bead. We homogenized the lung tissue with two 2-min 25 Hz passages on a Mixer Mill MM300 (Qiagen, Valencia, CA). RNA was purified from the aqueous phase of the lung homogenate with the Qiagen RNeasy Mini Kit, including RNase-free DNase treatment, according to the manufacturer's protocol. RNA concentrations were measured with a NanoDrop ND-1000 Spectrophotometer (Wilmington, DE). RNA quality and integrity was assessed using the Agilent RNA 6000 Nano Assay Kit and the Agilent 2100 BioAnalyzer (Santa Clara, CA). Total RNA was converted to cDNA using a High Capacity cDNA Archive Kit (Applied Biosystems; Foster City, CA) according to the manufacturer's protocol.

Quantitative Real Time RT-PCR. Quantitative RT-PCR (qRT-PCR) was performed on cDNA samples from lung homogenates with inventoried TaqMan Gene Expression Assays primer-

probe sets (Applied Biosystems) for the genes listed in Table 3.2. Reaction volumes were 25 µL, and 40 reaction cycles were performed for each gene in an Applied Biosystems 7300 Real Time PCR System. Relative gene expression was determined by the comparative cycle threshold ($\Delta\Delta C_T$) method, with each gene normalized to hypoxanthine guanine phosphoribosyl transferase (Hprt1) expression (Mamo *et al.* 2007), and then compared to the air controls. Results are reported as fold change over control ± standard error of the mean [($2^{-\Delta\Delta C_T}$) ± SEM].

Statistical Analysis. We used the UNIVARIATE and TTEST procedures of the SAS statistical package (version 9.1.3; SAS Institute, Inc., Cary, NC) to compare qRT-PCR data. A folded F test was used for each dataset to determine if the variance across the set was statistically 'equal', in which case the variances could be pooled for determining statistical differences. For the occasional cases of unequal variance across a dataset, Satterthwaite's approximation of degrees of freedom was used to determine statistical significance.

RESULTS

BALF Differentials. The differential distribution of BALF neutrophils and macrophages from air- and BDS-exposed mice as well as the respective particle burden of the macrophages are presented in Figure 3.1. In the air control samples, essentially all the BALF cells were macrophages with fewer than five particles per cell. Those particles likely represent incidental room air particles that escaped the HEPA filter, or food or cage litter particles. In the BDS samples, alveolar macrophages obviously had collected particles from the bronchoalveolar space (> 50% of the macrophages present are MΦ2 or MΦ3); and many neutrophils were recruited to the same space. The neutrophil concentration was profoundly increased (>10X) as a result of BDS exposure, and they rarely (< 1%) contained particles. With 16 hours of rest after BDS

exposure, there was a *further* significant increase (>2X; p=0.002) in the number of neutrophils collected in the BALF of BDS-exposed mice.

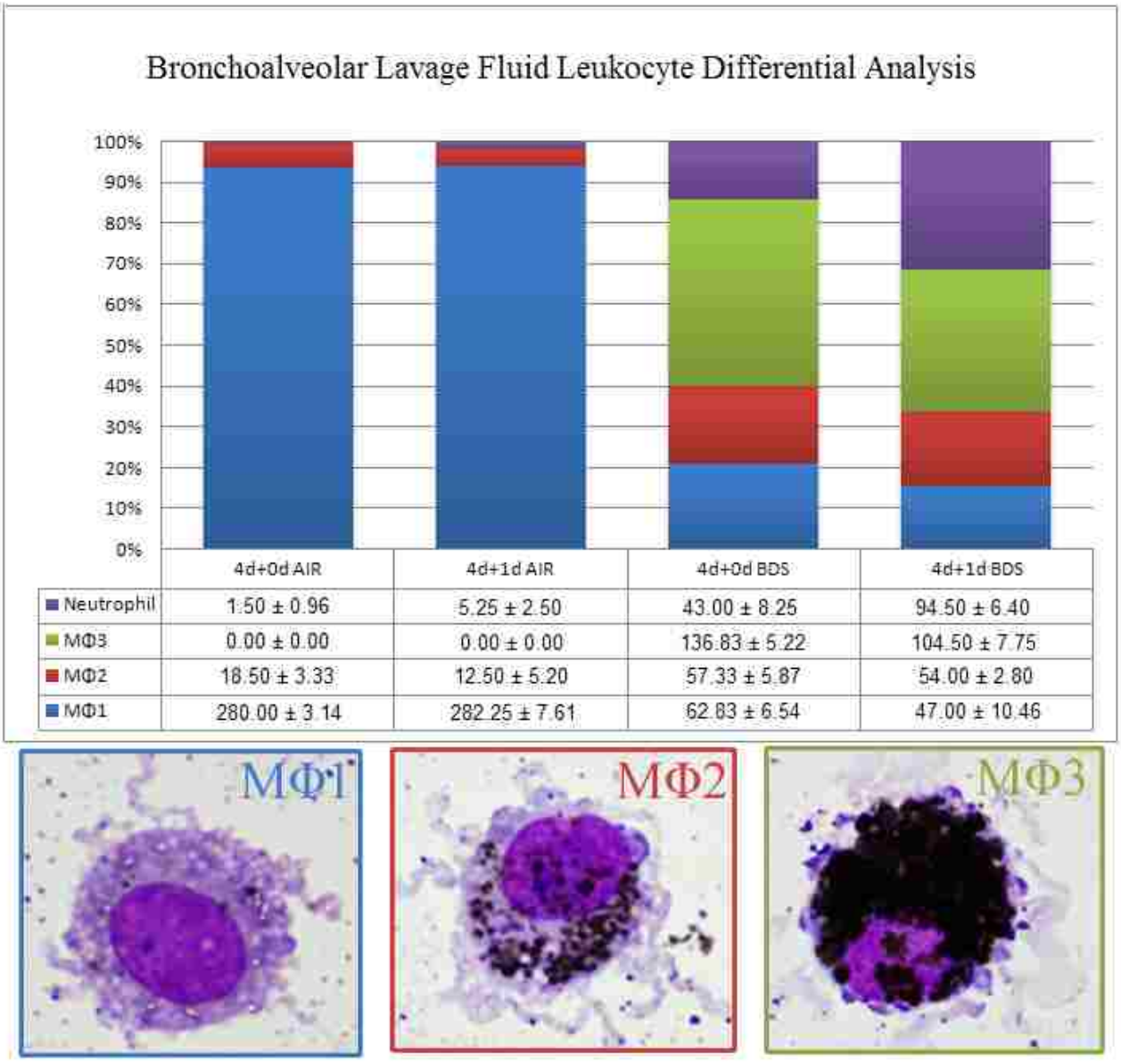

Figure 3.1. Differential Leukocyte Counts of BALF from Mice Exposed to Filtered Air or BDS. Exposure to BDS for four consecutive days leads to profound neutrophilic infiltration into the bronchoalveolar space. Alveolar macrophages (MΦ), the predominant cell found in BALF of normal mice, ingest the BDS particles. One day post-exposure, the neutrophilia is augmented and macrophages loaded with particulate material continue to be the predominant cell type (> 50% MΦ2 or MΦ3). Representative macrophages are demonstrated in the lower portion of the figure.

Lung Histopathology. Figure 3.2 shows examples of histopathological changes in the lung parenchyma of control (2A) and BDS-exposed (2B) animals. As shown in Table 3.1, the changes were quantified according to particles found within alveolar macrophages or macrophages that had migrated to the interstitium, particles apposed to or within cells of the bronchial epithelium, and neutrophil location (peribronchial or transmigratory). The values listed for macrophages and bronchiolar epithelial damage are based on the presence or absence of the characteristic in each lung sample. The neutrophil values are averages ± standard error of the mean of the score described below the table. These results demonstrate that inhaled freshly-generated BDS particles are able to reach the alveoli. Here, alveolar macrophages collect the particles and even carry them to the interstitium. This appears to be a time-dependent process, as only half of the mice displayed particle-laden interstitial macrophages immediately following

TABLE 3.1. Histopathological changes in lung parenchyma following inhalation exposure to butadiene soot reveal particle-laden macrophages and neutrophilic inflammation.

Treatment	Particles in Alveolar MΦs	Particles Associated With Epithelial Cells	Particles in Interstitial MΦs	Peribronchial Neutrophilia	Neutrophil Transmigration	Bronchiolar Epithelial Damage
4d+0d AIR	0/4	0/4	0/4	0.25±0.25	0.50±0.29	0/4
4d+1d AIR	0/4	0/4	0/4	0.50±0.29	0.25±0.25	0/4
4d+0d BDS	6/6	6/6	3/6	1.67±0.21	1.00±0.00	1/6
4d+1d BDS	4/4	4/4	4/4	3.00±0.00	1.50±0.29	3/4

Results are reported as either a) a ratio of samples displaying the labeled characterstic vs. total number of animals in the group, or b) an average score (as described below) ± standard error of the mean.

Peribronchial neutrophilia: 0=normal (rare, scattered neutrophils); 1=minimal (increased scattered individual or rare clusters of 3 or more); 2=mild (diffuse mild or scattered clusters of 3 or more), 3=moderate (diffuse moderate or multiple foci of 10 or more).

Neutrophil transmigration: 0=none, 1=minimal (rare individual cells), 2=mild (obviously increased).

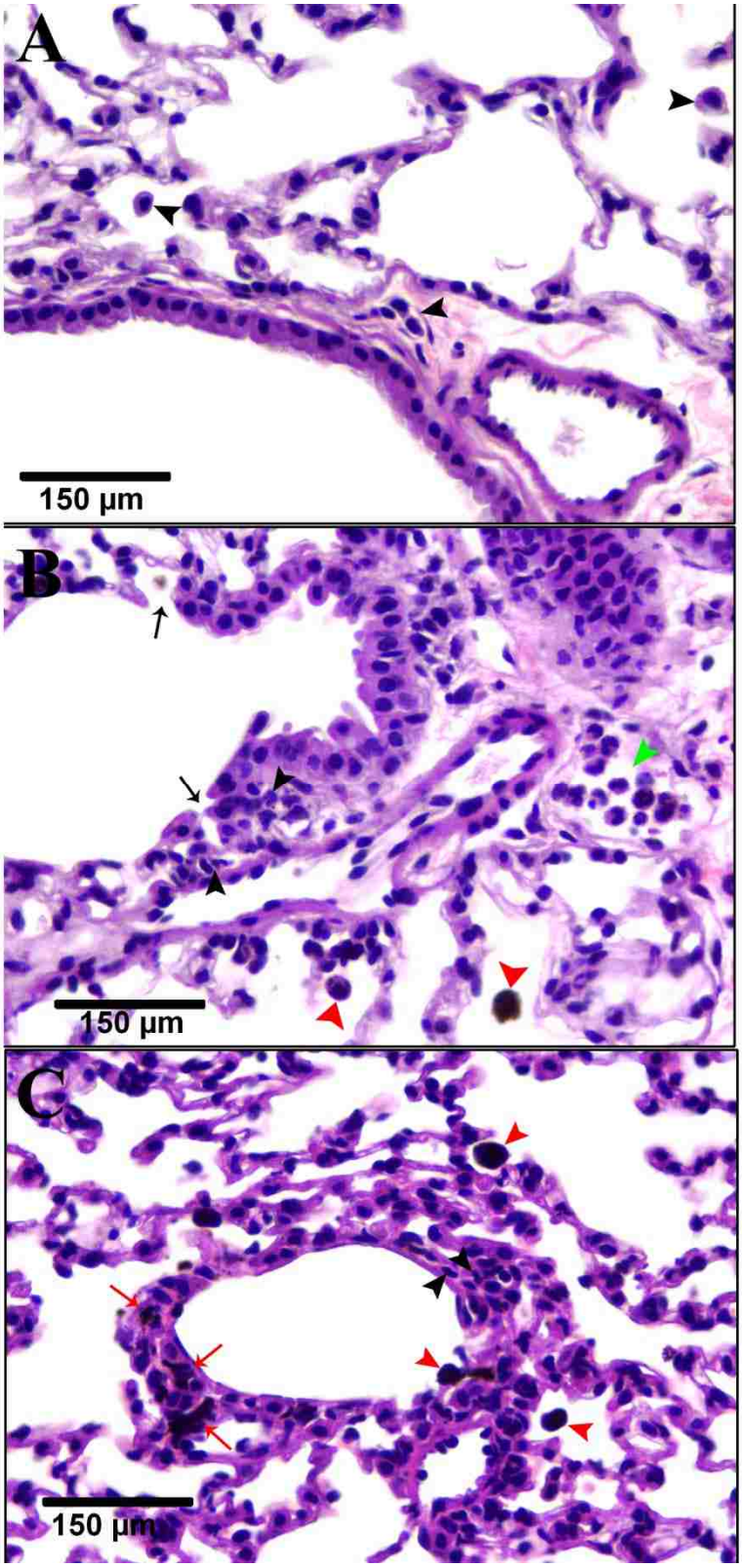

Figure 3.2. Lung Histopathology. (A) Photomicrograph of lungs from a mouse exposed to filtered air. Notice the scattered resident population of mononuclear inflammatory cells, mostly lymphocytes with few plasma cells and macrophages, in the interstitium and alveolar spaces (black arrowheads).
(B) Photomicrograph of lungs from a mouse exposed to 6.5 mg/m^3 of BDS for four consecutive days then allowed to rest for one day. Soot particles are within alveolar (red arrowheads) and interstitial macrophages. There is a focus of moderate neutrophil infiltration and transmucosal exocytosis (black arrowheads) with mild disruption of the continuity of the bronchiolar epithelium (black arrows). Small soot particles lie along the bronchiolar luminal surface and within epithelial cells. An interstitial lymphatic vessel is filled with neutrophils (green arrowhead), most of which contain 1-3 individual soot particles (not apparent at this magnification).
(C) Photomicrograph of lungs from a mouse exposed to 50 mg/m^3 of BDS for two consecutive days then rested for one week. Abundant soot is in the interstitium of the small bronchiole (red arrows) and in numerous alveolar macrophages (red arrowheads). Few neutrophils infiltrate the bronchiolar mucosa (black arrowheads).

exposure, whereas all of the mice did the following day. The particles also elicit a substantial inflammatory response, as evidenced by the peribronchial neutrophilia and migration of neutrophils into the bronchoalveolar space in the BDS-exposed mice. Both of these neutrophilic infiltrates were more pronounced following one day of recovery. In some BDS-exposed animals (4/10), especially after the recovery period (3/4), there was evidence of bronchiolar epithelial damage. This damage was described as foci of epithelial cell necrosis, epithelial denuding, or basement membrane disruption. Figure 3.2C is a representative photomicrograph from the study where mice were exposed to 50 mg/m^3 of BDS for two days, then allowed to rest for seven days. Alveolar macrophages were present that still contained soot particles, groups of particles were lodged in the interstitium, and some neutrophils persisted in the peribronchiolar area. Thus, the BALF and histopathology results reveal that inhalation of these combustion-derived ultrafine particles elicits a time-dependent increase in particle accumulation by alveolar macrophages and associated deep lung neutrophilia, including the persistence of particles in the pulmonary interstitium.

Quantitative RT-PCR. In light of the PAH load of BDS particles and the ultrafine size of the freshly-generated particles (Penn *et al.* 2005), we performed quantitative RT-PCR on lung tissue to determine whether 1) biotransformation enzyme expression was upregulated in response to AhR activation; 2) the particles elicited upregulation of an inflammatory cascade of cytokine gene expression; and 3) PAHs altered selected lipid metabolism or cell cycle pathways. The results of this expression analysis are presented in Table 3.2. In the lungs of BDS-exposed animals collected immediately after exposure, significant increases were observed in expression of selected AhR-responsive biotransformation enzymes: aldehyde dehydrogenase 3A1 (Aldh3a1), cytochrome P450 IA1 (Cyp1a1) and IB1 (Cyp1b1), as well as the AhR repressor

(Ahrr) and TCDD-inducible poly(ADP-ribose) polymerase (Tiparp), while expression of AhR itself was unchanged. In the lungs of mice after one day of recovery, the expression of these AhR-responsive genes was reduced; but, with the exception of Aldh3a1 and Tiparp, each was still significantly elevated over the controls.

Chemokine (C-X-C motif) ligand 2 (Cxcl2; MIP-2; human IL-8 analog) and IL-6 expression were elevated immediately following exposure. Their expression was reduced, yet still significantly elevated above controls, after one day of recovery. Although not significantly different from controls, the other cytokines that we examined [interferon-γ (Ifng), IL-1β, IL-4, transforming growth factor β1 (Tgfb1), and tumor necrosis factor (Tnf)] showed an increasing trend (as did the cellular inflammatory infiltrates) from immediately after exposure to the following day. These results show that uptake of the ultrafine particles by alveolar macrophages and airway epithelial cells is accompanied by upregulation of biotransformation enzymes and inflammatory cytokines.

Expression of serine (or cysteine) peptidase inhibitor, clade B, member 2 (Serpinb2; plasminogen activator inhibitor 2, PAI-2), which has been linked to progression of pulmonary fibrosis (Lardot *et al.* 1998), was increased following exposure to BDS; however, this increase was significantly different from controls only immediately after exposure.

Arachidonate 5-lipoxygenase activating protein (Alox5ap) and leukotriene A4 hydrolase (Lta4h) are responsible for producing leukotriene B4 (LTB4), a potent neutrophil chemotactic factor secreted by alveolar macrophages during inflammatory episodes (Martin *et al.* 1984). We observed a decrease in Alox5ap and Lta4h expression in lung tissue following BDS exposure.

TABLE 3.2. Quantitative RT-PCR of lung tissue reveals upregulation of aryl hydrocarbon receptor-responsive biotransformation genes and inflammatory cytokines following inhalation exposure to butadiene soot

Gene Abbreviation	Applied Biosystems Primer-Probe Set ID Number	4d+0d	4d+1d
AhR-Responsive Genes			
Ahr	Mm00478932_m1	-1.03 ± 0.16	1.00 ± 0.20
Ahrr	Mm00477443_m1	59.93 ± 8.95**	5.97 ± 1.22**
Aldh3a1	Mm00839312_m1	7.37 ± 1.05**	1.31 ± 0.28
Cyp1a1	Mm00487218_m1	35.87 ± 4.27**†	11.61 ± 2.44**
Cyp1b1	Mm00487229_m1	67.99 ± 9.83**	9.74 ± 2.11**
Tiparp	Mm00724822_m1	1.90 ± 0.28**	-1.19 ± 0.16
Cytokines			
Cxcl2 (MIP-2; IL-8)	Mm00436450_m1	7.82 ± 1.08**	4.94 ± 0.91**
Ifng	Mm00801778_m1	-1.37 ± 0.13	1.14 ± 0.30
Il-1b	Mm00434228_m1	1.22 ± 0.25	1.91 ± 0.44*
Il-4	Mm00445259_m1	-1.20 ± 0.14	1.07 ± 0.19†
Il-6	Mm00446190_m1	5.51 ± 1.30**	3.17 ± 0.72*
Tgfb1	Mm00441724_m1	1.01 ± 0.11	1.02 ± 0.15
Tnf	Mm00443258_m1	1.50 ± 0.24	1.63 ± 0.45
Lipid Metabolism And Other			
Alox5ap	Mm00802100_m1	-1.18 ± 0.12*	-1.20 ± 0.14*
Lta4h	Mm00521826_m1	-1.12 ± 0.09*	-1.20 ± 0.13*
Serpinb2 (PAI-2)	Mm00440905_m1	2.00 ± 0.51*	1.31 ± 0.21†

Results are reported as fold change from control ± standard error of the mean [($2^{-\Delta\Delta C_T}$) ± SEM].
*significance: $p<0.05$
**significance: $p<0.0001$
†Unequal variance among samples; therefore, Satterthwaite's approximation was used for degrees of freedom in determining significance.

DISCUSSION

We have demonstrated that inhalation exposure to a moderate dose of combustion-derived ultrafine particles causes acute pulmonary inflammation in the bronchoalveolar space of mice. As BDS is an oxygen- and metals-poor mixture of PAHs and ultrafine particles, it serves

as a unique model of particulate exposure when compared to metals-rich ROFA and oxygen (quinone)-rich DEPs, both of which cause inflammatory lung infiltrates.

PAHs found in ROFA and DEPs are metabolized for detoxification and excretion by mechanisms analogous to those described for B(a)P (Bonvallot *et al.* 2001; Kim *et al.* 2005). The paradox of how these mechanisms, designed to detoxify and eliminate noxious compounds from cells, are capable of producing even more toxic or carcinogenic compounds (bioactivation) is reviewed by Nebert *et al*. (2004). The first step in this process is Phase I biotransformation, most often carried out by microsomal oxidases such as CYP1A1, CYP1B1, and/or ALDH3A1. In contrast to the finding of Takano *et al*. (2002) that following exposure to DEPs AhR expression in the mouse lung is reduced in a concentration-dependent manner, we found no change in expression of the AhR subsequent to BDS exposure. Our results are more consistent with Yamamoto *et al.* (2004) who described the constitutive and PAH-induced expression of AhR, ARNT, AHRR, and CYP1A1 in various adult and fetal tissues. Expression of all four genes was constitutively high in adult lung tissue; however, after PAH exposure, AhR expression did not change in isolated mononuclear cells (monocytes and lymphocytes), while expression of ARNT, AHRR, and CYP1A1 increased. The decrease in Cyp1a1, Cyp1b1, Aldh3a1, and Tiparp that we observed in mice allowed one day to recover from BDS exposure may be explained by the activity of Ahrr. Once the majority of PAHs have been effectively metabolized, downstream effectors of AhR activation would decrease once the receptor becomes quiescent, especially if there is a repressor acting upon available receptors.

The oxidized products of cytochrome P450 activity on PAHs are capable of forming carcinogenic DNA adducts or eliciting oxidative stress responses in cells. These effects may be exacerbated by the presence of particles, as in the case of DEPs, where cellular oxidative stress

has been linked directly to inflammatory endpoints (Ma and Ma 2002). We have demonstrated that there is a significant influx of neutrophils to the bronchoalveolar space subsequent to BDS exposure. This infiltrate appeared to intensify after one day of rest. We have performed studies where mice exposed to 1, 5 or 50 mg/m^3 BDS for one to four days were allowed to rest for seven days. In each case, the neutrophilia persisted in the BALF of these animals along with the presence of MΦ2s and MΦ3s in the BALF and the pulmonary interstitium (Figure 3.2C). Furthermore, in mice exposed to 1 mg/m^3 BDS for four weeks then allowed to rest for 30 days, we still were able to collect several MΦ2s and MΦ3s even though the neutrophilia had subsided (data not presented). Thus, the retention of particles in alveolar macrophages, causing either physical irritation or persistent inflammation, may allow for long-term health effects following an acute exposure (Oberdorster *et al.* 1994).

Not only may inhalation exposure to particles elicit local effects in the respiratory tract, they also may contribute to disease processes in other organ systems. For example, increased circulating levels of inflammatory cytokines subsequent to PM_{10} exposure has been associated with progression of atherosclerosis (Suwa *et al.* 2002). Another study describes the direct translocation of *particles* from the respiratory tree to the systemic circulation as being responsible for subsequent cardiovascular disease conditions (Nemmar *et al.* 2004); however, this mechanism has been actively challenged by human exposure studies (Mills *et al.* 2006; Wiebert *et al.* 2006). Still others have found that ultrafine particles deposited in the nasopharyngeal area may gain access to the central nervous system via olfactory neuronal transport (Elder *et al.* 2006). Although our study deals only with effects of BDS in the lung parenchyma, we recognize the potential for ultrafine BDS particles to reach other organ systems. Studies in rats and dogs have demonstrated that pulmonary epithelial cells have a saturation point

with respect to PAHs (Ewing *et al.* 2006). Combustion-derived ultrafine particles may be able to translocate to extrapulmonary sites *with* their PAH payload if the PAH saturation point is exceeded. This is unlikely in the event of daily environmental exposure to ambient particles which have a low overall PAH burden (Allen *et al.* 1996), but the concentration might be exceeded during an acute exposure to high levels of such particles, *e.g.* firefighters, rescue workers reporting to petrochemical industrial accidents, or soldiers exposed to petroleum fires.

We have demonstrated that BDS-associated fluorescent PAHs localize to lipid droplets of lung cells *in vitro* (Murphy *et al*., manuscript submitted). Considering the neutrophilic infiltrate seen in the lungs of mice exposed to BDS, we selected two lipid metabolism genes involved in production of the eicosanoid LTB4. Inhaled BDS, however, does not alter the expression of Lta4h or Alox5ap in the MH-S murine alveolar macrophage cell line (Murphy, unpublished observations). Consistent with paradoxical results seen in cigarette smoke experiments where LTB4 secretion is reduced in cigarette smoke-exposed macrophages *in vitro* and *in vivo* (Laviolette *et al.* 1986; Tardif *et al.* 1990), we found reduced expression of Lta4h and Alox5ap in lungs of mice exposed to BDS. This situation would appear to impair the necessary immunologic response to particulate (or perhaps infectious agent) presence in the lungs. However, in light of the apparent reduction in LTB4 synthesis in the lungs as a whole, a profound neutrophilic response was still observed. Although LTB4 is considered to be one of the most potent chemoattractants for neutrophils, other molecules (including IL-8) are capable of recruiting neutrophils and macrophages to the lungs; these inflammatory effectors may be produced by pulmonary epithelial cells (Masubuchi *et al.* 1998) or even fibroblasts (Sato *et al.* 1999). Culture of alveolar macrophages collected from BDS-exposed mice followed by supernatant analysis (broad cytokine array) could provide further information on the

macrophage's role in orchestration of the inflammatory response to PAH-laden ultrafine particles.

Increased expression of plasminogen activator inhibitors has been linked to progression of pulmonary fibrosis (Lardot *et al.* 1998). In addition, increased PAI-2 expression has been found to be a favorable prognostic indicator for lung cancer metastasis, *i.e.* lung tumors with high PAI-2 expression were less likely to metastasize to local lymph tissue (Robert *et al.* 1999). Because we have presented an acute exposure scenario, we did not expect to find evidence of pulmonary fibrosis or neoplasia; nevertheless, we did observe increased PAI-2 expression. To investigate whether the PAI-2 expression persists and contributes to a fibrotic condition, gene expression and immunohistochemical analyses should be performed after a longer rest period.

In summary, we have described that brief inhalation exposure to a moderate dose of PAH-rich combustion-derived ultrafine particles causes 1) acute pulmonary inflammation, evidenced by inflammatory cell infiltrates and upregulated cytokine expression; and 2) increased expression of AhR-responsive genes that are capable of transforming PAHs into more toxic metabolites. Furthermore, our histopathological analyses have shown that freshly-generated ultrafine BDS particles reach the deepest bronchoalveolar spaces in mouse lungs.

REFERENCES

Allen, J. O., Dookeran, K. M., Smith, K. A., Sarofim, A. F., Taghizadeh, K., and Lafleur, A. L. (1996). Measurement of polycyclic aromatic hydrocarbons associated with size-segregated atmospheric aerosols in Massachusetts. *Environmental Science & Technology* **30**(3), 1023-1031.

Bermudez, E., Mangum, J. B., Wong, B. A., Asgharian, B., Hext, P. M., Warheit, D. B., and Everitt, J. I. (2004). Pulmonary responses of mice, rats, and hamsters to subchronic inhalation of ultrafine titanium dioxide particles. *Toxicol. Sci.* **77**(2), 347-357.

Bonvallot, V., Baeza-Squiban, A., Baulig, A., Brulant, S., Boland, S., Muzeau, F., Barouki, R., and Marano, F. (2001). Organic compounds from diesel exhaust particles elicit a proinflammatory response in human airway epithelial cells and induce cytochrome p450 1A1 expression. *Am. J. Respir. Cell Mol. Biol.* **25**(4), 515-521.

Campen, M. J., Babu, N. S., Helms, G. A., Pett, S., Wernly, J., Mehran, R., and McDonald, J. D. (2005). Nonparticulate components of diesel exhaust promote constriction in coronary arteries from ApoE-/- mice. *Toxicol. Sci.* **88**(1), 95-102.

Catallo, W. J., Kennedy, C. H., Henk, W., Barker, S. A., Grace, S. C., and Penn, A. (2001). Combustion products of 1,3-butadiene are cytotoxic and genotoxic to human bronchial epithelial cells. *Environ. Health Perspect.* **109**(9), 965-971.

Diaz-Sanchez, D., Tsien, A., Fleming, J., and Saxon, A. (1997). Combined diesel exhaust particulate and ragweed allergen challenge markedly enhances human in vivo nasal ragweed-specific IgE and skews cytokine production to a T helper cell 2-type pattern. *J. Immunol.* **158**(5), 2406-2413.

Dominici, F., Peng, R. D., Bell, M. L., Pham, L., McDermott, A., Zeger, S. L., and Samet, J. M. (2006). Fine particulate air pollution and hospital admission for cardiovascular and respiratory diseases. *JAMA* **295**(10), 1127-1134.

Dreher, K. L., Jaskot, R. H., Lehmann, J. R., Richards, J. H., McGee, J. K., Ghio, A. J., and Costa, D. L. (1997). Soluble transition metals mediate residual oil fly ash induced acute lung injury. *J. Toxicol. Environ. Health* **50**(3), 285-305.

Elder, A., Gelein, R., Silva, V., Feikert, T., Opanashuk, L., Carter, J., Potter, R., Maynard, A., Ito, Y., Finkelstein, J., and Oberdorster, G. (2006). Translocation of inhaled ultrafine manganese oxide particles to the central nervous system. *Environ. Health Perspect.* **114**(8), 1172-1178.

Ewing, P., Blomgren, B., Ryrfeldt, A., and Gerde, P. (2006). Increasing exposure levels cause an abrupt change in the absorption and metabolism of acutely inhaled benzo(a)pyrene in the isolated, ventilated, and perfused lung of the rat. *Toxicol. Sci.* **91**(2), 332-340.

Fujii, T., Hayashi, S., Hogg, J. C., Vincent, R., and Van Eeden, S. F. (2001). Particulate matter induces cytokine expression in human bronchial epithelial cells. *Am. J. Respir. Cell Mol. Biol.* **25**(3), 265-271.

Hamelmann, E., Schwarze, J., Takeda, K., Oshiba, A., Larsen, G. L., Irvin, C. G., and Gelfand, E. W. (1997). Noninvasive measurement of airway responsiveness in allergic mice using barometric plethysmography. *Am. J. Respir. Crit Care Med.* **156**(3 Pt 1), 766-775.

Institute of Laboratory Animal Resources (1996). Guide for the care and use of laboratory animals, National Academy Press, Washington, DC.

Kim, J. Y., Hecht, S. S., Mukherjee, S., Carmella, S. G., Rodrigues, E. G., and Christiani, D. C. (2005). A urinary metabolite of phenanthrene as a biomarker of polycyclic aromatic hydrocarbon metabolic activation in workers exposed to residual oil fly ash. *Cancer Epidemiol. Biomarkers Prev.* **14**(3), 687-692.

Kumagai, Y., Koide, S., Taguchi, K., Endo, A., Nakai, Y., Yoshikawa, T., and Shimojo, N. (2002). Oxidation of proximal protein sulfhydryls by phenanthraquinone, a component of diesel exhaust particles. *Chem. Res. Toxicol.* **15**(4), 483-489.

Kunzli, N., Kaiser, R., Medina, S., Studnicka, M., Chanel, O., Filliger, P., Herry, M., Horak, F., Jr., Puybonnieux-Texier, V., Quenel, P., Schneider, J., Seethaler, R., Vergnaud, J. C., and Sommer, H. (2000). Public-health impact of outdoor and traffic-related air pollution: a European assessment. *Lancet* **356**(9232), 795-801.

Lardot, C., Heusterpreute, M., Mertens, P., Philippe, M., and Lison, D. (1998). Expression of plasminogen activator inhibitors type-1 and type-2 in the mouse lung after administration of crystalline silica. *Eur. Respir. J.* **11**(4), 912-921.

Laviolette, M., Coulombe, R., Picard, S., Braquet, P., and Borgeat, P. (1986). Decreased leukotriene B4 synthesis in smokers' alveolar macrophages in vitro. *J. Clin. Invest* **77**(1), 54-60.

Li, N., Venkatesan, M. I., Miguel, A., Kaplan, R., Gujuluva, C., Alam, J., and Nel, A. (2000). Induction of heme oxygenase-1 expression in macrophages by diesel exhaust particle chemicals and quinones via the antioxidant-responsive element. *J. Immunol.* **165**(6), 3393-3401.

Lighty, J. S., Veranth, J. M., and Sarofim, A. F. (2000). Combustion aerosols: factors governing their size and composition and implications to human health. *J. Air Waste Manag. Assoc.* **50**(9), 1565-1618.

Lundborg, M., Dahlen, S. E., Johard, U., Gerde, P., Jarstrand, C., Camner, P., and Lastbom, L. (2006). Aggregates of ultrafine particles impair phagocytosis of microorganisms by human alveolar macrophages. *Environ. Res.* **100**(2), 197-204.

Ma, J. Y., and Ma, J. K. (2002). The dual effect of the particulate and organic components of diesel exhaust particles on the alteration of pulmonary immune/inflammatory responses and metabolic enzymes. *J. Environ. Sci. Health C. Environ. Carcinog. Ecotoxicol. Rev.* **20**(2), 117-147.

Mamo, S., Gal, A. B., Bodo, S., and Dinnyes, A. (2007). Quantitative evaluation and selection of reference genes in mouse oocytes and embryos cultured in vivo and in vitro. *BMC. Dev. Biol.* **7**, 14.

Martin, T. R., Altman, L. C., Albert, R. K., and Henderson, W. R. (1984). Leukotriene B4 production by the human alveolar macrophage: a potential mechanism for amplifying inflammation in the lung. *Am. Rev. Respir. Dis.* **129**(1), 106-111.

Masubuchi, T., Koyama, S., Sato, E., Takamizawa, A., Kubo, K., Sekiguchi, M., Nagai, S., and Izumi, T. (1998). Smoke extract stimulates lung epithelial cells to release neutrophil and monocyte chemotactic activity. *Am. J. Pathol.* **153**(6), 1903-1912.

Mills, N. L., Amin, N., Robinson, S. D., Anand, A., Davies, J., Patel, D., de la Fuente, J. M., Cassee, F. R., Boon, N. A., MacNee, W., Millar, A. M., Donaldson, K., and Newby, D. E. (2006). Do inhaled carbon nanoparticles translocate directly into the circulation in humans? *Am. J. Respir. Crit Care Med.* **173**(4), 426-431.

Murphy, S. A., Berube, K. A., and Richards, R. J. (1999). Bioreactivity of carbon black and diesel exhaust particles to primary Clara and type II epithelial cell cultures. *Occup. Environ. Med.* **56**(12), 813-819.

Nebert, D. W., Dalton, T. P., Okey, A. B., and Gonzalez, F. J. (2004). Role of aryl hydrocarbon receptor-mediated induction of the CYP1 enzymes in environmental toxicity and cancer. *J. Biol. Chem.* **279**(23), 23847-23850.

Nemmar, A., Hoylaerts, M. F., Hoet, P. H., and Nemery, B. (2004). Possible mechanisms of the cardiovascular effects of inhaled particles: systemic translocation and prothrombotic effects. *Toxicol. Lett.* **149**(1-3), 243-253.

Oberdorster, G., Ferin, J., and Lehnert, B. E. (1994). Correlation between particle size, in vivo particle persistence, and lung injury. *Environ. Health Perspect.* **102 Suppl 5**, 173-179.

Oberdorster, G., and Utell, M. J. (2002). Ultrafine particles in the urban air: to the respiratory tract--and beyond? *Environ. Health Perspect.* **110**(8), A440-A441.

Penn, A., Murphy, G., Barker, S., Henk, W., and Penn, L. (2005). Combustion-derived ultrafine particles transport organic toxicants to target respiratory cells. *Environ. Health Perspect.* **113**(8), 956-963.

Pope, C. A., III, Burnett, R. T., Thun, M. J., Calle, E. E., Krewski, D., Ito, K., and Thurston, G. D. (2002). Lung cancer, cardiopulmonary mortality, and long-term exposure to fine particulate air pollution. *JAMA* **287**(9), 1132-1141.

Pope, C. A., III, Burnett, R. T., Thurston, G. D., Thun, M. J., Calle, E. E., Krewski, D., and Godleski, J. J. (2004). Cardiovascular mortality and long-term exposure to particulate air pollution: epidemiological evidence of general pathophysiological pathways of disease. *Circulation* **109**(1), 71-77.

Rao, K. M., Ma, J. Y., Meighan, T., Barger, M. W., Pack, D., and Vallyathan, V. (2005). Time course of gene expression of inflammatory mediators in rat lung after diesel exhaust particle exposure. *Environ. Health Perspect.* **113**(5), 612-617.

Robert, C., Bolon, I., Gazzeri, S., Veyrenc, S., Brambilla, C., and Brambilla, E. (1999). Expression of plasminogen activator inhibitors 1 and 2 in lung cancer and their role in tumor progression. *Clin. Cancer Res.* **5**(8), 2094-2102.

Salvi, S., Blomberg, A., Rudell, B., Kelly, F., Sandstrom, T., Holgate, S. T., and Frew, A. (1999). Acute inflammatory responses in the airways and peripheral blood after short-term exposure to diesel exhaust in healthy human volunteers. *Am. J. Respir. Crit Care Med.* **159**(3), 702-709.

Sato, E., Koyama, S., Takamizawa, A., Masubuchi, T., Kubo, K., Robbins, R. A., Nagai, S., and Izumi, T. (1999). Smoke extract stimulates lung fibroblasts to release neutrophil and monocyte chemotactic activities. *Am. J. Physiol* **277**(6 Pt 1), L1149-L1157.

Sayes, C. M., Reed, K. L., and Warheit, D. B. (2007). Assessing toxicity of fine and nanoparticles: comparing in vitro measurements to in vivo pulmonary toxicity profiles. *Toxicol. Sci.* **97**(1), 163-180.

Schwartz, J., Dockery, D. W., and Neas, L. M. (1996). Is daily mortality associated specifically with fine particles? *J. Air Waste Manag. Assoc.* **46**(10), 927-939.

Suwa, T., Hogg, J. C., Quinlan, K. B., Ohgami, A., Vincent, R., and Van Eeden, S. F. (2002). Particulate air pollution induces progression of atherosclerosis. *J. Am. Coll. Cardiol.* **39**(6), 935-942.

Takano, H., Yanagisawa, R., Ichinose, T., Sadakane, K., Inoue, K., Yoshida, S., Takeda, K., Yoshino, S., Yoshikawa, T., and Morita, M. (2002). Lung expression of cytochrome P450 1A1 as a possible biomarker of exposure to diesel exhaust particles. *Arch. Toxicol.* **76**(3), 146-151.

Tardif, J., Borgeat, P., and Laviolette, M. (1990). Inhibition of human alveolar macrophage production of leukotriene B4 by acute in vitro and in vivo exposure to tobacco smoke. *Am. J. Respir. Cell Mol. Biol.* **2**(2), 155-161.

United States Environmental Protection Agency (1997). National Ambient Air Quality Standards for Particulate Matter. *Federal Registry* **62**(138).

Van Eeden, S. F., Tan, W. C., Suwa, T., Mukae, H., Terashima, T., Fujii, T., Qui, D., Vincent, R., and Hogg, J. C. (2001). Cytokines involved in the systemic inflammatory response induced by exposure to particulate matter air pollutants (PM(10)). *Am. J. Respir. Crit Care Med.* **164**(5), 826-830.

Warheit, D. B., Webb, T. R., Colvin, V. L., Reed, K. L., and Sayes, C. M. (2007). Pulmonary bioassay studies with nanoscale and fine-quartz particles in rats: toxicity is not dependent upon particle size but on surface characteristics. *Toxicol. Sci.* **95**(1), 270-280.

Wiebert, P., Sanchez-Crespo, A., Seitz, J., Falk, R., Philipson, K., Kreyling, W. G., Moller, W., Sommerer, K., Larsson, S., and Svartengren, M. (2006). Negligible clearance of ultrafine particles retained in healthy and affected human lungs. *Eur. Respir. J.* **28**(2), 286-290.

Yamamoto, J., Ihara, K., Nakayama, H., Hikino, S., Satoh, K., Kubo, N., Iida, T., Fujii, Y., and Hara, T. (2004). Characteristic expression of aryl hydrocarbon receptor repressor gene in human tissues: organ-specific distribution and variable induction patterns in mononuclear cells. *Life Sci.* **74**(8), 1039-1049.

CHAPTER 4

BRONCHOEPITHELIAL CELLS INTERNALIZE COMBUSTION-DERIVED ULTRAFINE PARTICLES *IN VITRO*: AN ULTRASTRUCTURAL INVESTIGATION

INTRODUCTION

Exposure to airborne particles has been a human health concern for many years (Seaton *et al.* 1995). Epidemiologic studies in urban communities have linked ambient particle exposure to such health effects as chronic obstructive pulmonary disease, lung cancer, and even heart failure (Dominici *et al.* 2006; Pope, III *et al.* 2002). Investigators have recognized that the pathogenesis of these conditions is complex because ambient particles are quite complex in composition. The particles vary greatly in origin, size, surface area, and elemental composition; plus a given particle type, such as those generated by petrochemical (gasoline, diesel, industrial substrate) combustion, may be coated with many other compounds, including polynuclear aromatic hydrocarbons (PAHs) (Lighty *et al.* 2000). Each of these characteristics may produce its own set of biological effects. For example, titanium dioxide particles in the ultrafine size range (particulate matter with an aerodynamic diameter of <0.1 μm; $PM_{0.1}$) can cause severe respiratory system inflammation (Bermudez *et al.* 2004; Oberdorster *et al.* 1994). Differences in crystal or surface structure of particles can also elicit variable inflammatory responses in the lung, including inflammatory cytokine expression (Renwick *et al.* 2004; Warheit *et al.* 2007).

In addition to recruiting inflammatory cells to the respiratory epithelial surface, particles can affect the activity of these cells. Renwick *et al*. (2001) found that macrophages exposed to particles, especially ultrafine particles, displayed a reduced phagocytic capacity. Others have shown that clearance of particle-laden macrophages from the respiratory tract is impaired, leading to the persistence of particles in the lung parenchyma (Bermudez *et al.* 2004; Oberdorster *et al.* 1994; Warheit *et al.* 1997). Macrophages incapacitated from particle overload

allow other particles to persist in contact with the epithelium, and these particles may include bacteria that normally would be cleared by active macrophages and neutrophils. Thus, particle exposure increases susceptibility to infection (Antonini *et al.* 2002; Lundborg *et al.* 2006).

Combustion-derived particles are often coated with a variety of chemical species. Diesel exhaust particles (DEPs) contain various oxygen-containing organics, such as quinones, in addition to PAHs and metal ions, all of which have toxic effects in the lung (Kumagai *et al.* 2002; Li *et al.* 2000; Murphy *et al.* 1999). The toxic effects of residual oil fly ash (ROFA), another complex particulate generated from fossil fuel combustion, have been attributed to the metals associated with the particles (Antonini *et al.* 2002; Dreher *et al.* 1997). 1,3-butadiene (BD) is a high-volume, aliphatic hydrocarbon byproduct of petroleum refining and is used in the manufacture of synthetic rubber and other elastomers. Butadiene soot (BDS), generated from the incomplete combustion of BD, is both a model mixture and a real-life example of a petrochemical product of incomplete combustion with the potential both for environmental contamination and for contributing to health problems. BDS is an organic-rich mixture of ultrafine (30-50 nm) carbonaceous particles (Penn *et al.* 2005) to which hundreds of PAH species, including benzo(a)pyrene [B(a)P] and other carcinogens, are adsorbed (Catallo *et al.* 2001; Penn *et al.* 2005). In contrast to DEPs and ROFA, BDS is oxygen- and metals-*poor* (Penn *et al.* 2005). Both human bronchoepithelial cells and mouse alveolar macrophages display a distinct punctate blue cytoplasmic fluorescence following exposure to BDS *in vitro*. The fluorescence is localized to cytoplasmic lipid droplets and is due to fluorescent PAHs delivered to the cells by the BDS particles, as particle-free organic extracts of BDS elicit the same fluorescent response as the native particles, but PAH-denuded particles do not (Penn *et al.* 2005; Murphy *et al.* manuscript submitted).

We have observed that BDS particles seem to associate strongly with human bronchoepithelial cells (BEAS-2B) *in vitro*, *i.e.* when collecting cells from the culture dish, there are black particles attached to large sheets of cells. After lysing the cells and centrifuging the resultant solution, a black pellet of particles is obtained; but whether these particles were simply adhered to the cell surface or actually endocytosed by the cells was unclear. Other investigators have shown that ultrafine DEPs and fluorescent polystyrene beads (40 nm in diameter) can be internalized by airway epithelial cells, as demonstrated by transmission electron microscopy and flow cytometry, respectively. They also reported that particle uptake by the epithelial cells was associated with increased secretion of inflammatory cytokines, including IL-6, IL-8, and GM-CSF (Auger *et al.* 2006; Boland *et al.* 1999).

The investigation presented here demonstrates that BDS particles are internalized by bronchoepithelial cells *in vitro* and phagocytosed by alveolar macrophages *in vivo*. In both cases, particle aggregates are contained within membrane-limited vesicles.

METHODS

Cell Culture. BEAS-2B cells (1.5×10^6), a human bronchoepithelial cell line (Reddel *et al.* 1988), were seeded into 25 cm^2 flasks (Corning, Corning, NY) containing bronchial-epithelial growth medium (BEGM), then expanded to confluence in 150 cm^2 flasks. BDS exposures were performed on cells at 90% confluence in 100 mm diameter petri dishes. BEGM is a basal medium (BEBM; Cambrex, Walkersville, MD) supplemented (per 500 mL) with 2 mL of 13 mg/mL bovine pituitary extract and 0.5 mL each of 0.5 mg/mL hydrocortisone, 0.5 μg/mL human recombinant epidermal growth factor, 0.5 mg/mL epinephrine, 10 mg/mL transferrin, 5 mg/mL insulin, 0.1 μg/mL retinoic acid, 6.5 μg/mL triiodothyronine, and 50 mg/mL gentamicin.

BDS Generation and Collection. The process of BDS generation and collection has been described in detail (Penn *et al.* 2005). Briefly, room temperature BD gas (≥ 99% purity; Sigma; St. Louis, MO) was passed through a back-flash-protected stainless steel two-stage regulator to a stainless steel Bunsen burner at flow rates of 5-7 mL/sec under normal atmosphere and ignited. Soot particles passing through the feed pipe were collected on acetone-washed Whatman cellulose filters placed in a porcelain Buchner funnel connected to a vacuum pump. The BDS was scraped gently off the filters and stored in aluminum-foil-wrapped glass vials capped with foil-lined lids.

BDS Exposures. A sonicated BDS (S-BDS) stock solution was prepared by suspending 10 mg BDS in 50 mL of BEGM and sonicating the suspension with three 15 second pulses of a Branson Sonifier (Model 450, Constant Duty Cycle; Danbury, CT). BEAS-2B cells were exposed to 20 μg/mL S-BDS for 24 hours prior to collection for transmission electron microscopy (TEM) processing.

BEAS-2B Cell Preparation. Cells were collected by scraping into 1 ml phosphate buffered saline (PBS). The cells were pelleted by gentle centrifugation (500 x g; 10 min). PBS was replaced with 1.25% glutaraldehyde, 2% formaldyhyde fixative in 0.1M sodium cacodylate buffer (NaCac). After washing with a solution of 0.1M NaCac and 5% sucrose, cell pellets were post-fixed in a 1% solution of osmium tetroxide in NaCac. After further washing, samples prepared for traditional TEM were stained *en bloc* with a 2% solution of uranyl acetate. These samples were washed again and dehydrated with a graded series of increasing ethanol concentrations (50%-100%). The samples were infiltrated with epoxy resin, which was polymerized prior to ultrathin sectioning. These sections were placed on colloidin-coated copper specimen grids. Finally, the sections were stained for increased contrast by inverting the grids

over a drop of uranyl acetate solution, then over a drop of Reynolds' lead citrate. These final steps were performed in a covered glass petri dish in which several sodium hydroxide crystals were placed to reduce atmospheric carbon dioxide within the dish. This is especially important during lead citrate staining where lead carbonate precipitates could form and introduce artifactual particulates to the sections. A subset of control and BDS-exposed cells were stained with ruthenium red to specifically distinguish the plasma membrane from other vesicular membranes within the cells. To stain with ruthenium red, the same procedure was followed as for traditional TEM, except that the fixation and post-fixation solutions each contained 0.1% ruthenium red and *en bloc* staining was not performed (Hayat 1989). Digital images were captured with a JEOL JEM-1011 (Tokyo, Japan) transmission electron microscope.

Mouse Macrophage Preparation. Bronchoalveolar lavage fluid (BALF) was collected from 18 mice, either exposed to HEPA-filtered air or 6.5 mg/m^3 BDS (as described by Murphy *et al.*, manuscript submitted), by flushing their lungs twice with 0.5 mL phosphate-buffered saline passed through a 19 gauge cannula anchored in the trachea. BALF was immediately placed on ice. After removing 400 µl of the raw BALF for cytospin preparation, the remaining fluid was centrifuged (500 x g; 10 min) and the supernatants were collected for archival at -80°C. The cell pellets were pooled according to exposure into 2.5% glutaraldehyde fixative in NaCac and processed for traditional EM.

RESULTS

Figure 4.1 displays electron micrographs of a negative control BEAS-2B cell (1A) and a cell that was exposed to S-BDS for 24 hours (4.1B/C). In 1B, there are membrane-limited areas within the cytoplasm containing soot particles and a group of particles in contact with the lower

membrane border of the cell. Figure 4.1C shows a magnified area of the same cell as in 1B where it appears that BDS particles are being internalized at the plasma membrane of the cell.

The micrographs in Figure 4.2 demonstrate ruthenium red staining of the plasma membrane of a negative control BEAS-2B cell (4.2A/B) and a cell exposed to S-BDS (4.2C/D). Ruthenium red clearly labeled the plasma membranes, and they appear as heavy black borders encompassing the cells. Subcellular structures are not as distinct as in Figure 4.1 or Figure 4.3 because *en bloc* uranyl acetate staining was not performed, but this helped to increase the contrast between the ruthenium red labeling of the plasma membrane and other membranes within the cytoplasm. Figure 4.2B is the same cell as in 4.2A, but it is presented at a higher magnification to highlight the character of the ruthenium red stain. Figure 4.2D demonstrates that the membrane surrounding the soot particles within the cell, as shown in the lower center portion of the less magnified Figure 4.2C, is discontinuous with the plasma membrane, *i.e.* the lack of ruthenium red staining of the membrane surrounding the soot particles indicates that the particles were completely internalized by the epithelial cell, rather than simply being apposed to a plasma membrane invagination (as shown in Figure 4.1B/C).

Figure 4.3 shows representative alveolar macrophages collected in BALF from mice exposed to HEPA-filtered air (4.3A) or 6.5 mg/m^3 BDS for four consecutive days (4.3B/C). Macrophages from the control group occasionally contained variable-sized particulates and several cytoplasmic vesicles. In contrast, virtually every macrophage from the BDS-exposed mice contained phagocytosed BDS particles. Many of these cells also had vesicles filled with electron-lucent whorls. Membranes of the vesicles surrounding soot particles and the membranous whorls are more clearly demonstrated at a higher magnification (4.3C).

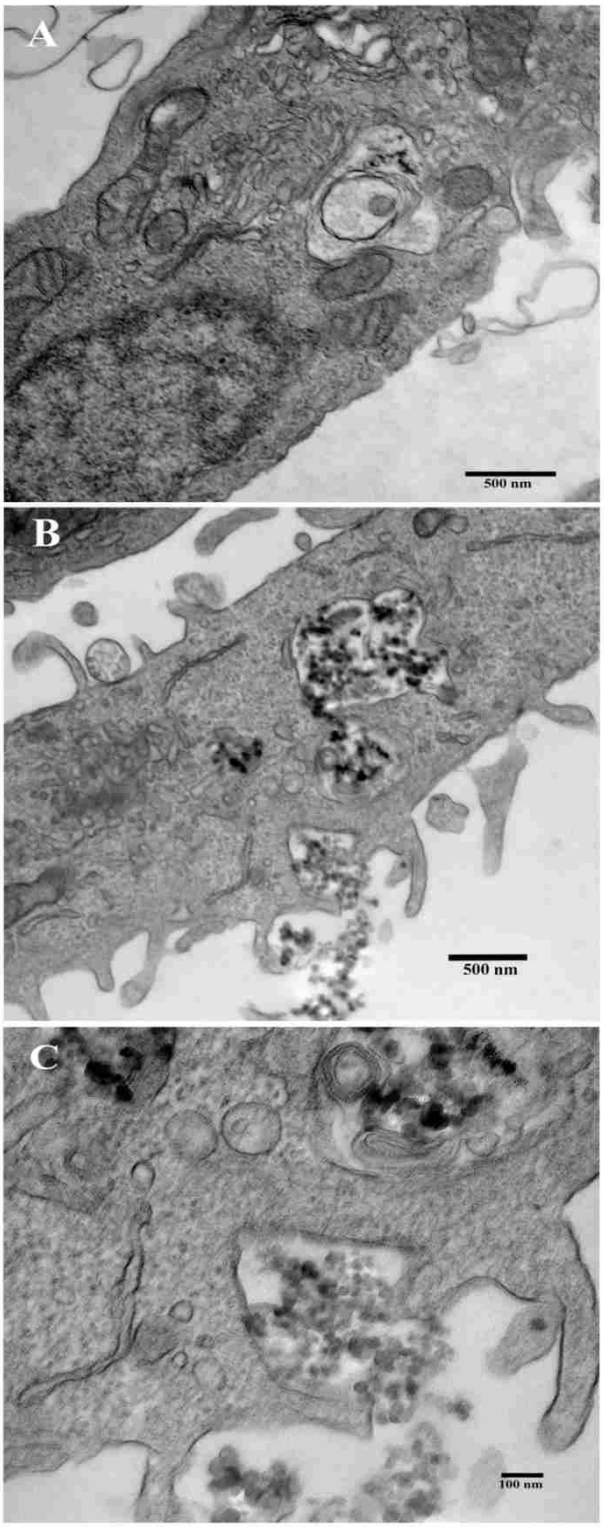

Figure 4.1. TEM micrographs of BEAS-2B cells. Panel A (40,000X) represents a typical negative control cell with no internalized particles and few vesicular structures. A cell exposed to S-BDS for 24 hours is displayed in panels B (30,000X) and C (100,000X). In panel B, there are membrane-limited areas within the cytoplasm containing soot particles and a group of particles in contact with the plasma membrane of the cell. Panel C is a more detailed display of the soot particles interacting with the plasma membrane of the same cell as shown in panel B.

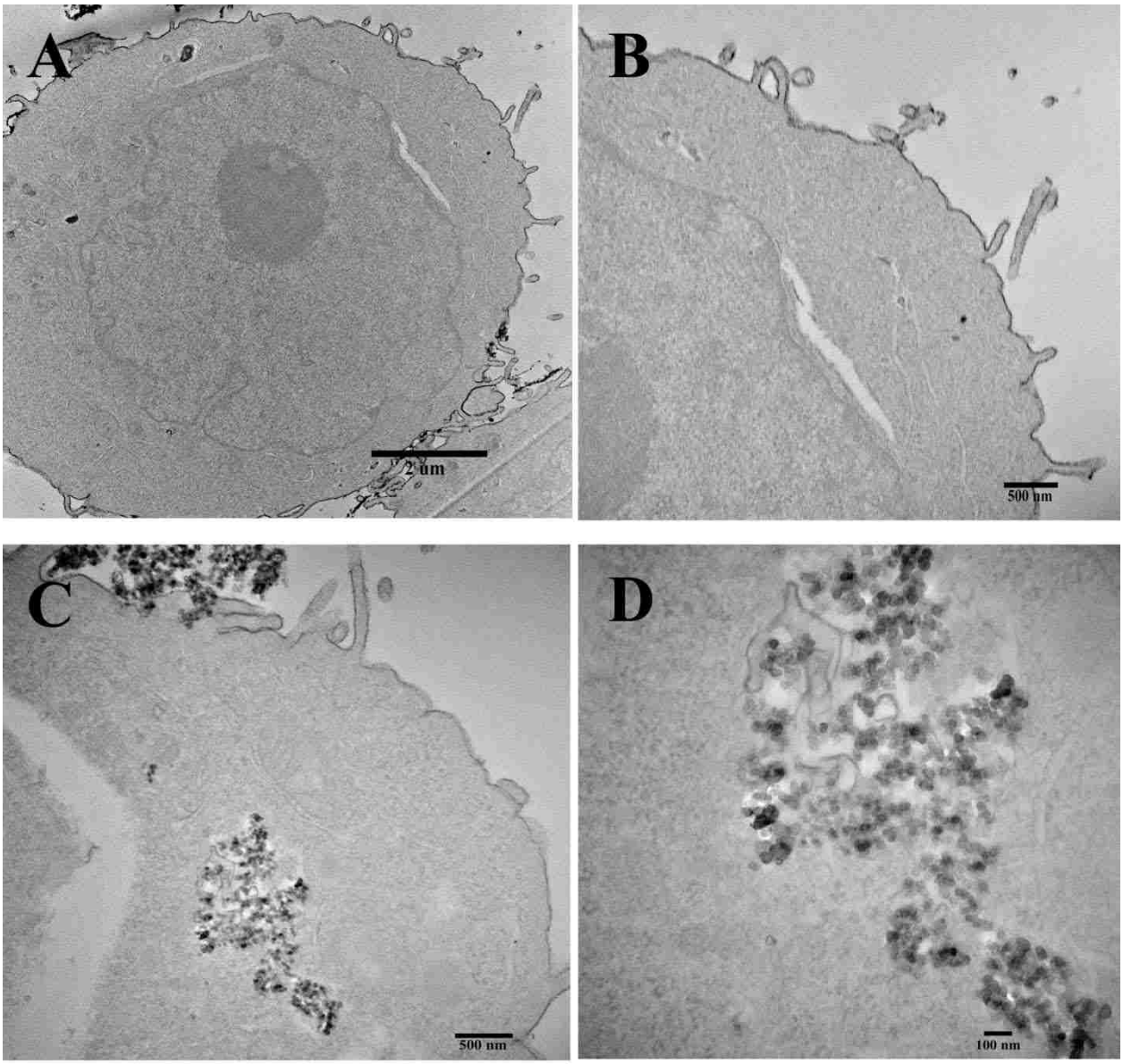

Figure 4.2. Ruthenium red staining of the plasma membrane of BEAS-2B cells. Panels A (12,000X) and B (30,000X) represent negative control cells, while panels C (30,000X) and D (80,000X) display a representative cell exposed to S-BDS. Ruthenium red clearly labeled the plasma membranes, and they appear as heavy black borders surrounding the cells. In panel D, the lack of ruthenium red staining of the membrane surrounding the soot particles demonstrates that this vesicle's membrane is discontinuous with the plasma membrane, indicating that the particles were completely internalized by the epithelial cell.

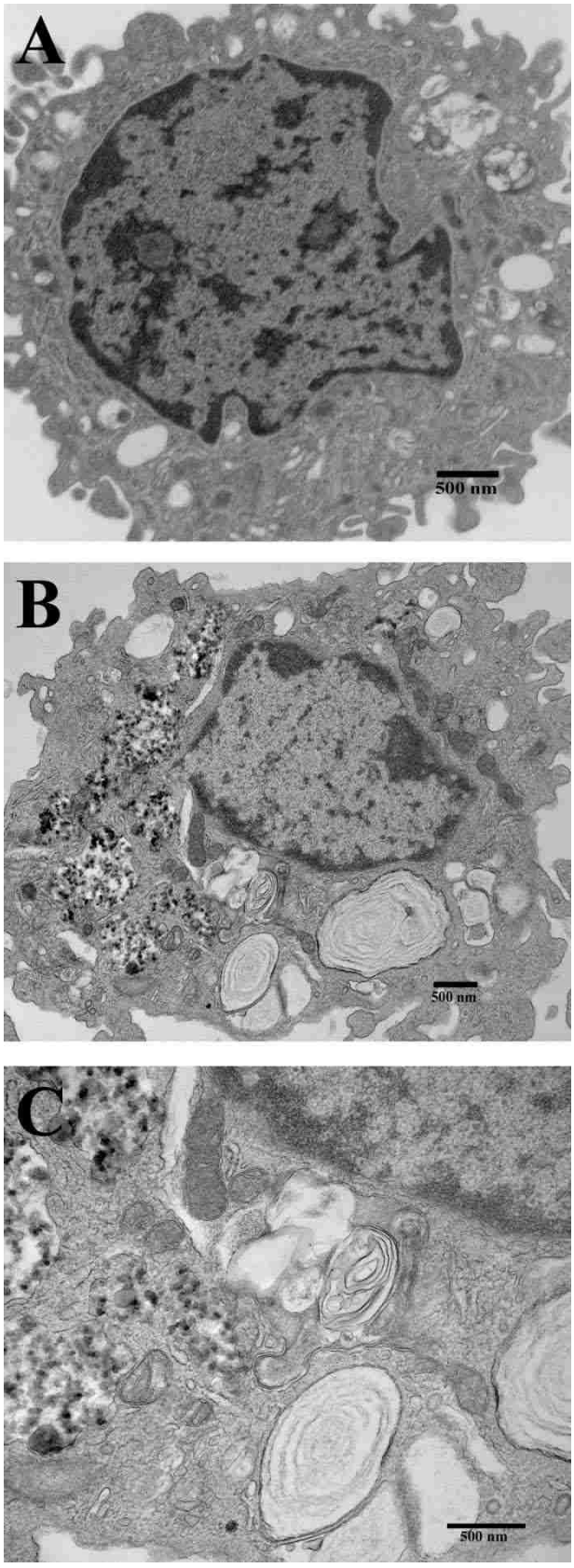

Figure 4.3. Alveolar macrophages collected from BALF *in vivo*. Panel A (15,000X) is a representative alveolar macrophage from a negative control mouse exposed to HEPA-filtered air. Panels B (15,000X) and C (40,000X) demonstrate the characteristics of most alveolar macrophages from mice exposed to 6.5 mg/m^3 BDS for four consecutive days. Although not shown in panel A, macrophages from the control group occasionally contained amorphous particulates and, as shown, several cytoplasmic vesicles. In contrast, virtually every macrophage from the BDS-exposed mice contained BDS particle-laden vesicles. Many of these cells also had vesicles filled with electron-lucent whorls. Membranes of the vesicles surrounding soot particles and the membranous whorls were more clearly demonstrated with higher magnifications, as in panel C.

DISCUSSION

Since retention of particles within respiratory tissues has been associated with adverse health effects, including persistent irritation and inflammation with the potential for carcinogenesis (Oberdorster *et al.* 1994; Warheit *et al.* 1997), it is important to determine which cells in the lung are capable of harboring particles and the ultimate fate of these particles.

Investigators have used magnetometry to track clearance of particles delivered by inhalation or intravenous injection. The particles were phagocytosed by alveolar macrophages and hepatic Kuppfer cells, respectively, which then attempted to eliminate the particles from the body. Alveolar macrophages appeared to phagocytose the particles more slowly than the Kuppfer cells, but the alveolar macrophages were able to clear the particle burden from the body more quickly than the Kuppfer cells (Brain 1992; Molina and Brain 2007; Weinstock and Brain 1988). The disparity in timing could be due to a time lag in the initial recruitment of a sufficient number of alveolar macrophages to the lung versus the more permanent population of Kuppfer cells in the liver, not to mention that the macrophages located in the spleen were not considered. Furthermore, once macrophages have ingested particles, alveolar macrophages have at least one direct outlet for clearance, the mucociliary elevator. Kuppfer cells must rely on the circulatory and/or digestive systems for clearance; but the authors speculated that Kuppfer cells, through a slower process than the escalator, solubilized the particles, causing them to lose their magnetic character and be lost to further investigation (Weinstock and Brain 1988). Movement of particle-laden macrophages to more permanent locations, such as the pulmonary interstitium, was not considered in these magnetometry studies; but this fate of alveolar macrophages loaded with silica particles or asbestos fibers can contribute to debilitating disease conditions, such as pulmonary fibrosis (Adamson *et al.* 1989; Adamson *et al.* 1991). Fibrotic conditions also appear

to be promoted when secretion of IL-6 and IL-8 (Takizawa *et al.* 1997), as well as plasminogen activator inhibitors (PAIs), is increased in pulmonary tissue (Lardot *et al.* 1998). We have observed retention of particles within pulmonary interstitial macrophages of mice exposed to BDS along with upregulation of IL-6, IL-8, and PAI-2 in lung tissue (Murphy *et al*. manuscript submitted) suggesting that BDS, as a model for petrochemical combustion-derived ultrafine particles, could promote pulmonary fibrosis.

There has been an intense debate over the mechanism of cardiotoxicity following inhalation exposure to ambient particles. One hypothesis is that inflammatory mediators, including cytokines, produced by lung cells enter the systemic circulation in sufficient quantity to affect other organ systems (Van Eeden *et al.* 2001). In support of this, Suwa *et al.* (2002) correlated increased circulating levels of inflammatory cytokines subsequent to PM_{10} exposure with progression of atherosclerosis. Another study described the direct translocation of particles from the respiratory tree to the systemic circulation as being responsible for subsequent cardiovascular disease conditions (Nemmar *et al.* 2004); however, this mechanism has been challenged by human exposure studies (Mills *et al.* 2006; Wiebert *et al.* 2006). Still others have found that ultrafine particles deposited in the nasopharyngeal area may gain access to the central nervous system via olfactory neuronal transport (Elder *et al.* 2006). Also, Geiser *et al.* (2005) reported that ultrafine particles enter respiratory and circulatory system cells by non-phagocytic or non-endocytic mechanisms. They found non-membrane-bound particles within the cytoplasm of cells *in vivo* and *in vitro*, and *no* evidence of endocytosis. Further, they proposed that ultrafine particles may enter the systemic circulation through such a diffusive-type process across alveolar or capillary epithelia. Nemmar *et al.* (2006) applauded these findings, only faulting the lack of

attention to surface charge of the particles in reaching their conclusions about the mechanisms of particle distribution in the body.

Our results demonstrate that the 'diffusion' of ultrafine particles across biological membranes is *not* a defining characteristic of all ultrafine particles. We have no evidence that ultrafine BDS particles reach non-membrane-bound areas within the cytoplasm of cells *in vitro* or *in vivo*. Furthermore, we have confirmed that epithelial cells *in vitro* are capable of internalizing petrochemical combustion-derived ultrafine particles into membrane-bound vesicles, similar to the compartmentalization seen in alveolar macrophages *in vivo*.

REFERENCES

Adamson, I. Y., Letourneau, H. L., and Bowden, D. H. (1989). Enhanced macrophage-fibroblast interactions in the pulmonary interstitium increases fibrosis after silica injection to monocyte-depleted mice. *Am. J. Pathol.* **134**(2), 411-418.

Adamson, I. Y., Letourneau, H. L., and Bowden, D. H. (1991). Comparison of alveolar and interstitial macrophages in fibroblast stimulation after silica and long or short asbestos. *Lab Invest* **64**(3), 339-344.

Antonini, J. M., Roberts, J. R., Jernigan, M. R., Yang, H. M., Ma, J. Y., and Clarke, R. W. (2002). Residual oil fly ash increases the susceptibility to infection and severely damages the lungs after pulmonary challenge with a bacterial pathogen. *Toxicol. Sci.* **70**(1), 110-119.

Auger, F., Gendron, M. C., Chamot, C., Marano, F., and Dazy, A. C. (2006). Responses of well-differentiated nasal epithelial cells exposed to particles: role of the epithelium in airway inflammation. *Toxicol. Appl. Pharmacol.* **215**(3), 285-294.

Bermudez, E., Mangum, J. B., Wong, B. A., Asgharian, B., Hext, P. M., Warheit, D. B., and Everitt, J. I. (2004). Pulmonary responses of mice, rats, and hamsters to subchronic inhalation of ultrafine titanium dioxide particles. *Toxicol. Sci.* **77**(2), 347-357.

Boland, S., Baeza-Squiban, A., Fournier, T., Houcine, O., Gendron, M. C., Chevrier, M., Jouvenot, G., Coste, A., Aubier, M., and Marano, F. (1999). Diesel exhaust particles are taken up by human airway epithelial cells in vitro and alter cytokine production. *Am. J. Physiol* **276**(4 Pt 1), L604-L613.

Brain, J. D. (1992). Mechanisms, measurement, and significance of lung macrophage function. *Environ. Health Perspect.* **97**, 5-10.

Catallo, W. J., Kennedy, C. H., Henk, W., Barker, S. A., Grace, S. C., and Penn, A. (2001). Combustion products of 1,3-butadiene are cytotoxic and genotoxic to human bronchial epithelial cells. *Environ. Health Perspect.* **109**(9), 965-971.

Dominici, F., Peng, R. D., Bell, M. L., Pham, L., McDermott, A., Zeger, S. L., and Samet, J. M. (2006). Fine particulate air pollution and hospital admission for cardiovascular and respiratory diseases. *JAMA* **295**(10), 1127-1134.

Dreher, K. L., Jaskot, R. H., Lehmann, J. R., Richards, J. H., McGee, J. K., Ghio, A. J., and Costa, D. L. (1997). Soluble transition metals mediate residual oil fly ash induced acute lung injury. *J. Toxicol. Environ. Health* **50**(3), 285-305.

Elder, A., Gelein, R., Silva, V., Feikert, T., Opanashuk, L., Carter, J., Potter, R., Maynard, A., Ito, Y., Finkelstein, J., and Oberdorster, G. (2006). Translocation of inhaled ultrafine manganese oxide particles to the central nervous system. *Environ. Health Perspect.* **114**(8), 1172-1178.

Geiser, M., Rothen-Rutishauser, B., Kapp, N., Schurch, S., Kreyling, W., Schulz, H., Semmler, M., Im, H., V, Heyder, J., and Gehr, P. (2005). Ultrafine particles cross cellular membranes by nonphagocytic mechanisms in lungs and in cultured cells. *Environ. Health Perspect.* **113**(11), 1555-1560.

Hayat, M. A. (1989). Principles and Techniques of Electron Microscopy: Biological Applications, Cambridge University Press, Cambridge, UK.

Kumagai, Y., Koide, S., Taguchi, K., Endo, A., Nakai, Y., Yoshikawa, T., and Shimojo, N. (2002). Oxidation of proximal protein sulfhydryls by phenanthraquinone, a component of diesel exhaust particles. *Chem. Res. Toxicol.* **15**(4), 483-489.

Lardot, C., Heusterpreute, M., Mertens, P., Philippe, M., and Lison, D. (1998). Expression of plasminogen activator inhibitors type-1 and type-2 in the mouse lung after administration of crystalline silica. *Eur. Respir. J.* **11**(4), 912-921.

Li, N., Venkatesan, M. I., Miguel, A., Kaplan, R., Gujuluva, C., Alam, J., and Nel, A. (2000). Induction of heme oxygenase-1 expression in macrophages by diesel exhaust particle chemicals and quinones via the antioxidant-responsive element. *J. Immunol.* **165**(6), 3393-3401.

Lighty, J. S., Veranth, J. M., and Sarofim, A. F. (2000). Combustion aerosols: factors governing their size and composition and implications to human health. *J. Air Waste Manag. Assoc.* **50**(9), 1565-1618.

Lundborg, M., Dahlen, S. E., Johard, U., Gerde, P., Jarstrand, C., Camner, P., and Lastbom, L. (2006). Aggregates of ultrafine particles impair phagocytosis of microorganisms by human alveolar macrophages. *Environ. Res.* **100**(2), 197-204.

Mills, N. L., Amin, N., Robinson, S. D., Anand, A., Davies, J., Patel, D., de la Fuente, J. M., Cassee, F. R., Boon, N. A., MacNee, W., Millar, A. M., Donaldson, K., and Newby, D. E. (2006). Do inhaled carbon nanoparticles translocate directly into the circulation in humans? *Am. J. Respir. Crit Care Med.* **173**(4), 426-431.

Molina, R. M., and Brain, J. D. (2007). In vivo comparison of cat alveolar and pulmonary intravascular macrophages: phagocytosis, particle clearance, and cytoplasmic motility. *Exp. Lung Res.* **33**(2), 53-70.

Murphy, S. A., Berube, K. A., and Richards, R. J. (1999). Bioreactivity of carbon black and diesel exhaust particles to primary Clara and type II epithelial cell cultures. *Occup. Environ. Med.* **56**(12), 813-819.

Nemmar, A., Hoet, P. H., and Nemery, B. (2006). Translocation of ultrafine particles. *Environ. Health Perspect.* **114**(4), A211-A212.

Nemmar, A., Hoylaerts, M. F., Hoet, P. H., and Nemery, B. (2004). Possible mechanisms of the cardiovascular effects of inhaled particles: systemic translocation and prothrombotic effects. *Toxicol. Lett.* **149**(1-3), 243-253.

Oberdorster, G., Ferin, J., and Lehnert, B. E. (1994). Correlation between particle size, in vivo particle persistence, and lung injury. *Environ. Health Perspect.* **102 Suppl 5**, 173-179.

Penn, A., Murphy, G., Barker, S., Henk, W., and Penn, L. (2005). Combustion-derived ultrafine particles transport organic toxicants to target respiratory cells. *Environ. Health Perspect.* **113**(8), 956-963.

Pope, C. A., III, Burnett, R. T., Thun, M. J., Calle, E. E., Krewski, D., Ito, K., and Thurston, G. D. (2002). Lung cancer, cardiopulmonary mortality, and long-term exposure to fine particulate air pollution. *JAMA* **287**(9), 1132-1141.

Reddel, R. R., Ke, Y., Gerwin, B. I., McMenamin, M. G., Lechner, J. F., Su, R. T., Brash, D. E., Park, J. B., Rhim, J. S., and Harris, C. C. (1988). Transformation of human bronchial epithelial cells by infection with SV40 or adenovirus-12 SV40 hybrid virus, or transfection via strontium phosphate coprecipitation with a plasmid containing SV40 early region genes. *Cancer Res.* **48**(7), 1904-1909.

Renwick, L. C., Brown, D., Clouter, A., and Donaldson, K. (2004). Increased inflammation and altered macrophage chemotactic responses caused by two ultrafine particle types. *Occup. Environ. Med.* **61**(5), 442-447.

Renwick, L. C., Donaldson, K., and Clouter, A. (2001). Impairment of alveolar macrophage phagocytosis by ultrafine particles. *Toxicol. Appl. Pharmacol.* **172**(2), 119-127.

Seaton, A., MacNee, W., Donaldson, K., and Godden, D. (1995). Particulate air pollution and acute health effects. *Lancet* **345**(8943), 176-178.

Suwa, T., Hogg, J. C., Quinlan, K. B., Ohgami, A., Vincent, R., and Van Eeden, S. F. (2002). Particulate air pollution induces progression of atherosclerosis. *J. Am. Coll. Cardiol.* **39**(6), 935-942.

Takizawa, H., Satoh, M., Okazaki, H., Matsuzaki, G., Suzuki, N., Ishii, A., Suko, M., Okudaira, H., Morita, Y., and Ito, K. (1997). Increased IL-6 and IL-8 in bronchoalveolar lavage fluids

(BALF) from patients with sarcoidosis: correlation with the clinical parameters. *Clin. Exp. Immunol.* **107**(1), 175-181.

Van Eeden, S. F., Tan, W. C., Suwa, T., Mukae, H., Terashima, T., Fujii, T., Qui, D., Vincent, R., and Hogg, J. C. (2001). Cytokines involved in the systemic inflammatory response induced by exposure to particulate matter air pollutants (PM(10)). *Am. J. Respir. Crit Care Med.* **164**(5), 826-830.

Warheit, D. B., Hansen, J. F., Yuen, I. S., Kelly, D. P., Snajdr, S. I., and Hartsky, M. A. (1997). Inhalation of high concentrations of low toxicity dusts in rats results in impaired pulmonary clearance mechanisms and persistent inflammation. *Toxicol. Appl. Pharmacol.* **145**(1), 10-22.

Warheit, D. B., Webb, T. R., Reed, K. L., Frerichs, S., and Sayes, C. M. (2007). Pulmonary toxicity study in rats with three forms of ultrafine-TiO2 particles: differential responses related to surface properties. *Toxicology* **230**(1), 90-104.

Weinstock, S. B., and Brain, J. D. (1988). Comparison of particle clearance and macrophage phagosomal motion in liver and lungs of rats. *J. Appl. Physiol* **65**(4), 1811-1820.

Wiebert, P., Sanchez-Crespo, A., Seitz, J., Falk, R., Philipson, K., Kreyling, W. G., Moller, W., Sommerer, K., Larsson, S., and Svartengren, M. (2006). Negligible clearance of ultrafine particles retained in healthy and affected human lungs. *Eur. Respir. J.* **28**(2), 286-290.

CONCLUDING REMARKS

RESEARCH SUMMARY

At this point, we have presented experiments that were designed to continue the characterization of butadiene soot (BDS), including its physicochemical properties (Chapter 1), its effects on bronchoepithelial cells and macrophages *in vitro* (Chapter 2 and Chapter 4), and its effects on the respiratory system of mice *in vivo* (Chapter 3).

In Chapter 1, we demonstrated that the overwhelming majority of freshly generated BDS particles are of respirable size, have a predictable chemical composition, and act to transport adsorbed, bioactive chemicals (primarily PAHs) to target cells. These results also indicated that uptake of airborne ultrafine particles by target cells is not necessary for the particles to exert their toxic effects on the cells.

The results presented in Chapter 2 demonstrated that fluorescent PAH compounds adsorbed to inhalable combustion-derived ultrafine particles traffic to lipid droplets of respiratory cells, including bronchial epithelial cells, alveolar macrophages, and adipocytes. Furthermore, *in vitro* exposure of epithelial cells and alveolar macrophages to BDS stimulated AhR-responsive xenobiotic metabolism pathways known to potentiate the toxicity of certain PAHs, including several found in BDS.

In Chapter 3, we described that brief inhalation exposure to a moderate dose of PAH-rich combustion-derived ultrafine particles causes 1) acute pulmonary inflammation, evidenced by inflammatory cell infiltrates and upregulated cytokine expression; and 2) increased expression of AhR-responsive genes that are capable of transforming PAHs into more toxic metabolites. The histopathological analyses showed that freshly-generated ultrafine BDS particles reached the deepest bronchoalveolar spaces in mouse lungs.

In Chapter 4, we challenged the results from other research groups by demonstrating that the 'diffusion' of ultrafine particles across biological membranes is not a defining characteristic of all ultrafine particles. We found no evidence that ultrafine BDS particles reach non-membrane-bound areas within the cytoplasm of cells *in vitro* or *in vivo*. We confirmed that epithelial cells *in vitro* are capable of internalizing petrochemical combustion-derived ultrafine particles into membrane-bound vesicles, similar to the compartmentalization seen in alveolar macrophages *in vivo*.

In contrast to diesel exhaust particles (DEPs) and residual oil fly ash (ROFA), we propose that oxygen- and metals-poor, PAH-rich BDS is a unique 'real-world' model for inhalation exposure to ambient petrochemical combustion-derived ultrafine particles. BDS elicits similar effects as DEPs and ROFA *in vitro* and *in vivo*, including the observed alterations in gene expression and inflammation; however, the localization of PAHs from BDS within lipid droplets of target cells in the lung has not been described for DEPs or ROFA.

FUTURE RESEARCH

Future research may focus on the fate of the PAHs within cells. Because of the fluorescent nature of BDS-associated PAHs in lipid droplets, advanced fluorometry could be used to measure the accumulation of fluorescence in the droplets, and any subsequent reduction in fluorescence also may be quantified if the cells metabolize or otherwise eliminate the PAHs. Isolation of lipid droplets from BDS-exposed cells and analysis of this fraction by mass spectrometry could allow for identification of the specific PAHs responsible for the observed fluorescent responses, and this identification may allow for predictive investigation of the fate of the individual compounds within cells.

Recent advances in molecular biology have made possible gene expression analysis of the entire genome of several species. We have already begun to use this technology to investigate genome-wide changes in gene expression due to BDS exposure *in vitro* and *in vivo*; however, careful interpretation of the complex results obtained from this type of investigation is essential to reach meaningful conclusions. For example, a simple list of genes that are upregulated or downregulated is useless, unless the results are arranged according to gene families or along effector pathways. Thus, future analyses of our genomic data shall rely on bioinformatics and computational biology to organize and catalogue the biological and toxicological effects of BDS.

VITA

Gleeson Murphy, Jr. was born in Picayune, Mississippi, on June 10, 1979. He grew up in the rural Piney Woods of South Mississippi and attended public schools in Hancock County until he graduated as Salutatorian from Hancock High School (Kiln, Mississippi) in 1997. He then accepted a scholarship to attend Louisiana State University in Baton Rouge, Louisiana. There he received a Bachelor of Science degree in zoology *summa cum laude* in 2000. He was then fortunate enough to be accepted into the School of Veterinary Medicine at Louisiana State University, where he earned a Doctor of Veterinary Medicine degree, again as Salutatorian, in 2005.

During his second year of veterinary school, Gleeson entered the DVM/PhD program. The program was quite challenging and stressful, but worth the effort. In fact, he attracted the attention of the United States Army and was awarded an Army Health Professions Scholarship to fund his third and fourth years of veterinary school. In an extraordinary show of support for higher education of military officers, the Army awarded Captain Murphy a Long Term Health Education and Training grant, which gave him the time and financial compensation necessary to complete the Doctor of Philosophy degree. Upon completion of his degree requirements at Louisiana State University and the Officer Basic Leader's Course at Fort Sam Houston in San Antonio, Texas, Captain Murphy will report to his first duty station at the United States Army Medical Research Institute of Chemical Defense at Aberdeen Proving Ground, Maryland.